

Climate change is a pressing global issue that is caused by the consumption of fossil fuels, which releases greenhouse gases into the atmosphere. Cell factories are biological systems that are engineered to produce a wide range of products, such as biofuels, bioplastics, and pharmaceuticals which can play a crucial part in reducing the dependency on fossil fuels. Additionally, cell factories can be made more efficient and sustainable by using advanced technologies such as metabolic engineering and synthetic biology.

This thesis aimed to expand the genetic toolbox of *Pseudomonas taiwanensis* VLB120 and implement them for the generation of a chassis strain to enlarge the product portfolio of this emerging industrial-relevant cell factory. Sigma-70 dependent promoter libraries were generated and integrated into the single genomic locus *attTn7* of *P. taiwanensis* VLB120 and *E. coli* TOP10 and characterized using a standardized promoter strength unit. Such characterization standards gave an insight into how a specific promoter behaves in each organism and create sets of promoters relevant to metabolic engineering purposes. This thesis also focused on the assessment of an optimized gene expression architecture to achieve high gene expression. This module achieved high gene expression across several expression vectors of two fluorescent reporter genes by incorporating mRNA stabilizing and translation-enhancing genetic parts. This module was also applied to increase the productivities of a short acetoin pathway and the relevance of mRNA stability was proven through qPCR-based mRNA decay rates. These tools were a component in the development of a *P. taiwanensis* VLB120 propionyl-CoA chassis strain to expand the portfolio of this pseudomonad to odd-chain products. The successful incorporation of propionyl-CoA in the metabolism of *P. taiwanensis* VLB120 was confirmed by the production of propionate after identifying the deletion of the methylcitrate synthase as a crucial factor.

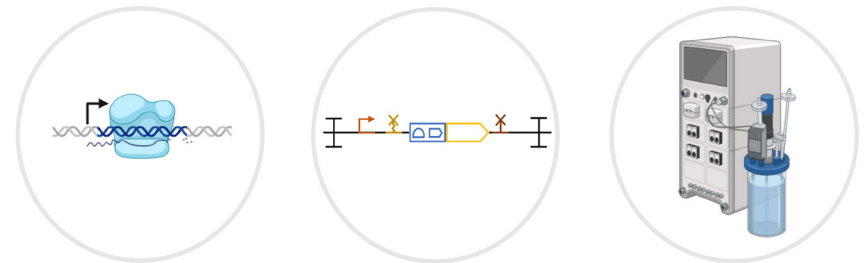
In summary, this thesis contributes to the development of *P. taiwanensis* VLB120 as an emerging industrial-relevant workhouse by expanding the available genetic toolbox and setting the first stone to produce odd-chain products in this organism. It also contributes to the standardization of genetic tools characterization and cross-species studies to aid the identification of the most suitable microbe for specific biotechnological applications and fasten the human independence of fossil fuels.

Pseudomonas taiwanensis VLB120 synthetic biology: parts, modules, and chassis

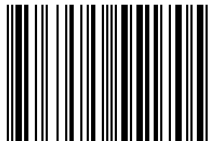
Dário Silva Neves

Dário Silva Neves

Pseudomonas taiwanensis VLB120 synthetic biology: parts, modules, and chassis



ISBN 978-3-98555-170-5



Pseudomonas taiwanensis VLB120 synthetic biology: parts, modules, and chassis

Von der Fakultät für Mathematik, Informatik und Naturwissenschaften der
RWTH Aachen University zur Erlangung des akademischen Grades eines
Doktors der Naturwissenschaften genehmigte Dissertation

vorgelegt von

Dário Jorge Silva Neves, M. Sc.

aus

Louriçal, Leiria, Portugal

Berichter:

Univ.-Prof. Dr.-Ing. Lars M. Blank

Dr.-Ing. Birgitta Ebert

Tag der mündlichen Prüfung: 03 Juli 2023

Diese Dissertation ist auf den Internetseiten der Universitätsbibliothek verfügbar.

Bibliografische Information der Deutschen Nationalbibliothek

Die Deutsche Nationalbibliothek verzeichnet diese Publikation in der Deutschen Nationalbibliografie; detaillierte bibliografische Daten sind im Internet über <https://portal.dnb.de> abrufbar.

Dário Silva Neves:

Pseudomonas taiwanensis VLB120 synthetic biology: parts, modules, and chassis

1. Auflage, 2023

Gedruckt auf holz- und säurefreiem Papier, 100% chlorfrei gebleicht.

Copyright Apprimus Verlag, Aachen, 2023

Wissenschaftsverlag des Instituts für Industriekommunikation und Fachmedien
an der RWTH Aachen

Steinbachstr. 25, 52074 Aachen

Internet: www.apprimus-verlag.de, E-Mail: info@apprimus-verlag.de

Alle Rechte, auch das des auszugsweisen Nachdruckes, der auszugsweisen oder vollständigen Wiedergabe, der Speicherung in Datenverarbeitungsanlagen und der Übersetzung, vorbehalten.

Printed in Germany

ISBN 978-3-98555-170-5

Eidesstattliche Erklärung

Ich erkläre hiermit, dass diese Dissertation und die darin dargelegten Inhalte die eigenen sind und selbstständig, als Ergebnis der eigenen originären Forschung, generiert wurden.

Hiermit erkläre ich an Eides statt

1. Diese Arbeit wurde vollständig oder größtenteils in der Phase als Doktorand dieser Fakultät und Universität angefertigt;
2. Sofern irgendein Bestandteil dieser Dissertation zuvor für einen akademischen Abschluss oder eine andere Qualifikation an dieser oder einer anderen Institution verwendet wurde, wurde dies klar angezeigt;
3. Wenn immer andere eigene- oder Veröffentlichungen Dritter herangezogen wurden, wurden diese klar benannt;
4. Wenn aus anderen eigenen- oder Veröffentlichungen Dritter herangezogen wurde, wurde stets die Quelle hierfür angegeben. Diese Dissertation ist vollständig meine eigene Arbeit, mit der Ausnahme solcher Zitate;
5. Alle wesentlichen Quellen von Unterstützung wurden benannt;
6. Wenn immer ein Teil dieser Dissertation auf der Zusammenarbeit mit anderen basiert, wurde von mir klar gekennzeichnet, was von anderen und was von mir selbst erarbeitet wurde;
7. Ein Teil oder Teile dieser Arbeit wurden zuvor veröffentlicht, und zwar in:

D. Neves, U. Liebal, S. C. Nies, T. B. Alter, C. Pitzler, L. M. Blank and B. E. Ebert, "Cross-species synthetic promoter library: finding common ground between *Pseudo-monas taiwanensis* VLB120 and *Escherichia coli*." *ACS Syn. Bio.*, 2023, doi: 10.1021/acssynbio.3c00084

D. Neves, S. Vos, L. M. Blank, and B. E. Ebert, "Pseudomonas mRNA 2.0: Boosting Gene Expression Through Enhanced mRNA Stability and Translational Efficiency," *Front. Bioeng. Biotechnol.*, 2020, doi: 10.3389/fbioe.2019.00458.

D. Neves, D. Meinen, T. B. Alter, L. M. Blank and B. E. Ebert, "Expanding *Pseudomonas taiwanensis* VLB120's acyl-CoA portfolio: propionate production in mineral salt medium." *Microb. Biotechnol.*, 2023. doi: 10.1111/1751-7915.14309

Konstanz, 06.07.2023

Dário Jorge Silva Neves

Note of Thanks

First of all, I want to express my gratitude to Prof. Lars M. Blank and Dr. Birgitta Ebert for granting me the opportunity to complete my doctorate at the Institute of Applied Microbiology and for being an important part of my development as a scientist.

Lars, I want to thank you for providing me the exceptional research work conditions and even more for showing me how to maintain a friendly and joyful working atmosphere. I will remember how during our discussions you would always provide me with the bigger picture and remind me of the impact that our research could (and most certainly will!) have in our daily life. But what I am truly thankful for is you showing me how to lead a group not with an authoritarian mindset but rather with a team spirit where autonomous thinking is encouraged and a contribution mindset is pursued. I will take these as the foundations of my leadership style.

Birgitta, I want to thank you for also giving me the freedom to pursue my projects and having an important role in defining my leadership values. I thank you for your patience during our brainstorming sessions, where I sometimes got overwhelmed with all the logical reasoning cascades, and for guiding me whenever it was needed. But what I am truly thankful for is supporting me during adversities that were out of our hands and encouraging me to tread my path which lead to this thesis.

I want to thank the students that helped me with the laboratory work, without them this thesis would have only half the data: Daniel Meinen, Annika Lenic, Nicola Freyer, Stefan Vos, Nadine Runge, Simon Briel, Simone Weingarten, Sarah Schlesse and Sussanne Thierry.

I want to thank all my iAMB colleagues who made my time at the iAMB rememberable and contributed to it in their unique way! Thank you to Ahmed Zahoor ul Hasan, Andrea Germer, Andreas Schmitz, Annette Schreer, Apilaasha Tharmasothirajan, Bastian Molitor, Bernd Leuchtle, Birthe Halmschlag, Carola Berger, Christian Carl Blesken, Christoph Halbfeld, Christoph Lenzen, Christoph Thiel, Conrad Müller, Dieter Weber, Eda Sarikaya, Eik Czarnotta, Elena von Helden, Erick Bosire, Gisela Beissel, Hao Guo, Hendrik Ballerstedt, Henrik Cordes, Isabel Bator, Isabel Reuter, Ivan Schlembach, Jan Förster, Jan Schirawski, Johanna Loevenich, Jonas Christ, Juan Ramirez, Julia Schütte, Kalle Hüser, Kristina Kirchner, Liesa Pötschke, Malte Heyer, Manja Kropp, Mariam Dianat Sabet Gilani, Maike Otto, Matthias Lehen, Martin Zimmermann, Miriam Agler-Rosenbaum, Monika Brehm, Philipp Demling, Rabea Zauter, Roberta Lovaglio, Romualdus Nugraha Catur Utomo, Salome Nies, Sandra Hartmann, Sandra Schulte, Sebastian Köbbing, Sebastian Zobel, Suresh Sudarsan, Tatiana de Campos Rodrigues, Theresia Desy Askitosari, Thiemo Zambanini, Thomas Heise, Thomas Kirchner, Thuy An Phan Nguyen, Till Tiso, Tobias Alter, Ulf Liebal, Ulrike Schmitt, Valeria Agostino, Vanessa Baier, Vinícius Luiz da Silva and Wing-Jin Li! I would like to especially thank Matthias, Hamed, Isabel, Birthe, Sebastian, Ahmed, Till, Eik, Christoph, Carl, Ulf, Maïke, and Benedikt for all the fun and great memories that I will take with me. Who I want to thank from the bottom of my heart is Tobias Alter, I will always have nostalgic memories from our conversations at Sowieso (there will always be a round of Beer and Mexicaner for us there), the crazy futsal tournament applications and the legendary parties in the corridor. I thank you for being there to hear my doubts and support me when I most needed it.

I want to thank Marita Weiss for her patience with me during the rough times of this thesis and for not letting me doubt myself. The world should learn what kindness and tolerance are from you, especially in these times.

I want to thank Antony Gonçalves for our lifelong friendship and for listening to the tales of iAMB during my visits to Portugal.

I want to thank Nuno Marques, even though I just met you after leaving the iAMB, your regular inquiries about the status of the thesis helped me to push it to the end and I am grateful to have you as my friend Gato!

I want to thank my family for which the next paragraph will be in Portuguese so they do not have to use Google translate.

Eu quero agradecer aos meus pais Mila e Manuel pelo apoio durante esta tese. Obrigado pela ajuda no meu retorno à Alemanha e por me apoiarem à distância ao ouvirem os meus lamentos e esperanças! Também quero agradecer à minha irmã Lili pela companheirismo e desabafos de irmão. Eu quero também agradecer à minha madrinha São e padrinho António não especialmente por algo relacionado com a tese, mas por uma fase da minha vida alguns capítulos anteriores a este.

Lastly, I want to thank Paula Narimatsu. We met shortly after I left the iAMB and you were the person with the most follow-up updates on this thesis. You tried to motivate me with deadlines and bets but the one that helped the most was to simply remind me that it just has to be done. Our relationship went through different stages just like this thesis, and both ended with a happy ending! Thank you for always listening to me and supporting me whenever I need it!

Funding



This work was funded by the ERA SynBio project SynPath (Grant ID 031A459) with the financial support of the German Federal Ministry of Education and Research.

Summary	III
Zusammenfassung.....	V
List of Abbreviations.....	VII
List of Figures.....	XI
List of Tables.....	XIII
1. General Introduction.....	3
1.1. Towards a circular bioeconomy based on renewable carbon	3
1.1.1. Climate Change and the urge for a circular bioeconomy.....	3
1.1.2. Integration of bioeconomy and circular economy- the concept of a circular bioeconomy..	7
1.2. Cell factories and their development.....	8
1.3. <i>Pseudomonas taiwanensis</i> VLB120 as a cell factory	11
1.4. Scope and outline of the thesis.....	13
2. Material and methods.....	17
2.1. Media and culture conditions	17
2.2. Plasmid and Strain Construction.....	18
2.3. Gravimetric cell dry weight determination.....	21
2.4. Growth rate determination.....	21
2.5. Fluorescent measurements	21
2.6. Sequence statistics.....	22
2.7. Flow Cytometry and cell sorting	22
2.8. qPCR assays for mRNA stability assessment.....	23
2.9. Analytical methods.....	24
2.10. LC-MS analysis of propionyl-CoA	24
2.11. Fermentation	24
3. Results.....	29
3.1. Cross-species synthetic promoter library: finding common ground between <i>Pseudomonas taiwanensis</i> VLB120 and <i>Escherichia coli</i>	29
3.1.1. Abstract	29
3.1.2. Introduction.....	29
3.1.3. Results and Discussion	30
3.1.3.1. Design and generation of the synthetic promoter libraries	30
3.1.3.2. Sequence diversity of generated promoter.....	33
3.1.3.3. Characterization of the synthetic promoter libraries in <i>E. coli</i> TOP10.	34
3.1.3.4. Characterization of the synthetic promoter libraries in <i>Pseudomonas taiwanensis</i> VLB120.	36
3.1.3.5. Common ground and disparities of σ_{70} -dependent promoters between <i>P. taiwanensis</i> VLB120 and <i>E. coli</i>	38

Table of contents

3.1.4. Conclusion	41
3.2. <i>Pseudomonas</i> mRNA 2.0: Boosting Gene Expression Through Enhanced mRNA Stability and Translational Efficiency.....	45
3.2.1. Abstract	45
3.2.2. Introduction.....	45
3.2.3. Results and Discussion.....	47
3.2.3.1. Characterization of plasmid-based, constitutive fluorescent protein expression.....	47
3.2.3.2. Characterization of plasmid-based, inducible fluorescent protein expression.....	50
3.2.3.3. Characterization of inducible fluorescence expression of single, genome-integrated constructs.....	51
3.2.3.4. Evaluation of a recombinant acetoin production pathway employing the optimized expression cassette	52
3.2.3.5. qPCR based elucidation of mRNA stability	53
3.2.4. Conclusion	54
3.3. Expanding <i>Pseudomonas taiwanensis</i> VLB120's acyl-CoA portfolio: propionate production in mineral salt medium.....	57
3.3.1. Abstract	57
3.3.2. Introduction.....	57
3.3.3. Results and Discussion.....	59
3.3.3.1. Extending the acyl-CoA portfolio of <i>P. taiwanensis</i> VLB120 by expressing the sleeping beauty mutase.....	59
3.3.3.2. Propionate production in <i>P. taiwanensis</i> VLB120	60
3.3.3.3. Benchmarking of fed-batch fermentation strategies for propionate production.....	62
3.3.4. Conclusion	65
4. General Discussion	69
4.1. Development of cross-species genetic tools.....	69
4.2. Development of enhanced gene expression architectures	71
4.3. Extending the acyl-CoA portfolio of <i>Pseudomonas taiwanensis</i>	71
4.4. Conclusion	73
Appendix.....	75
References.....	83
Curriculum vitae	99

Summary

Climate change is a pressing global issue that is caused by the consumption of fossil fuels, which releases greenhouse gases into the atmosphere. One of the ways to reduce dependency on fossil fuels and mitigate the effects of climate change is by using cell factories. Cell factories are biological systems that are engineered to produce a wide range of products, such as biofuels, bioplastics, and pharmaceuticals. These products can be produced using renewable resources such as plant matter or algae, rather than fossil fuels. Additionally, the production process of these products in cell factories can be made more efficient and sustainable by using advanced technologies such as metabolic engineering and synthetic biology. Synthetic biology aims to engineer biologically based systems with novel functions by either applying a rational and systematic approach or exploring the vast combinatorial potential of DNA to create new-to-nature molecular biology tools. Due to the intrinsic complexity of DNA shuffling and the current limitations in predicting accurate outcomes of synthetic biology parts, it is crucial to properly standardize and characterize synthetic biology tools to aid cell factory developments.

This thesis aimed to expand the genetic toolbox of *Pseudomonas taiwanensis* VLB120 and implement them for the generation of a chassis strain to enlarge the product portfolio of this emerging industrial-relevant cell factory. Sigma-70 dependent promoter libraries were generated and integrated into the single genomic locus *attTn7* of *P. taiwanensis* VLB120 and *E. coli* TOP10. Each promoter was characterized using a standardized promoter strength unit developed within this work that calibrates device-specific fluorescence output with fluorescein and accounts for cell growth-specific differences. Such characterization standards allow us to give an insight into how a specific promoter behaves in each organism and create sets of promoters relevant to metabolic engineering purposes. This thesis also focused on the assessment of an optimized gene expression architecture to achieve high gene expression without relying on strong promoters. This module achieved high gene expression across several expression vectors of two fluorescent reporter genes by incorporating mRNA stabilizing and translation-enhancing genetic parts. This module was also applied to increase the productivities of a short acetoin pathway and the relevance of mRNA stability was proven through qPCR-based mRNA decay rates. These tools were a component in the development of a *P. taiwanensis* VLB120 propionyl-CoA chassis strain to expand the portfolio of this pseudomonad to odd-chain products. The successful incorporation of propionyl-CoA in the metabolism of *P. taiwanensis* VLB120 was confirmed by the production of propionate after identifying the deletion of the methylcitrate synthase as a crucial factor. The propionate-producing *P. taiwanensis* VLB120 was evaluated in bioreactor fermentations under three different fed-batch strategies to assess how feeding regimes and feast-famine switches affect the production of propionyl-CoA-dependent products.

In summary, this thesis contributes to the development of *P. taiwanensis* VLB120 as an emerging industrial-relevant workhouse by expanding the available genetic toolbox and setting the first stone to produce odd-chain products in this organism. It also contributes to the standardization of genetic tools characterization and cross-species studies to aid the identification of the most suitable microbe for specific biotechnological applications and fasten the human independence of fossil fuels.

Zusammenfassung

Der Klimawandel ist ein dringendes globales Problem, das durch den Verbrauch von fossilen Brennstoffen verursacht wird, die Treibhausgase in die Atmosphäre freisetzen. Eine Möglichkeit, die Abhängigkeit von fossilen Brennstoffen zu reduzieren und die Auswirkungen des Klimawandels abzumildern, besteht darin, Zellfabriken zu verwenden. Zellfabriken sind biologische Systeme, die dafür entwickelt wurden, eine breite Palette von Produkten herzustellen. Diese Produkte können mithilfe erneuerbarer Ressourcen wie Pflanzenmaterial oder Algen hergestellt werden, anstatt von fossilen Brennstoffen. Zusätzlich kann der Produktionsprozess dieser Produkte in Zellfabriken durch den Einsatz fortgeschrittener Technologien wie metabolischem Engineering und synthetischer Biologie effizienter und nachhaltiger gemacht werden. Synthetische Biologie zielt darauf ab, biologisch basierte Systeme mit neuen Funktionen durch Anwendung einer rationalen und systematischen Methode oder Erforschung des großen Kombinationspotentials von DNA zu entwickeln. Aufgrund der intrinsischen Komplexität von DNA-Shuffling und der aktuellen Einschränkungen bei der Vorhersage präziser Ergebnisse von synthetischen Biologie-Teilen ist es wichtig, synthetische Biologie-Tools ordnungsgemäß zu standardisieren und zu charakterisieren, um die Entwicklung von Zellfabriken zu unterstützen.

Diese Arbeit hatte zum Ziel, das genetische Werkzeugkasten von *Pseudomonas taiwanensis* VLB120 zu erweitern und diese zur Generierung eines Chassis-Stamms zu verwenden, um das Produktportfolio dieser aufstrebenden industriell relevanten Zellfabrik zu erweitern. Sigma-70-abhängige Promoter-Bibliotheken wurden erstellt und in den einzelnen Genomlocus *attTn7* von *P. taiwanensis* VLB120 und *E. coli* TOP10 integriert. Jeder Promoter wurde mithilfe einer in dieser Arbeit entwickelten standardisierten Promoterstärkeinheit charakterisiert, die die gerätespezifische Fluoreszenzausgabe mit Fluorescein kalibriert und Unterschiede im Zellwachstum berücksichtigt. Diese Charakterisierungsstandards ermöglichen es, einen Einblick darüber zu gewinnen, wie sich ein bestimmter Promoter in jedem Organismus verhält und Sets von Promotern zu erstellen, die für metabolische engineering Zwecke relevant sind. Diese Arbeit konzentrierte sich auch auf die Bewertung einer optimierten Gene expression Architektur, um eine hohe Gene expression ohne Abhängigkeit von starken Promotoren zu erreichen. Dieses Modul erreichte eine hohe Gene expression in mehreren Expressionvektoren von zwei fluoreszierenden Reportergenen durch die Aufnahme von mRNA stabilisierenden und Translation verbessernden genetischen Teilen. Dieses Modul wurde auch angewendet, um die Produktivität eines kurzen Acetoin-pathway zu erhöhen und die Relevanz der mRNA Stabilität wurde durch qPCR-basierte mRNA Abbauraten bewiesen. Diese Werkzeuge waren ein Bestandteil in der Entwicklung einer *P. taiwanensis* VLB120 Propionyl-CoA Chassis-Stamm, um das Portfolio dieser Pseudomonade auf ungerade Kettenprodukte zu erweitern. Die erfolgreiche Aufnahme von Propionyl-CoA in den Stoffwechsel von *P. taiwanensis* VLB120 wurde durch die Produktion von Propionat bestätigt, nachdem die Löschung des Methylcitrat-Synthase als wichtiger Faktor identifiziert wurde. Der Propionat produzierende *P. taiwanensis* VLB120 wurde in Bioreaktor Fermentationsprozessen unter drei verschiedenen Fed-Batch-Strategien bewertet, um zu untersuchen, wie Fütterungsregime und Feast-Famine-Schaltungen die Produktion von propionyl-CoA abhängigen Produkten beeinflussen.

Summary

Zusammenfassend trägt diese Arbeit zur Entwicklung von *P. taiwanensis* VLB120 als aufstrebende industriell relevante Werkstatt bei, indem sie das verfügbare genetische Werkzeugkasten erweitert und den ersten Schritt zur Produktion ungerader Kettenprodukte in diesem Organismus setzt. Es trägt auch zur Standardisierung der genetischen Werkzeugcharakterisierung und der Querspezies-Studien bei, mit dem Ziel, die Identifizierung des am besten geeigneten Mikroorganismus für spezifische biotechnologische Anwendungen zu unterstützen und die Unabhängigkeit von fossilen Brennstoffen zu beschleunigen

List of Abbreviations

%	percent
#	number
°C	degree Celsius
μL	microliter
acpC	CoA transferase
AcCoA	acetyl-CoA
AckA	acetate kinase
Acr	acryloyl-CoA reductase
AcrCoA	acroyoyl-CoA
αCTD	α C-terminal domain of RNA polymerase
AFU	arbitrary fluorescence units
ALE	adaptive laboratory evolution
aldB	acetolactate decarboxylase
Asd	aspartate-semialdehyde dehydrogenase
Asp	Aspartate
AspAld	aspartate-semialdehyde
AspC	aspartate aminotransferase
AspP	aspartyl-phosphate
AtoAD	acetate CoA-transferase subunit BD
ATP	adenosine triphosphate
BCD	bicistronic design
BiTerm	bidirectional terminator
bp	base pairs
CEPI	confederation of european paper industries
CDW	cell dry weight
CimA	citramalate synthase
CO ₂	carbon dioxide
CoA	coenzyme A
CRISPR	clustered regularly interspaced short palindromic repeats
DIS	discriminator promoter region
DNA	deoxyribonucleic acid
DO	dissolved oxygen
<i>E. coli</i>	<i>Escherichia coli</i>
ED	Entner Doudoroff
EXT	extended -10 promoter element
<i>e.g.</i>	exempli gratia
EMP	Emden-Meyerhof-Parnas
FadA	3-ketoacyl-CoA thiolase
FadB	fatty acid oxidation complex subunit alpha
FadD	long chain fatty acid-CoA ligase
FadE	acyl-CoA dehydrogenase

List of abbreviations

FBA	flux balance analysis
g	gram
gDNA	genomic DNA
gmR	gentamycin resistance
GOI	gene of interest
h	hour(s)
HoSer	homoserine
HoSerP	homoserine-phosphate
H ₂ O	water
H ₂ SO ₄	sulfuric acid
3-HP	3-hydroxypropionate
3-HPCoA	3-hydroxypropionyl-CoA
3HPCD	3-hydroxypropionyl-CoA dehydratase
3HPCS	3-hydroxypropionyl-CoA synthase
HPLC	high-performance liquid chromatography
iAMB	Institute of Applied Microbiology
icIR	transcriptional repressor
ilvA	threonine dehydratase
ilvB	acetolactate synthase
IPCC	intergovernmental panel on climate change
IPTG	isopropyl β-D-1-thiogalactopyranoside
2-ketobut	2-ketobutyrate
K ₂ HPO ₄	dipotassium hydrogen phosphate
L	liter
LB	lysogeny broth
LB _{mod}	LB supplemented with glucose
log	logarithm
MalAld	malonic semialdehyde
MalCoA	malonyl-CoA
Mcr	malonyl-CoA reductase
MetL	aspartokinase/homoserine dehydrogenase
MFE	μmoles of fluorescein equivalents
mg	milligram
min	minutes
mL	milliliter
mm	millimeter
mM	millimolar
MmCoA	methylmalonyl-CoA
mRNA	messenger ribonucleic acid
<i>msfGFP</i>	monomeric superfolder green fluorescent protein
<i>mCherry</i>	monomeric red fluorescent proteins
MSM	mineral salt medium
Msr	malonic semialdehyde reductase

NADH	nicotinamide adenine dinucleotide (reduced)
NADPH	nicotinamide adenine dinucleotide phosphate (reduced)
NaH ₂ PO ₄	sodium dihydrogen phosphate
NCA	national climate assessment
nm	nanometer
NTG	N-methyl-N'-nitro-N-nitrosoguanidine
OD ₆₀₀	optical density at 600 nm
PHA	polyhydroxyalkanoates
<i>P. aeruginosa</i>	<i>Pseudomonas aeruginosa</i>
<i>P. putida</i>	<i>Pseudomonas putida</i>
<i>P. taiwanensis</i>	<i>Pseudomonas taiwanensis</i> VLB120
CO ₂	carbon dioxide
PCR	polymerase chain reaction
Pfk	6-phosphofructokinase
P _{ow}	partition coefficient between a 1:1 mixture of n-octanol and water
PPP	pentose phosphate pathway
Prop	propionate
PropCoA	propionyl-CoA
PropP	propionyl-phosphate
RBS	ribosome binding site
RiboZ	synthetic ribozyme
RNA	ribonucleic acid
rpm	revolutions per minute
rpoB	β subunit of bacterial RNA polymerase
rRNA	ribosomal ribonucleic acid
RWTH	Rheinisch-Westfälische Technische Hochschule
<i>S. cerevisiae</i>	<i>Saccharomyces cerevisiae</i>
sbm	sleeping beauty mutase operon
ScpA	methylmalonyl-CoA mutase
ScpB	methylmalonyl-CoA decarboxylase
sdhA	catalytic subunit of succinate-ubiquinone oxidoreductase
SPA	promoter library with randomized spacer region
Sp.	Species
SPL35/42	promoter libraries with randomized -35 and -10 boxes
SucCoA	succinyl-CoA
tetA	tetracycline resistance
ThrA	aspartokinase/homoserine dehydrogenase
ThrB	homoserine kinase
ThrC	threonine synthase
Threo	threonine
TSS	transcription start site
UP	upstream promoter element
USA	United States of America

List of abbreviations

USGCRP	united states global change research program
UTR	untranslated region
VtmoJ	synthetic ribozyme
v/v	volume per volume
w/v	weight per volume
WT	wildtype
yciA	acyl-CoA hydrolase

List of Figures

Figure 1- Interrelation of Carbon Dioxide levels in the atmosphere and Land-Ocean temperature index over the past decades [3]–[5].	3
Figure 2- Temperature anomalies of a model projected 30-year temperature average.	4
Figure 3- Percentage of greenhouse gas emissions by social and economic sectors by 2017 [37].	6
Figure 4. Structure of bacterial σ_{70} -dependent promoters and RNA polymerase interactions with promoter DNA.	31
Figure 5. Promoter library construction and characterization workflow.	32
Figure 6. Statistical overview of the mutational landscape of the promoter libraries.	34
Figure 7. Comparison of promoter ranking based on the performance indicators.	35
Figure 8. Overview of the expression strength of the three promoter libraries genomically integrated into A) <i>E. coli</i> TOP10 and B) <i>P. taiwanensis</i> VLB120.	35
Figure 9. Representation of nucleotide frequency deviation of quartiles Q1, Q2, and Q3-4 from mean nucleotide frequencies for <i>E. coli</i> and <i>P. taiwanensis</i> VLB120.	37
Figure 10. Performance comparison of the three promoter libraries SPA (blue), SPL42 (orange), and SPL35 (green) in <i>P. taiwanensis</i> VLB120 (Pt) and <i>E. coli</i> TOP10 (Ec).	38
Figure 11. The variance of the mean for normalized expression for all nucleotide positions for the spacer region (-29 to -13) of the SPA library between <i>E. coli</i> and <i>P. taiwanensis</i> VLB120.	39
Figure 12. Normalized average expression for each nucleotide at each position for the SPA library in <i>E. coli</i> (A) and <i>P. taiwanensis</i> VBL120 (B).	39
Figure 13. Gene expression cassette architectures represented with glyphs compliant with the Synthetic Biology Open Language Visual (SBOLv).	46
Figure 14. Gene expression constructs evaluated within this work.	48
Figure 15. Evaluation of the developed gene expression constructs.	49
Figure 16. Acetoin production pathway comprising the C83S ilvB mutant from <i>E. coli</i> and aldB from <i>Brevibacillus brevis</i> (A).	53
Figure 17. qPCR based elucidation of mRNA stability of <i>msfGFP</i> transcripts from the plasmid-based traditional (light-colored) and optimized (dark-colored) expression cassettes harboring the constitutive SPA75 promoter.	54
Figure 18. Strategies for propionyl-CoA production.	58
Figure 19. Specific propionate production by the propionyl-CoA chassis <i>P. taiwanensis</i> Tn7_sbm Δ PVLB_08385 expressing either the <i>yciA</i> or <i>aarC</i> in the pTN1 traditional (Tra) and optimized (Opt) variants using MSM _{B12} medium supplemented with 50 mM glucose with balanced amounts of nitrogen (bal.; C:N ratio of 6) or limited nitrogen content (lim.; C:N of 12).	62
Figure 20. Representative fermentation profiles of the three evaluated fed-batch modes, DO triggered addition of 25 mM of glucose with a (A) 50 mM of initial glucose and (B) with 100 mM of initial glucose concentration and, (C) feedback-loop controlled fed-batch maintaining a constant glucose concentration of 25 mM.	64

List of Figures

Figure 21. FACS distribution of the promoter libraries templates BG42 (SynPro 42) and BG35 (SynPro 35) and the three generated promoter libraries SPL35, SPL42 and SPA expressed in the pTn7 plasmid in <i>E. coli</i> PIR2.	77
Figure 22. Nucleotide abundances in the promoter libraries SPL35 and SPL42 in <i>P. taiwanensis</i> VLB120.	80
Figure 23. Specific GFP production rate quartiles of the SPA promoter library in <i>P. taiwanensis</i> VLB120.	81
Figure 24. Evaluation of the developed inducible gene expression constructs under induced (dark blue) and non-induced (light blue) conditions.	82
Figure 25. Time course of mRNA abundance of the <i>msfGFP</i> gene normalized with the transcript level of the housekeeping gene <i>rpoB</i> for the traditional (A) and the optimized expression cassette (B).82	

List of Tables

Table 1. Timeline of the evolution of the scientific evidence supporting the contribution of carbon emissions towards global warming and the most recent measures taken to tackle this threat..	5
Table 2. Bacterial strains used in this study.	19
Table 3. The number of clones at each step of the integration workflow for each library.	33
Table 4. Pairwise fold-changes of specific fluorescence (fluorescence per g cell dry weight) between the optimized and traditional gene expression cassettes.....	50
Table 5. Theoretical yields of propionate production from glucose for the three alternative propionyl-CoA pathways expressed in <i>P. taiwanensis</i> VLB120.	59
Table 6. Propionyl-CoA levels in constructed strains.	60
Table 7. Comparison of yields, productivities, and glucose uptake rates of the <i>P. taiwanensis</i> VLB120 propionate production strain during the three evaluated fed-batch strategies.	65
Table 8. Sequence and characterization of each promoter in <i>E. coli</i> TOP10 and <i>P. taiwanensis</i> VLB120.78	
Table 9. Inter-species promoter sets containing promoters with similar and opposite expression strength in <i>E. coli</i> and <i>P. taiwanensis</i> VLB120.	81

Chapter 1

General introduction

Contributions

This chapter was written by Dário Neves and reviewed by Lars M. Blank.

1. General Introduction

1.1. Towards a circular bioeconomy based on renewable carbon

1.1.1. Climate Change and the urge for a circular bioeconomy

The topic of Climate change has matured over the past decades as a possible concern in the distant future, mainly defended by environmentalists, to an imminent major threat to human society and organic life now acknowledged by the United Nations. Climate change, defined as a long-term change in the average weather patterns, observed in the past decades has been linked with a 95% probability to human activities in the Fifth Assessment Report of the Intergovernmental Panel on Climate Change (IPPC) [1]. Such Climate Change is directly related to global warming resulting from a human expansion of the greenhouse effect, warming resulting from the entrapment of the radiating heat leaving from Earth. Gases that contribute to the greenhouse effect and which are produced by human activity are mainly, nitrous oxide (N_2O), methane (CH_4), and carbon dioxide (CO_2). Nitrous oxide is a powerful greenhouse gas arising from commercial and organic fertilizers, fossil fuel combustion, nitric acid production, and biomass burning. Methane, on the other hand, is produced in landfills through the decomposition of wastes, agriculture (especially rice cultivation), and domestic livestock, and, on a molecular base, methane entraps 25 times more heat than a carbon dioxide molecule [2]. Carbon dioxide is released through natural events, such as respiration and volcanic activity but also through human activities such as deforestation and the combustion of fossil fuels. Since the Industrial Revolution, the CO_2 concentration in the atmosphere increased by 47% and is one of the main driving forces for the incremental temperature increase of the atmosphere and consequent climate change (Figure 1) [3]–[5].

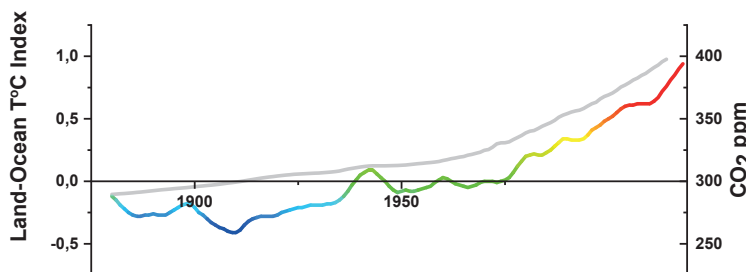


Figure 1- Interrelation of Carbon Dioxide levels in the atmosphere and Land-Ocean temperature index over the past decades [3]–[5].

The increase of the Land-Ocean temperature index, which indicates the global temperature increase on land and water bodies, has led to undeniable consequences to the diverse planetary habitats. Evidence of these consequences is the continued shrinking of ice sheets, as recorded by NASA's Gravity Recovery and Climate Experiment which shows an average yearly loss of 279 billion tons of ice in Greenland since 1993 while Antarctica lost around 148 billion tons of ice per year, the global Sea level rise, which rose 20 centimeters in the last century or the increase of extreme weather events [6]–[8].

The temperature rise in a future scenario in which no global environmental concerns are emphasized and future social-economic development is accompanied by higher greenhouse gas emissions (scenario B in Figure 2) can reach a maximum of 8°C as extrapolated by the National Climate Assessment (NCA) from the U.S. Global Change Research Program (USGCRP) [9]. In this scenario, the temperature rise would lead to a decrease of precipitation volumes during spring times in the western part of the USA of up to 25%, accompanied by a respective increase of rain in Antarctica and northern Canada. The precipitation anomalies would lead to a decrease in soil moisture, which would increase the probability of a megadrought, a drought lasting more than three decades, from the current 12% to 80% [10]–[12].

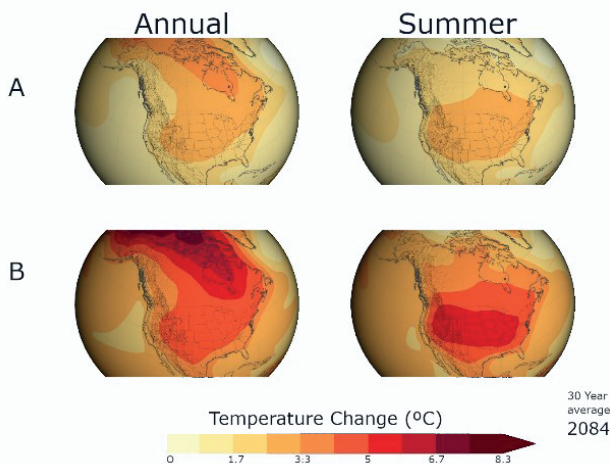
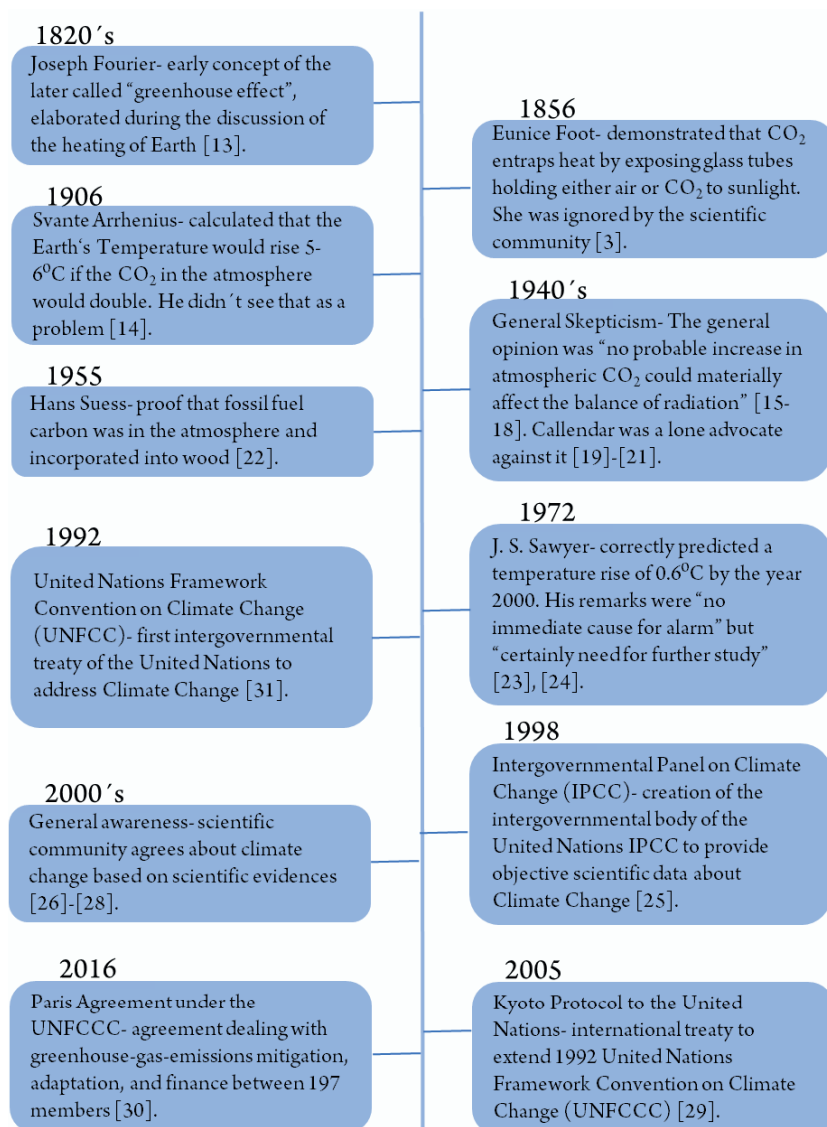


Figure 2- Temperature anomalies of a model projected 30-year temperature average. of scenario A (lower greenhouse emissions) and scenario B (higher greenhouse emissions) with the 1970-1999 average. Adapted from [9]. On the other hand, if greenhouse gas emissions are tackled and efforts to a carbon-neutral economy are put in place the temperature rise would be halted which would diminish the effects of climate change (scenario A in Figure 2).

The topic of climate change might seem to only have arisen during the last decade, however, the early concept of the Greenhouse effect was postulated in the 1820s by Joseph Fourier and since then several warnings have been sent by the scientific community about the negative effect of fossil fuel combustion on large scale. A summary of the warnings and evolution of the scientific evidence supporting the contribution of carbon emissions towards global warming is summarized in Table 1.

Table 1. Timeline of the evolution of the scientific evidence supporting the contribution of carbon emissions towards global warming and the most recent measures taken to tackle this threat.



Public awareness of climate change did increase over the past years but still encompasses a percentage of indifferent or non-believers [32]–[35]. On an intergovernmental level, the threat of climate change is taken as a high-priority concern and discussions emphasize which steps are necessary to halt its effects. The necessary steps to combat climate change can be crystalized

into two approaches: adaptation and mitigation [36]. Adaptation encompasses all actions to reduce the susceptibility to the harmful consequences of climate change, like sea-level rise, extreme weather episodes, and food insecurity, but also encloses taking advantage of beneficial opportunities, such as harnessing the energy of stronger winds or longer growing seasons which could lead to increased yields. Simultaneously, mitigation efforts should be made to halt climate change by reducing the number of greenhouse gases in the atmosphere arising from the combustion of fossil fuels or by enhancing the natural resources which capture the heat-trapping gases.

Mitigation efforts cannot only rely on stopping the use of fossil fuels but also need to present sustainable alternatives which maintain the social requirements. Almost all relevant social and economic sectors are heavily dependent on fossil fuels and greenhouse gas emissions (Figure 3).

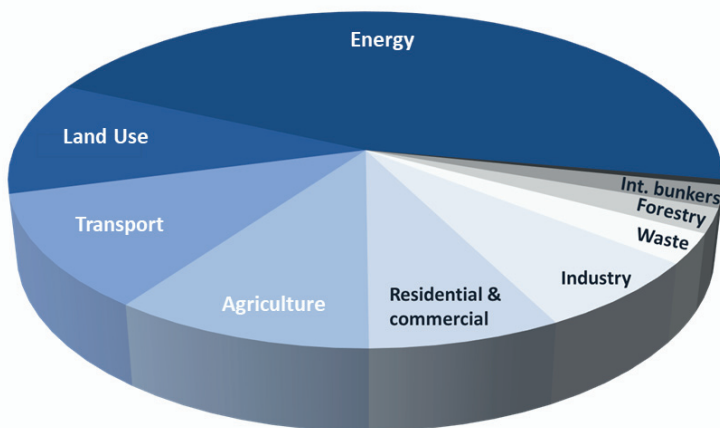


Figure 3- Percentage of greenhouse gas emissions by social and economic sectors by 2017 [37].

For societal sectors, which mainly require the combustion of fossil fuels, like energy and transport, the carbon-neutral alternatives mainly focus on using sustainable energy sources like solar, wind, hydro, tidal, geothermal, and biomass energy. To tackle the greenhouse gas emissions emitted in agriculture the solutions focus more on adopting a plant-rich diet and avoiding especially bovine meat since it is one of the major methane sources. Other solutions, which are not directly related to greenhouse gas emissions but still have an impact on climate change, are the adoption of vertical farms or the use of insect-based protein to reduce the required farm areas, water and energy requirements and, optimize the crop productivities.

Fossil resources are also used to retrieve all the chemicals and molecules required to produce daily used products. The usage and processing of these fossil resources are based on a take-make-waste extractive industrial model which frames a linear economy. Such a linear economy leads to major amounts of waste which end up in the environment disrupting the habitats and contributing to climate change. The global population is predicted to increase to 9.7 billion by 2050, leading to a further increase in energy and resource demands on a finite-resource planet, making it necessary to find a sustainable alternative [38]. A sustainable alternative is the so-called

circular economy which entails the decoupling of economic activity from the consumption of finite resources and where regeneration is key [39]. The circular economy model holds two types of cycles, biological and technical. The biological cycle engulfs consumption products like food and biologically based materials which are after consumption fed back into the system through fermentation, composting, or anaerobic digestion. Technical cycles hold materials that can be recovered by strategies based on reuse, repair, remanufacture, or recycling. The circular economy strategy was embraced by the European Commission through its action plan ‘Closing the loop’ in 2015 which emphasized ‘The transition to a more circular economy, where the value of products, materials, and resources is maintained in the economy for as long as possible, and the generation of waste minimized, is an essential contribution to the EU's efforts to develop a sustainable, low carbon, resource efficient and competitive economy’.

1.1.2. Integration of bioeconomy and circular economy- the concept of a circular bioeconomy

The circular economy concept focuses on maintaining the value of products, materials, and resources for as much as possible in the economy and thus reducing the amount of waste, but it does not emphasize the generation of new renewable resources or the exploration of alternative raw material sources to fossil-based ones.

A sector that aims for the obtention of raw materials sustainably is the so-called bioeconomy which pursues to substitute fossil carbon with renewable biomass carbon arising from agriculture, forestry, and marine sources. Bioeconomy and circular economy are different but complementary approaches that share the common traits of attempting to improve resource and eco-efficiency, lowering the greenhouse gas footprint, reducing the dependency on fossil carbon, and valorizing waste [40]. Rather than focusing on recycling and reuse approaches, bioeconomy handles product or service functionality such as new chemical building blocks, processing routes, and, the identification of new functionalities and properties of products. Bioeconomy activities can be categorized into the direct exploitation of biological resources (such as the primary sectors of agriculture, fishery, and forestry), the further processing of biomass (like food or wood processing), or novel activities that process biomass and biomass residues into bioenergy or bio-based chemicals [41]. Examples of how these goals are achieved are precision and vertical farming allied to gene editing for efficient agriculture and forestry developments, new processing pathways with lower toxicities and reduced use of harsh chemicals, biotechnology to produce sustainable bulk and fine chemicals, and, healthier and nature-compatible bio-based products [40]. In the past decade the bioeconomy concept has been on the policy agenda on a global scale, such as the National Bioeconomy Blueprint from the United States of America, the European Green Deal, and European Bio-Based Industries Joint Undertaking, or the implementation of bioeconomy in the growth strategies of emerging economies [42]–[45].

However, bioeconomy and circular economy are per se not necessarily sustainable and require a symbiosis between the two, the circular bioeconomy, to come closer to that end. For instance, biobased products should not harm the ecosystem nor incite the linear economy model whereas the circular economy should reduce its dependency on fossil resources. The definition of circular bioeconomy can be crystallized into an economy mainly fueled by bio-based products with properties to be able to be reused, remanufactured, or recycled to foment a cascading use until the greenhouse gas emissions required for the cycling are lower than the ones to produce virgin

bio-based products [40], [46]. The concept of circular bioeconomy is already adopted and promoted by industrial associations such as CEPI (Confederation of European Paper Industries) and EuropaBio (The European Association for Bioindustries) [47], [48].

However, certain regulatory challenges are still in place which hinders the development of a circular bioeconomy. From a European perspective, several regulatory blocks are still present such as the heavy regulation on the use of CRISPR/Cas technologies for plant breeding (in contrast to the United States Department of Agriculture that since 2018 does not regulate genome-edited plants if they could have been developed through traditional breeding), the longer and more expensive approval of new products and the tendency for a court ruling on a process-based approach rather than the regulation of the resulting product as it is followed by other nations [49]–[52].

Despite these hindrances for a circular bioeconomy, several indicators show that relevant steps are being taken to reach this goal. One indicator is the increase in public and private investment in biotechnology, more specifically in cell factories and synthetic biology. Cell factories and synthetic biology play a crucial role in the challenge to reduce the dependency on fossil fuels since they allow the obtention of a wide spectrum of chemicals ranging from fine and bulk chemicals to bioactive molecules from renewable sources. The development of cell factories and respective synthetic biology tools will be discussed in this work.

1.2. Cell factories and their development

Modern society is only able to thrive on the base of materials and chemicals that fulfill all its demands. These chemicals and materials have until recently either been directly extracted or converted from unrenewable sources. As discussed in the previous section, the need for a sustainable alternative is urgent since the foundations that made modern society thrive might become the same which will make it crumble. Biologically sustainable alternatives are already present as shown by the estimation of Carlson that 25% of the chemicals produced in the USA are biologically based [53], [54]. Microbial cell factories harness the capability of obtaining most of these materials and chemicals from renewable feedstocks and further contribute to the increase of this percentage [55]. One successful example is the industrial applicable bio-based production of 1,3-propanediol in *E. coli* with a titer of 135 g/L requiring 42% less energy consumption and 56% fewer greenhouse gas releases than the respective fossil fuel alternative [56]. However, being proven that these chemicals can be produced at large scale by cell factories, the strain development pipeline to reach capabilities for industrial scale production still requires further breakthroughs. For some target chemicals, it is possible to find natural producers which do not require extensive engineering to achieve industrial-relevant production levels since they already possess high tolerance and robust metabolic fluxes towards the target product. Some examples are *Mannheimia succiniciproducens* for succinic acid, *Corynebacterium glutamicum* for amino acids; *Clostridium* sp. for butanol, and *Yarrowia lipolytica* for oleochemicals [57]. Rational approaches to boost the production of native metabolites can be summarized into the following strategies: a) pathway overexpression: this strategy encompasses the increase of activity by either overexpressing the biosynthetic activity or engineering the enzymes to have higher specific activities. One example is the improved production of ganoderic acid in *Ganoderma lucidum* [58]; b) transporter engineering: product yields can be affected by the intracellular accumulation of

product due to interferences in enzyme kinetics, feedback inhibition or cellular toxicity making the overexpression of efflux pumps a very important strategy for improved productivities as shown by Dunlop et al for the production of biofuels in *E. coli* [59]; c) de-branching: branching or competing pathways tend to reduce productivities due to decreased carbon flux towards the product. Deletion of non-lethal competing pathways or decreasing the activity of lethal knockouts by knockdown, tunable promoters, or mRNA silencing is a common approach in metabolic engineering and a rather relevant one as shown for isoleucine production in *E. coli* [60]; d) product degradation: the arguably most intuitive strategy from the ones described here is the deletion of non-essential reactions which consume the desired product being one example the deletion of threonine dehydrogenase for the production of L-threonine [61]; e) co-factor engineering: in biosynthetic pathways were intermediate steps require co-factors (NADH/NAD⁺, NADPH₂, NADP⁺, acetyl-CoA, etc.) their limitation can become the bottleneck for enhanced productivities [62], [63]. To overcome this bottleneck two strategies that can be followed to increase the available amount of co-factors are deleting non-essential enzymes which consume the required co-factor or replacing enzymes with ones that have an alternative co-factor dependency. Some successful examples of co-factor engineering are the substitution by an enzyme with an alternative co-factor requirement for sesquiterpene production [64] or in the specific case of NADH and NADPH the overexpression of an *E. coli* transhydrogenase for interconversion of these co-factors [65]; f) removal of feedback inhibition: some biosynthetic pathways are tightly regulated by feedback inhibition, for example, amino acids, which hampers the possibility to achieve desired high carbon fluxes. Random or targeted mutagenesis of feedback-inhibited enzymes allied to screening methodologies based on irreversible binding analogs of the product do sometimes allow to find variants that lost this property as shown for the production of different amino acids in *E. coli* [66]–[68]; g) de-regulation of carbon catabolism: some of the required biosynthetic pathways for a given product are under the control of general metabolic regulators which hamper the possibility to achieve higher fluxes. Disruption of such global regulators has been reported to lead to higher productivity as shown for ethanol production in *Pichia guilliermondii* [69] the last strategy is the signal transduction engineering in which the production is not regulated by carbon or nitrogen sources but by micronutrients or other steps within the pathway which once engineered can retrieve higher productivities [70].

For the majority of the desired target molecules, however, no natural producers can be found, or have been found yet, imposing the introduction of heterologous pathways to well-known organisms and further engineer them to achieve industrial-relevant production levels. One example of a successful heterologous expression in non-native producing strains with further strain engineering is the production of astaxanthin in *E. coli*, an antioxidant molecule with pharmaceutical and cosmetic applications, in which the *crt* and *trC* operons from *Pantoea ananitis* and *Chlamydomonas reinhardtii* where respectively introduced and further engineered with signal and solubility tags to improve their expression. Besides the heterologous pathway expression, the native methylerythritol phosphate pathway metabolism was engineered based on *in silico* metabolic flux analysis leading to the production of 430 mg/L in fed-batch fermentation. [71]. Furthermore, for some of the required molecules, no natural pathways have been found yet, and therefore non-natural occurring enzymatic activities have to be generated, or novel synthetic pathways have to be assembled. Due to the combinatorial complexity of pathway assembly and

the growing amount of known enzymatic reactions, computational model-based pathway assembly has been used to explore this vast potential for novel metabolic pathways of products. Several prediction tools have been developed like BNICE, DESHARRY, RetroRules, RetroPath, GEM-Path, or SimPheny and, despite the peculiarities of each, most are based on generalized reaction rules and enzymatic reaction databases exploration. Successful examples of how these prediction tools lead to the production of compounds that are not naturally produced are the conversion of syngas to monoethylene glycol based on BNICE analysis or the identification of a novel biosynthetic pathway using the SimPheny BioPathway Predictor for the synthesis of 1,4-butanediol [72], [73]. In the example of the production of 1,4-butanediol, another type of model-driven cell factory engineering principle was applied which consists of Flux Balance Analysis (FBA) of genome-scale reconstructions of metabolic networks. These models allow to identify possible flux bottlenecks in the pathway and suggest knockouts to increase the productivity of the desired target compound. In the example of 1,4-butanediol, several knockout targets were identified through OptKnock simulations, and once these were applied a final production of 18 g/L of 1,4-butanediol was achieved [72], which was further commercialized by Genomatica (USA). Another example of FBA-driven knockout identification, which leads to a relevant increase of production titers is the synthesis of methyl ketones by *Pseudomonas taiwanensis* VLB120 [74]. The above-mentioned engineering strategies for improving natural producers are also applicable to cell factories that rely on heterologous pathways. Further required strategies for heterologous pathway expression aim to allocate the enzymes to the proper cellular compartment and transcription engineering to assure that the genes are properly expressed in the selected host.

The previously described rational approaches to engineer cell factories are sometimes not applicable for some target molecules due to a lack of prior knowledge between genotype and phenotype. In such cases, resorting to evolutionary engineering is a resourceful alternative since it explores either the natural capabilities of cells to adapt to their environment or the potential of mutagenesis. Two disciplines can be delineated in evolutionary engineering, directed evolution and adaptive laboratory evolution (ALE). Directed evolution is initiated with mutagenesis of proteins or cells to create mutants which are further screened for the desired traits. In the protein engineering realm, it is an important approach to achieve enhanced catalytic activities, desired substrate/product specificity, and protein stability which might be further integrated into cell factories, whereas directed evolution of cells by chemical and/or physical mutagenic treatments allows the identification of mutants with higher resistance levels towards chemicals, higher productivities or enhanced growth on specific carbon sources [75]. The keystone of the directed evolution cycle is the screening methodology to identify the beneficial variants, which can be further mutagenized until the desired trait is reached. Examples of successfully directed evolution workflows are the doubling of L-arginine production titers in *C. glutamicum* after an N-methyl-N-nitro-N'-nitroguanidine (NTG) and ultraviolet treatment or the evolution of cytochrome C from *Rhodothermus marinus* to produce chiral organoboranes on a gram-scale through whole cell biosynthesis [76], [77]. The second discipline, ALE, does not rely on forced mutagenesis as in directed evolution but rather on natural mutagenic rates during cell growth under the conditions which are targeted. ALE is a powerful application to increase growth efficiency on specific carbon sources or adaptation to either external toxic compounds or self-produced metabolic by-products. In both cases, the cells are grown in the presence of these

compounds and re-inoculated until the growth rate achieves a defined threshold. For the increase of resistance levels towards toxic compounds, once the growth rate threshold is achieved the concentration of the toxic compound is increased and further adaptation cycles are performed. Once the desired growth rates are achieved in both application cases, substrate adaptation and resistance acquirement, cells are harvested and sequenced to identify the genetic modifications which lead to the phenotypic upgrade. Examples of increased growth efficiency achieved through ALE are the increased growth of *E. coli* with glycerol, glucose, and citrate or the metabolization of ethylene glycol by *P. umsongensis* GO16 as the sole carbon source, a major step in the upcycle of post-consumer polyethylene terephthalate to medium chain-length polyhydroxyalkanoates (PHA) and a novel bio-based polyamide urethane (bio-PU) [78]–[81]. Successful examples of *E. coli* ALE to toxic compounds are the adaptation to ethanol, iso- and n-butanol, and ionic liquids [82]–[84].

All the so far mentioned approaches to improve cell factories are powerful synthetic biology tools that could allow modern society to obtain most of the required chemicals from renewable sources using microorganisms.

The awareness of the potential of synthetic biology for cell factory development such as for other sectors like diagnostics and healthcare has already been translated to an increase in small and medium enterprises and has also gained interest from investors [85], [86]. In 2018, SYNBIOCHEM, the University of Manchester-based SBRC, summarized guidelines for the development of materials using synthetic biology showing the growing potential and interest in this field [87].

1.3. *Pseudomonas taiwanensis* VLB120 as a cell factory

Microorganisms have been used by humans for several millennia as catalysts to produce bioactive molecules, way before the existence of unicellular organisms was even known to mankind. The use of yeast to modify food and beverages has been over the past millennia the major fermentative process to occur on earth and its leading position is enforced by the use of these fungi to produce bioethanol, the most important biomolecule by mass of annual production [88]. The designation of microorganisms as cell factories for biotechnological use to produce diverse molecules and materials has only been coined in the 1990s with its adoption as a Key Action in the 5th Framework Programme of the European Union [89]. This boosted the interest in biotechnological processes for the biomanufacturing of molecules and materials using mainly model organisms such as *E. coli* and *S. cerevisiae* [90]. The designation of *E. coli* and *S. cerevisiae* as model organisms have emerged due to their recurrent use which increased the understanding of their metabolism and further developed their respective genetic toolboxes. However, the interest in alternative organisms harboring biotechnological advantageous traits has been increasing since the development of genetic tools for these organisms has been facilitated by the CRISPR/Cas system such as the increased amount of annotated genomes [91]–[95]. Some of the most promising microorganisms harboring unique traits are *Acinetobacter baylyi*, due to their natural competence for synthetic biology, *Shewanella* species for their electro-active properties, *Vibrio natriegens* for its rapid-growth properties, *Halomonas* for its ability to grow in saline media under non-sterile conditions and, the species on which this work

will focus on, *Pseudomonas* for their stress-resistant properties that can be exploited for the production of new-to-nature products [96]–[100].

Pseudomonads are Gram-negative, rod-shaped bacteria belonging to the class of Gammaproteobacteria usually featuring fast growth, low production of by-products, and low nutritional demand [101]. These soil-dwelling bacteria are usually found in challenging ecosystems which bolster the evolution of complex genetic repertoire granting them for example the capability to degrade toxic xenobiotic aromatics like benzene, toluene, styrene, and phenol [102], [103]. Besides the ability to degrade toxic compounds, this genus has also been used for the synthesis of bulk and fine chemicals like aliphatic alcohols [104], prodiginines [105], polyhydroxyalkanoate (PHA), polyesters [106], rhamnolipids [107], and methyl ketones [74].

The *Pseudomonas* strain on which this work focuses on is *Pseudomonas taiwanensis* VLB120, a strictly aerobic gram-negative bacterium isolated as a styrene degrader in a German forest and with its genome being sequenced in 2013 [108]. This non-pathogenic bacterium, with a safety level 1 status, harbors several industrial-relevant traits since it can grow on D-xylose via the Weimberg pathway and shows an inherent tolerance towards inhibitors from biomass hydrolysates [109], [110]. Besides its industrial applicability for cellulosic feedstocks, this strain has metabolic peculiarities which broaden its industrial relevance. This strain does not contain the gene encoding the 6-phosphofructokinase (Pfk) in its genome, which halts the glycolytic compounds to be catabolized via the Emden-Meyerhof-Parnas (EMP) route but mainly diverts them to the Entner-Doudoroff (ED) pathway and to a minor extent to the pentose phosphate pathway (PPP). This peculiarity results in a lower ATP generation but allows higher reduction rates of NADP⁺ by the partial recycling of triose-phosphates [111]. The lower ATP generation rate and also the necessity for even higher reduction rates of NADP⁺ have been shown in a phylogenetical proximal strain, *Pseudomonas putida* KT2440, to be satisfied with an increased carbon source uptake rate [112]. This higher reducing power grants the strain a tolerance towards oxidative stress and fitness for redox-intensive pathways [113], [114]. It was also shown that NADH-dependent processes can also profit from this high NADPH regeneration through the activity of pyridine nucleotide transhydrogenases [115]. Besides the glycolytic metabolic peculiarity, *P. taiwanensis* VLB120 also contains mechanisms that confer resistance towards solvents with a logP_{o/w} (the logarithmic partition coefficient in a 1:1 mixture of octanol and water) between 2.11 (toluol and styrene) and 4, which is generally linked to cytotoxicity since the solubility of these molecules allows direct contact with the cellular membrane [116]–[120]. One of the mechanisms which grant the solvent-resistant phenotype to this strain is the expression of resistance-nodulation-cell division (RND)-type efflux pumps (TtgGHI localized on the pSTY megaplasmid) which are driven by proton motive force to expel solvents from the cytoplasm [108], [121]. A second mechanism that contributes to the solvent-resistant phenotype of this strain is the ability to reduce the membrane fluidity by enforcing a denser lipid packing. This denser lipid packing is achieved by changing the unsaturated fatty acids in the membrane from *cis* to *trans*, by incorporating saturated fatty acids in the membrane, and by changing the phospholipid hydrophilic group [122]–[124].

1.4. Scope and outline of the thesis

This work aimed to further develop *Pseudomonas taiwanensis* VLB120 as a cell factory by further expanding the genetic tools portfolio of this strain for heterologous gene expression and providing an insight into how certain genetic parts function in this organism and the model organism *E. coli*. Besides the insight into the genetic tools of this strain, emphasis was laid on the creation of a chassis strain to expand the possible product range of this strain.

Chapter 3.1 focuses on the creation of a σ_{70} promoter library expressing the reporter gene *msfGFP* which was further integrated as a single copy into the genome of *P. taiwanensis* VLB120 and *E. coli* TOP10. The promoter library was further characterized in both organisms through online measurements of cellular density and fluorescence during exponential growth. The performance of each promoter in both organisms was described by a specific *msfGFP* expression rate in which the specific growth rate was considered. This allowed insight into how specific genetic parts behave between these two organisms.

Chapter 3.2 describes the evaluation of a previously proposed optimized gene expression architecture to achieve higher gene expression by focusing on mRNA stability and translation initiation rather than reaching high gene expression using strong promoters. This optimized gene expression architecture was tested on a plasmid basis and after single genomic integration using different promoters and reporter genes to evaluate the applicability of this optimized gene expression architecture in different scenarios.

Chapter 3.3 aims to extend the acyl-CoA product portfolio of *Pseudomonas taiwanensis* VLB120 to odd-chain products by enabling the production of propionyl-CoA. Propionyl-CoA production was enabled by expressing the sleeping beauty mutase operon from *E. coli* as a single integration copy. Assessment of this propionyl-CoA chassis strain for odd-chain products was done by expressing an acyl-CoA hydrolase enabling the synthesis of propionate. Fermentation strategies were evaluated during bioreactor fermentations to evaluate further the potential of this strain for the synthesis of odd-chain products.

The achievements and outcomes of the above-mentioned chapters are discussed in chapter 4 and debated from a broader perspective.

Chapter 2

Materials and methods

Partially published as

D. Neves, U. Liebal, S. C. Nies, T. B. Alter, C. Pitzler, L. M. Blank and B. E. Ebert, "Cross-species synthetic promoter library: finding common ground between *Pseudo-monas taiwanensis* VLB120 and *Escherichia coli*." *ACS Syn. Bio.*, 2023, doi: 10.1021/acssynbio.3c00084

D. Neves, S. Vos, L. M. Blank, and B. E. Ebert, "Pseudomonas mRNA 2.0: Boosting Gene Expression Through Enhanced mRNA Stability and Translational Efficiency," *Front. Bioeng. Biotechnol.*, 2020, doi: 10.3389/fbioe.2019.00458.

D. Neves, D. Meinen, T. B. Alter, L. M. Blank and B. E. Ebert, "Expanding *Pseudomonas taiwanensis* VLB120's acyl-CoA portfolio: propionate production in mineral salt medium." *Microb. Biotechnol.*, 2023. doi: 10.1111/1751-7915.14309

Contributions

This chapter was written by Dário Neves. The growth rate determination part was written by Tobias Alter. The sequence statistics part was written by Ulf Liebal. This chapter was reviewed by Lars M. Blank and Birgitta Ebert.

2. Material and methods

2.1. Media and culture conditions

Strains used and constructed during this work can be found in Table 2. Liquid cultures were grown in a horizontal rotary shaker with a shaking frequency of 200 rpm and a throw of 50 mm in LB medium or LB medium supplemented with 5 g/L glucose and buffered with 11.64 g/L K_2HPO_4 and 4.89 g/L NaH_2PO_4 (LBmod). *Pseudomonas* strains were grown at 30°C, whereas *E. coli* was grown at 37°C. Solid LB was prepared by adding 1.5 % (w/v) agar to the medium. Antibiotics were supplemented to the medium for plasmid maintenance and selection purposes. Kanamycin sulfate was added at a concentration of 50 mg/L for *Pseudomonas* and *E. coli*. Gentamycin was used at a concentration of 25 mg/L for both species. Tetracycline was added only to solid media at a concentration of 30 mg/L for *Pseudomonas* and 10 mg/L for *E. coli*. To induce the pTN1-derived plasmids harboring the *nagR/P_{nagAa}* promoter system controlling the expression of the fluorescent proteins or the acetoin pathway, 0.01 mM or 1 mM of sodium salicylate was added, respectively. The inducer isopropyl- β -D-1 thiogalactopyranoside (IPTG) was used at a concentration of 1 mM to induce the P_{trc}-controlled constructs integrated into the *attTn7* site of *Pseudomonas* strains.

Precultures for the fluorescence measurements of *Pseudomonas* were performed in 96-well plates whereas *E. coli* was propagated in 15 mL glass. The online-fluorescence measurements for either the promoter characterization or optimized expression cassette evaluation were performed on cultures in continuous shaken 96-well microtiter plates (μ clear-bottom, Greiner bio one) sealed with a gas-permeable sealing foil (Greiner Bio One) in LB medium w/o antibiotics in the Biolector (m2p-labs, Baesweiler, Germany). Plates were incubated at 900 rpm and a shaking diameter of 3 mm. Cell density measurements were retrieved at 620 nm with a gain of 30; fluorescence was excited at 488 nm and read at 520 nm with a gain of 70. Both outputs were measured every 15 minutes until the stationary phase was reached.

The acetoin-producing strains evaluated w/o the optimized expression cassette were cultivated in airtight 500 mL serum flasks containing 50 mL of LBmod supplemented with gentamycin (see above). The main cultures were inoculated from an overnight pre-culture to an OD₆₀₀ of 0.1. The plasmid-based acetoin pathway genes were induced with sodium salicylate once the cultures reached an OD₆₀₀ of 1. Afterwards, samples were collected for HPLC analysis.

The propionate production experiments were performed in mineral salt medium according to Hartmans et al. in triple buffered conditions (11.64 g/L K_2HPO_4 and 4.89 g/L NaH_2PO_4) supplemented with 0.22 μ M vitamin B12 (MSM_{B12}), which was required to observe the activity of ScpA and, required antibiotics [125]. For the screening of *yciA* and *arrC* constructs for propionate production, 50 mM Glucose was added to the MSM_{B12}. The main cultures were inoculated from an overnight pre-culture in mineral salt medium to an OD₆₀₀ of 0.1. The expression constructs were induced with sodium salicylate once the cultures reached an OD₆₀₀ of 1. Samples were collected for HPLC analysis at regular time points after induction.

The chemicals used were purchased from Merck (Darmstadt, Germany), Sigma-Aldrich (St. Louis, MO, USA), or Carl Roth (Karlsruhe, Germany) unless stated otherwise. Pharmaceutical-grade glycerol was kindly provided by Bioetol (Kyritz, Germany).

2.2. Plasmid and Strain Construction

All plasmids were constructed through Gibson assembly[126] using the NEBuilder HiFi DNA Assembly kit (New England Biolabs, Ipswich, MA, USA). Primers used in this work were purchased from Eurofins Genomics (Ebersberg, Germany) as unmodified DNA oligonucleotides. PCR amplification of DNA for cloning purposes was performed using the Q5 High-Fidelity Polymerase (New England Biolabs, Ipswich, MA, USA). The *sbm* operon from *E. coli* K-12 MG1655 was amplified from genomic DNA and assembled into the mini-Tn7 vector backbone together with the *nagR/P_{nagAa}* promoter system and the tetracycline resistance cassette. The genes *ilvB* (from *E. coli* K-12 MG1655, Uniprot P08142, with C83S mutation for improved kcat/Km), *aldB* (from *B. brevis*, Uniprot P23616), *yciA* gene from *H. influenzae* (UniProt P44886) and *aarC* from *P. shermanii* (UniProt A0A160VKNK6) were codon-optimized for *P. taiwanensis* VLB120 using the online tool OPTIMIZER [127]. Settings were as follows: genetic code, eubacterial; method, guided random; undesired restriction sites were manually excluded, and rare codons with <6% usage were avoided by manipulating the input codon usage table. Both codon-optimized genes and their corresponding optimized gene expression parts were ordered as synthetic DNA fragments from Thermo Fisher Scientific. The assembled plasmids were transformed into either NEB® 5-alpha chemically competent *E. coli* (New England Biolabs, Ipswich, MA, USA) or One Shot™ PIR2 Chemically Competent *E. coli* (Thermo Fisher Scientific) cells through heat shock according to the supplier's protocol. Assembled plasmids were transformed into *P. taiwanensis* VLB120 by electroporation using a GenePulser Xcell (BioRad, Hercules, CA, USA) (settings: 2 mm cuvette gap, 2.5 kV, 200 Ω , 25 μ F). For DNA integration into the *attTn7* locus, the mini-Tn7 delivery vector backbone developed by Zobel et al.[128] was used and deployed through mating procedures. For mating events, the *E. coli* donor harboring the mini-Tn7 vector with the constructs to be integrated, the helper strain *E. coli* HB101 pRK2013, the *E. coli* DH5 λ pir expressing the transpose operon *tnsABCD* and the recipient strain were streaked on top of each other on an LB agar plate and incubated at 30°C for 12–24 h. Further on, cell material was taken from the bacterial lawn, resuspended in 0.9% (w/v) sodium chloride solution, and plated on selective ceftrimide agar plates. *E. coli* and *Pseudomonas* transformants were screened through colony PCR using the OneTaq 2xMaster Mix with standard buffer after lysing colony cell material in alkaline polyethylene glycol, as described by Chomczynski and Rymaszewski[129]. Gene deletion of Δ PVLB_08385 was based on the I-SceI-based method developed by Martinez-Garcia et al.[130] with an adapted protocol by Wynands et al. [131]. Successful plasmid constructions and genome integrations were confirmed by Sanger sequencing performed by Eurofins Genomics (Ebersberg, Germany).

For the synthetic promoter library work, degenerate primers in the target promoter regions were used to generate the libraries using pTn7_BG35 and _BG42[128] as templates. All PCR fragments were purified with the High Pure PCR product purification Kit (Roche, Basel, Switzerland). The fragments with randomized promoters were cloned into the multiple cloning site of plasmid pTn7-M with the Golden Gate Assembly (New England Biolabs, Ipswich, MA, USA) to create the SPL35, SPL42 promoter library. The SPA library was created similarly, here the spacer was randomized based on the strong promoter BG42. The Golden Gate Assembly Mix was transformed into electrocompetent *E. coli* PIR2 cells. The FACS-sorted *E. coli* PIR2 cells containing

the pTn7-SPL35_XXX/ SPL42_XXX/ SPA_XXX libraries were individually sequenced and used for genomic integration at the *attTn7* site in streptomycin-resistant *E. coli* Top10, and into *P. taiwanensis* VLB120. To identify positive clones the plates were examined under blue light to pre-screen for integration. All strains used in this study are shown in Table 2.

Table 2. Bacterial strains used in this study.

Strain	Description	References
<i>E. coli</i>		
DH5a	<i>supE44, ΔlacU169 (φ80lacZΔM15), hsdR17 (rK-mK +), recA1, endA1, gyrA96, thi-1, relA1</i>	[132]
PIR2	<i>F- Δlac169 rpoS(Am) robA1 creC510 hsdR514 endA recA1 uidA(ΔMluI)::pir</i>	[133] iAMB #322
PIR2	Bearing the pTn7-Gm_SPL35_XXX plasmids	This study
PIR2	Bearing the pTn7-Gm_SPL42_XXX plasmids	This study
PIR2	Bearing the pTn7-Gm_SPA_XXX plasmids	This study
PIR2	Bearing the plasmid pTn7-tetA_P _{trc} Tra_GFP	This study
PIR2	Bearing the plasmid pTn7-tetA_P _{trc} Opt_GFP	This study
PIR2	Bearing pTn7-tetA <i>nagR</i> /P _{nagAa} _scpA_argK_scpB	This study
HB101 pRK2013	Sm ^R , <i>hsdR-M⁺, proA2, leuB6, thi-1, recA</i> ; bears plasmid pRK2013	[134] iAMB #2037
DH5a pSW-2	DH5a bearing pSW-2	[130] iAMB #2404
DH5aλpir pTNS1	DH5aλpir bearing plasmid pTNS1	[130] iAMB #3221
TOP10	Wild type	[135]
TOP10	<i>attTn7::Gm_SPL35-XXX_BCD2_GFP_T0</i>	This study
TOP10	<i>attTn7::Gm_SPL42-XXX_BCD2_GFP_T0</i>	This study
TOP10	<i>attTn7::Gm_SPA-XXX_BCD2_GFP_T0</i>	This study
<i>P. taiwanensis</i>		
VLB120	Wild type	[114] iAMB #2060
VLB120 pTN1_35_T_G	bearing plasmid pTN1_SynPro35_Tra_GFP	This study iAMB #6004
VLB120 pTN1_35_O_G	bearing plasmid pTN1_SynPro35_Opt_GFP	This study iAMB #6005
VLB120 pTN1_35_T_C	bearing plasmid pTN1_SynPro35_Tra_mCherry	This study iAMB #6006
VLB120 pTN1_35_O_C	bearing plasmid pTN1_SynPro35_Opt_mCherry	This study iAMB #6007
VLB120 pTN1_42_T_G	bearing plasmid pTN1_SynPro42_Tra_GFP	This study iAMB #5987
VLB120 pTN1_42_O_G	bearing plasmid pTN1_SynPro42_Opt_GFP	This study iAMB #5988
VLB120 pTN1_42_T_C	bearing plasmid pTN1_SynPro42_Tra_mCherry	This study iAMB #5991

Table 2. (continued)

Materials and methods

Strain	Description	References
VLB120 pTN1_42_O_Ch	bearing plasmid pTN1_SynPro42_Opt_mCherry	This study iAMB #5992
VLB120 pTN1_75_T_G	bearing plasmid pTN1_SPA75_Tra_GFP	This study iAMB #5993
VLB120 pTN1_75_O_G	bearing plasmid pTN1_SPA75_Opt_GFP	This study iAMB #5994
VLB120 pTN1_75_T_C	bearing plasmid pTN1_SPA75_Tra_mCherry	This study iAMB #5995
VLB120 pTN1_75_O_C	bearing plasmid pTN1_SPA75_Opt_mCherry	This study iAMB #5996
VLB120 pTN1_nagR_T_G	bearing plasmid pTN1_nagR/P _{nagAa} _Tra_GFP	This study iAMB #5997
VLB120 pTN1_nagR_O_G	bearing plasmid pTN1_nagR/P _{nagAa} _Opt_GFP	This study iAMB #5998
VLB120 pTN1_nagR_T_C	bearing plasmid pTN1_nagR/P _{nagAa} _Tra_mCherry	This study iAMB #5999
VLB120 pTN1_nagR_O_C	bearing plasmid pTN1_nagR/P _{nagAa} _Opt_mCherry	This study iAMB #6000
VLB120 attTn7::trc_T_GFP	attTn7::tetA_P _{trc} _Tra_GFP	This study iAMB #6094
VLB120 attTn7::trc_O_GFP	attTn7::tetA_P _{trc} _Opt_GFP	This study iAMB #6095
VLB120 pTN1_nagR_T_acetoin	bearing plasmid pTN1_nagR/P _{nagAa} _Tra_ilvB_aldB	This study iAMB #6001
VLB120 pTN1_nagR_O_acetoin	bearing plasmid pTN1_nagR/P _{nagAa} _Opt_ilvB_aldB	This study iAMB #6002
VLB120 Tn7_sbm	attTn7::tetA_nagR/P _{nagAa} _scpA_argK_scpB	This study iAMB #6015
VLB120 ΔPVLB_08385 Tn7_sbm	attTn7::tetA_nagR/P _{nagAa} _scpA_argK_scpB ΔPVLB_08385	This study iAMB #6016
VLB120 ΔPVLB_08385 Tn7_sbm pTN1_Tra_yciA	attTn7::tetA_nagR/P _{nagAa} _scpA_argK_scpB ΔPVLB_08385 bearing plasmid pTN1_Tra_yciA	This study iAMB #6104
VLB120 ΔPVLB_08385 Tn7_sbm pTN1_Opt_yciA	attTn7::tetA_nagR/P _{nagAa} _scpA_argK_scpB ΔPVLB_08385 bearing plasmid pTN1_Opt_yciA	This study iAMB #6106
VLB120 ΔPVLB_08385 Tn7_sbm pTN1_Tra_aarC	attTn7::tetA_nagR/P _{nagAa} _scpA_argK_scpB ΔPVLB_08385 bearing plasmid pTN1_Tra_aarC	This study iAMB #6105
VLB120 ΔPVLB_08385 Tn7_sbm pTN1_Opt_aarC	attTn7::tetA_nagR/P _{nagAa} _scpA_argK_scpB ΔPVLB_08385 bearing plasmid pTN1_Opt_aarC	This study
VLB120	attTn7::Gm_SPL35-XXX_BCD2_GFP_T0	This study
VLB120	attTn7::Gm_SPL42-XXX_BCD2_GFP_T0	This study
VLB120	attTn7::Gm_SPA-XXX_BCD2_GFP_T0	This study

2.3. Gravimetric cell dry weight determination

Overnight cultures of *P. taiwanensis* VLB120 were diluted to pre-established optical densities and filtered through membrane filters with a pore size of 0.2µM which were previously weighted (w0) after being dried in a microwave for 3 min at 350W. The filter cake was washed three times with distilled water, dried in the microwave for 8min at 350W, and cooled down in a desiccator before weighing (w1). The cell dry weight (CDW) was calculated by subtracting w0 from w1 and dividing by the volume of the filtered suspensions. One hundred and ninety microliters of the same cell suspensions were transferred to a 96-well microtiter plate (Greiner Bio One), and scattered light signals were recorded at 620 nm with a gain of 30. Linear regression between the CDW and scattered light signals of the pre-established cell suspensions retrieved the conversion factor between these two units.

2.4. Growth rate determination

Determination of growth rates from Biolector cultivation experiments was done by fitting the exponential growth law to CDW data. This approach required identifying the exponential growth phase from the cultivation data, for which a protocol from Hemmerich et al. was applied [136]. To determine the onset of the exponential growth, the CDW data is sequentially scanned using a data frame consisting of five consecutive data points. The data frame is thereby shifted one data point at a time. t_0 is identified as soon as the confidence score (ordinary R^2 value) from fitting the exponential growth law (Equation 1) to the data within the data frame exceeds a critical value of 0.98.

$$X = X_0 e^{\mu(t-t_0)} \quad \text{Equation 1}$$

Here, X is the biomass concentration, t the time, and μ the specific growth rate which is used as the fitting parameter. The subscript 0 denotes the biomass concentration and time at the first time point of a data frame. All following data points within frames showing R -squared values greater than 0.98 additionally belong to the exponential growth phase. As soon as a data frame fit yields an R^2 value below 0.98, the previous data frame marks the end of exponential growth and determines t_1 . The final growth rate is computed by fitting Equation 1 to all CDW data points between t_0 and t_1 . The fitting procedure involves a linear regression using logarithmic CDW data as predictors, where, according to a logarithmic Equation 1, the growth rate is the regression coefficient. Data handling and all computations for determining growth rates were conducted in MATLAB 2018a on a Windows 7 machine with 16 GB of RAM and an AMD FX-8350 eight-core (at 4.00 GHz) processor.

2.5. Fluorescent measurements

All *Pseudomonas* strains expressing fluorescent reporter proteins were characterized in the microbioreactor system BioLector (m2p-labs, Baesweiler, Germany). Cultivations were performed at 30°C with a shaking frequency of 900 rpm, shaking diameter of 3 mm, and, 85% humidity in a 96-well microtiter plate (Greiner Bio One) containing 190 µL of LB media supplemented with required antibiotics for plasmid maintenance and sealed with evaporation

reducing foil (μclear-bottom, Greiner Bio One). The main cultures were inoculated from an overnight pre-culture to an OD₆₀₀ of 0.1. Growth was measured through the scattered light signal at 620 nm with a gain of 30, *msfGFP* fluorescence was excited at 485 nm and emission was measured at 520 nm. The measurements were performed with gains of 50 and 70 due to signal overflow of the stronger constructs. *mCherry* fluorescence was excited at 580 nm, and emission was measured at 610 nm with a gain of 100. Scattered light values were converted into cell dry weight concentrations with a predetermined calibration curve. Inducer was added to the cultures during the early exponential growth phase. To allow a comparison of fluorescence values recorded with different gains, we adapted a published protocol[137] to convert the *msfGFP* signals into μM units of fluorescein (MFE, μmoles of fluorescein equivalents). We utilized the Fluorescein NIST-traceable standard (Molecular Probes Inc., Eugene, USA), a calibrated 50μM solution of fluorescein in 100 mM borate buffer. This molecular probe exhibits its highest fluorescence at pH 9.0. Dilution series of the fluorescein standard were performed with 100mM sodium borate buffer to maintain the pH above 9 since below this value fluorescein can exist in multiple ionization states which can interfere with calibration.

The specific fluorescence intensity was retrieved from the linear coefficient between the fluorescence signal and CDW and used to characterize the expression constructs. Biological triplicates were performed, and errors were presented as the standard deviation of the mean.

2.6. Sequence statistics

We identified enriched or depleted nucleotides for expression level quartiles (Q1, 100-75%; Q2, 75-50% and Q3+4, <50%) within each organism. For the three expression segments (Q1, Q2, Q3+4), the average and standard deviation of the frequency of nucleotides were calculated. The difference of the nucleotide frequency for the segments to the average of frequencies for all promoters was calculated and all differences larger than the standard deviation were visualized in a Logo-plot.

The position-dependent average activity of each nucleotide was computed for SPA constructs as follows. First, the expression values were compared by centering the mean expression to zero with unit standard deviation. Then, a matrix was generated with four columns representing the four nucleotides and 17 rows representing the tested spacer region. For each sequence, the corresponding nucleotide at a given position in the matrix was set to '1' and '0' otherwise. The matrices were multiplied to the respective normalized expression value resulting in a matrix for each measured sequence with the activity at matrix positions for corresponding nucleotide and position. The host-specific expression matrices allowed the calculation of mean expression and cross-host expression variance. Different expressions were selected by performing Welch's t-test of independent samples with different variances and with the null hypothesis of identical average values (Scipy' `ttest_ind` function).

2.7. Flow Cytometry and cell sorting

Single-cell analysis and respective sorting were performed with a BD Influx cell sorter (BD Biosciences, San Jose, CA). The flow cytometer was equipped with a 100 μm nozzle whereas phosphate-buffered saline (1.05 mM KH₂PO₄, 3 mM Na₂HPO₄, 155 mM NaCl) was used as sheath fluid. Cells of each species expressing the BG42 and BG35 genomic integrated construct were

used to calibrate forward and side scatter such as fluorescence intensity (excitation 580nm/emission 610 nm). Cells were sorted at a rate of 5000 events/s, collected in PBS, and plated onto LB with the required antibiotics.

2.8. qPCR assays for mRNA stability assessment

Biological triplicates from *P. taiwanensis* VLB120 harboring either the plasmid pTN1_75_T_G or pTN1_75_O_G were grown overnight in LBmod supplemented with 25 mg/mL gentamycin from a glycerol stock. On the following day, the main cultures with the same medium were inoculated to an initial OD₆₀₀ of 0.1. Once the cultures reached an OD of 1, 1 mg/mL rifampicin and 40µg/mL nalidixic acid were added simultaneously to cease DNA replication and transcription, respectively. Two milliliters of samples were retrieved, centrifuged, and cell pellets flash-frozen in liquid nitrogen and stored at -80°C until further sample treatment. Cell pellets were suspended in 800 µL of DNA/RNA protecting buffer from the Monarch Total RNA MiniPrep kit (New England Biolabs, Ipswich, MA, USA), transferred into the ZR S6012-50 Bashing beads lysis tubes (Zymo Research, Irvine, CA, USA), and mechanically disrupted for 1min. The lysate was transferred into a fresh reaction tube and centrifuged for 2min at 13,000 rpm. The supernatant was transferred into a fresh tube, and the protocol proceeded as described in the Monarch Total RNA MiniPrep kit. qPCR experiments with *msfGFP* and *rpoB* primers pairs were performed with 1 µL of each RNA sample to confirm that the samples were not contaminated with either genomic or plasmid DNA. Eighty nanograms of RNA of each sample were converted into cDNA using the LunaScript RT SuperMix kit (New England Biolabs, Ipswich, MA, USA). qPCR experiments were performed with the Luna Universal qPCR Master Mix (New England Biolabs, Ipswich, MA, USA). qPCR of samples was performed with 1 µL of the reverse transcription reaction mixtures. The qPCR was performed with the CFX96 Real-Time PCR Detection System (Biorad, Hercules, CA, USA). qPCR reactions were performed in technical triplicates. Absolute amounts of mRNA transcripts of *msfGFP* and *rpoB* were quantified using the linear calibration curves used for primer pairs efficiencies, which were constructed with either the plasmid harboring the traditional *msfGFP* expression cassette under the control of the SPA75 or genomic DNA, respectively. The data were analyzed with the Bio-Rad CFXManager and Microsoft Excel software. As we normalized the *msfGFP* mRNA abundance data with the transcript abundance of the housekeeping gene *rpoB*, the determination of an absolute decay rate for the *msfGFP* mRNA was not possible. We calculated the delta between the decay rates of the *msfGFP* and *rpoB* mRNA instead. Assuming a first-order degradation kinetic for the mRNA of both genes, the time profile of the normalized mRNA data can be described with Equation 2.

$$\begin{aligned} \frac{mRNA_{msfGFP}(t)}{mRNA_{rpoB}(t)} &= \frac{mRNA_{msfGFP,0} \cdot \exp^{k_{msfGFP} \cdot t}}{mRNA_{rpoB,0} \cdot \exp^{k_{rpoB} \cdot t}} \\ &= \frac{mRNA_{msfGFP,0}}{mRNA_{rpoB,0}} \cdot \exp^{(k_{rpoB} - k_{msfGFP}) \cdot t} \end{aligned} \quad \text{Equation 2}$$

A non-linear least square algorithm was used in Matlab (The MathWorks Inc., Natick, MA, USA) to fit the experimental data to Equation (1) and to determine the difference in the decay rates of the *rpoB* and the *msfGFP* gene.

2.9. Analytical methods

The samples taken during the acetoin-producing cultivations were centrifuged at 13,000 rpm for 1min, and the supernatant was stored at -20°C until further analysis. To follow the consumption of glucose and production of acetoin, a Beckman System Gold 126 Solvent Module with an organic acid resin column (Polystyrene divinylbenzene copolymer (PS DVB), $300 \times 8.0\text{mm}$, CS-Chromatographie) was used with $5\text{mM H}_2\text{SO}_4$ as eluent at a flow of 0.6 mL h^{-1} for 30 min at 30°C . Detection was realized with a SystemGold 166 UV detector (Beckman Coulter) and a Smartline RI Detector 2300 (KNAUER Wissenschaftliche Geräte, Berlin, Germany).

2.10. LC-MS analysis of propionyl-CoA

Cells, ranging from $1.13\text{--}1.71\text{ mg}$, were harvested during exponential growth, retained on a $0.2\text{ }\mu\text{m}$ pore size filter, and quenched by washing the cells with ice-cold 50% (v/v) methanol. The intracellular content of the samples was extracted by submerging the filter in 2 mL of ice-cold 50% (v/v) methanol and incubating overnight under vigorous shaking at 4°C . The extraction solution was centrifuged at $13,000\text{ g}$ for 5 min at 4°C to remove cellular debris and filtered through a 3 kDa MW centrifuge filter at $13,000\text{ g}$ for 45 min at 4°C to remove proteins. For acyl-CoA quantification, liquid chromatography-mass spectrometry (LC-MS) analysis was employed. The chromatographic separation was achieved with a Kinetex® XB C18 100\AA column (100 mm , 2.1 mm , $2.6\text{ }\mu\text{m}$ particle size) using an Agilent 1290 Infinity LC system. The mobile phase, gradient profile, and flow rate were as described in Yuzawa et al. [138]. The LC system was coupled to an Agilent 6495 Triple quadrupole LC-MS with iFunnel Technology. Ionization and mass measurement were performed as in Yuzawa et al. [138].

2.11. Fermentation

Bioreactor fermentations were performed in 2 L stirred-tank bioreactors (Eppendorf, Germany), which were controlled by BioFlo120 units and DASware Control Software 5.3.1 (Eppendorf, Germany). A working volume of $1.5\text{ L MSM}_{\text{B12}}$ containing the required antibiotics was inoculated to an initial OD_{600} 0.1 using an overnight cultivation in the same medium. Once an OD_{600} of 1 was reached, 0.5 mM of sodium salicylate was added to induce gene expression. The pH was monitored with pH probes (phferm, Hamilton Bonaduz, Switzerland) and maintained constant with $4\text{ M H}_2\text{SO}_4$ and 2 M KOH . During the cultivation, the dissolved oxygen (DO) tension was maintained above 30% by a cascaded agitation ($400\text{--}1000\text{ rpm}$) to prevent oxygen limitation. The DO tension was measured with an InPro 6800 Polarographic oxygen sensor (Mettler Toledo, Giessen, Germany). The aeration rate was kept constant at 0.7 L/min and the cultivation temperature was set to 30°C . Glucose feeding during fed-batch fermentation was triggered by the DO levels. When the DO reached levels above 50% , the feed pump was activated to replenish glucose to a concentration of 25 mM . This procedure was repeated until the addition of glucose did not lead to a decrease in the DO tension indicating that the cells were no longer metabolically active. To maintain a fixed glucose concentration of 5 g/L throughout the fed-batch, the glucose concentration was monitored online with an enzyme-based TRACE C2 Control unit (TRACE Analytics GmbH, Germany), which controlled the feed pump.

Chapter 3

Results

Chapter 3.1

Cross-species synthetic promoter library: finding common ground between *Pseudomonas taiwanensis* VLB120 and *Escherichia coli*

Partially submitted as

D. Neves, U. Liebal, S. C. Nies, T. B. Alter, C. Pitzler, L. M. Blank and B. E. Ebert, "Cross-species synthetic promoter library: finding common ground between *Pseudo-monas taiwanensis* VLB120 and *Escherichia coli*." *ACS Syn. Bio.*, 2023, doi: 10.1021/acssynbio.3c00084

Contributions

Dário Neves and Salome Nies performed the experiments with the help from the students Sarah Schleese, Simone Weingarten and Simon Briel. Ulf Liebal performed the statistically data analysis. Dário Neves and Christian Pitzler did the FACS experiments. Birgitta Ebert conceived and supervised the study. Dário Neves, Ulf Liebal and Birgitta Ebert prepared the figures and wrote the manuscript with the help of Tobias Alter and Lars M. Blank.

3. Results

3.1. Cross-species synthetic promoter library: finding common ground between *Pseudomonas taiwanensis* VLB120 and *Escherichia coli*

3.1.1. Abstract

The potential of non-model organisms for industrial biotechnology is increasingly becoming evident since advances in systems and synthetic biology have made it possible to explore their unique traits. However, the lack of adequately characterized genetic elements that drive gene expression poses obstacles to benchmarking non-model with model organisms. Promoters are one of the genetic elements that contribute significantly to gene expression, but information about their performance in different organisms is limited. This work addresses this bottleneck by generating libraries of synthetic σ_{70} -dependent promoters controlling the expression of *msfGFP* and integrating and characterizing these in *Escherichia coli* and *Pseudomonas taiwanensis* VLB120, a less explored microbe with industrially attractive attributes. We adopted a standardized method for comparing gene promoter strength across species and laboratories. Our approach uses fluorescein calibration and adjusts for cell growth variation, enabling accurate cross-species comparisons. The quantitative description of promoter strength is a valuable expansion of *P. taiwanensis* VLB120's genetic toolbox, while the comparison with the performance in *E. coli* facilitates the evaluation of *P. taiwanensis* VLB120's potential as chassis for biotechnology applications. Of the characterized promoters, only 10% had similar expression strength in both of the organisms, showing that efforts are required to find common ground between these two organisms.

3.1.2. Introduction

Precision engineering of metabolic activities is critical in synthetic biology, e.g., to build genetic circuits that control metabolic outputs and to develop superior and robust cell factories. The gene expression strength is a crucial determinant of enzyme activity and largely depends on the promoter region mediating RNA polymerase binding[139]. Consequently, well-characterized sets of promoters with fine-graded expression strengths covering broad ranges are invaluable in engineering biological systems. To extend beyond the natural diversity, several libraries of up to several thousand artificial promoters have been generated by randomizing the promoter sequence or mix-and-match variants of essential promoter elements [140]–[142]. The quantitative and massive datasets also form the basis for developing mathematical models that, when appropriately mature, can be used for the *a priori* design of promoters with specified strength [143].

However, available data and associated studies have limitations, especially for metabolic engineering applications. Most promoter libraries have been generated for and characterized in *E. coli*, and only a handful exist for other organisms. Although a promoter's expression strength likely differs in different species, the applicability of data derived from *E. coli*-based studies on other host organisms has not been shown, severely limiting the reusability of the data and knowledge. The lack of measurement standards for expression strength further reinforces this impasse. Promoter strength prediction and analysis using machine learning methods have been

developed but are to our knowledge still not applicable to forecast expression strength in different organisms due to the lack of cross-species data.[144], [145] Typically, a promoter's expression strength is characterized by the fluorescence intensity of a fluorescent protein expressed under the promoter's control. These expression constructs can be analyzed in high-throughput, and hence, vast promoter libraries have been characterized through plate reader assays or flow cytometry [143]. Another approach to distinguish promoters, which does not rely on fluorescence, is based on RNAseq in which the strength linearly correlates to the copy number of the transcript [146]. However, a significant fraction of these promoters have marginal to no activity. While of interest for deferring basic knowledge on sequence-activity relationships and model development, those very weak or inactive promoters have no applicability in metabolic engineering.

Moreover, fluorescent intensity measurements are specific for the device and analysis parameters used and most often reported in arbitrary units, prohibiting inter-laboratory or inter-experiment comparisons. The absolute fluorescence value reflects the amount of protein in the sample and is usually normalized to the cell mass or reported as per cell value (flow cytometry). It depends on transcriptional and post-transcriptional factors, including translational activity and protein stability. Transcription itself is also influenced by a variety of factors other than the promoter, such as copy number of the constructs, the cell's growth stage, and growth rate [147]–[149]. These factors should be considered when reporting data on promoter expression strength. We further argue that a cell-specific protein synthesis rate is more meaningful than cell-specific fluorescence values for metabolic engineering projects, where the aim is to achieve a particular metabolic activity.

This study aimed to characterize promoter variants in *E. coli* and *Pseudomonas*, addressing the abovementioned shortcomings of promoter characterization by implementing a standardized fluorescence unit, correcting for growth rate, and abolishing copy number variances of the expression construct by relying on a single genomic integration. *Pseudomonads* are becoming an established and preferred host in industrial biotechnology because of favorable traits such as diverse stress tolerance (chemical, oxidative, solvent), outstanding metabolic versatility, and adaptability [150]. The dual characterization in the two chassis shall shed light on interspecies differences in promoter behavior, which is of fundamental interest and relevant for, e.g., cross-species synthetic promoter design and exchange of expression constructs.

3.1.3. Results and Discussion

A library of synthetic promoters recruiting the σ_{70} transcription factor was expressed in *E. coli* and *P. taiwanensis*. All promoters were characterized on single genome integration basis, and cell mass-specific GFP production rates are presented. The results are discussed in the scope of metabolic engineering applications but also form a basis for deeper sequence analysis and elucidating promoter interaction with the σ_{70} RNA polymerase.

3.1.3.1. Design and generation of the synthetic promoter libraries

We opted for using σ_{70} -dependent promoters because these constitutive promoters are often used for microbial strain engineering. The core promoter structure consists of an upstream region containing the -35 and -10 consensus boxes, separated by a spacer sequence typically

containing around 17 nucleotides (nts), a -15 motif embedded in the spacer, a discriminator upstream of the -10 box consisting of 6 nts directly followed by the transcription start site (TSS) (Figure 4). The promoter structure and the σ factor are conserved and highly resemble each other in *Pseudomonas* and *Escherichia*; therefore, it could be argued that the promoter variants would behave similarly in both organisms [151], [152]. However, previous studies have shown that RNA polymerase libraries of point mutations in functional domains were sufficient to obtain different expression levels from standard promoters [153]–[156]. This strengthens the need for a standardized characterization of promoters in both organisms to construct expression cassettes with similar expression output for cross-species comparison.



Figure 4. Structure of bacterial σ_{70} -dependent promoters and RNA polymerase interactions with promoter DNA. Representation of the randomized regions of the three promoter libraries generated SPL42, SPL35, and SPA. UP, upstream element; -35, -35 element; -10, -10 element; EXT, extended -10 element; DIS, discriminator region; TSS transcription start site; α CTD, α C-terminal domain of RNA polymerase; σ x.y specific σ_{70} subunit. Optimal UP and consensus sequences are shown. W = A or T; N = any base. Figure adapted from [157].

We inserted a bicistronic design (BCD) preceding the gene of interest (GOI). This standardized translational architecture avoids variability in translation efficiency due to (structural) differences in the 5'-upstream region of the GOI and results in GOI-independent expression strength [158]. BCD expression constructs have previously been compared with the traditional, monocistronic design in *Pseudomonas* and *E. coli*, where the improved interaction with ribosomes mediated by the BCD increased overall translation efficiency [158], [159]. Importantly, this design also highly facilitates the promoter library reusability and prevents certain combinations of promoter/GOI from not being expressed due to structural hindrances of ribosomes.

Episomal expression is often used for the characterization of synthetic biology tools due to simplicity, but plasmid copy number variations during different growth stages, between single cells, and even more between species can lead to misinterpretation of the reporter output. To mitigate this risk, we integrated single constructs into the *attTn7* insertion site downstream of the *glmS* gene, which is present in both species. The expression from a single copy might affect the evaluation of very weak promoters because of technical limits in fluorescence detection.

Overall, we constructed three libraries of the prokaryotic σ_{70} promoter using degenerated primers as described by Solem et al. [159]. The promoters were used to drive the expression of *msfGFP*, a monomeric, superfolder green fluorescent protein (Figure 5).

The two synthetic promoters, BG42 and BG35, which share the consensus sequences of the -10 and -35 boxes but differ in the spacer sequence, served as templates for the synthetic promoter libraries (SPLs) [159]. Both promoters were previously characterized for having distinct expression strengths in *Pseudomonas putida* KT2440. Strong activity was reported for BG42 and low activity for BG35, providing an excellent starting point for further diversification [128].

Results

We randomized either the -35 and -10 consensus boxes or the 17 nts spacer of the BG42 sequence to retrieve the promoter libraries SPL42 and SPA, respectively. The third library, SPL35, was created by randomizing the two consensus box sequences of BG35.

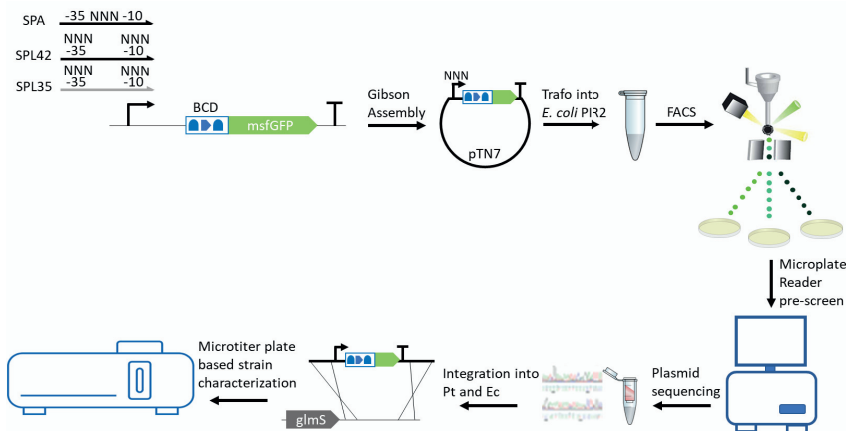


Figure 5. Promoter library construction and characterization workflow. Promoter variants were generated using degenerated primers in the desired regions and assembled into the integration plasmid pTN7. The Gibson Assembly mixtures were transformed into *E. coli* PIR2 and single cells from the transformation recovery culture were sorted onto agar plates based on fluorescence phenotype. The obtained colonies were grown overnight in 96-well plates and pre-screened for fluorescence using a microtiter plate reader with online fluorescence readings. Colonies that showed a fluorescent phenotype were selected, and plasmids were extracted for sequencing to integrate the respective fluorescence expression cassette into *P. taiwanensis* VLB120 (Pt) and *E. coli* TOP10 (Ec). Strains that fulfilled all requirements were characterized through online fluorescence and scatter-light measurements.

The sequence length of the promoters (40 nts) and the single segments (spacer, -35/-10 box, up-/downstream region) were maintained in all promoters. While in the SPA library, all spacer positions were randomized, certain positions were kept constant in SPL42 and SPL35. In the -35 box, the first two positions were held constant ($^{-35}\text{TTNNNN}^{-30}$) (Figure 4), and the first and last two nucleotides were kept unchanged in the randomization of the -10 box ($^{-12}\text{TANNNTT}^{-6}$). This strategy of retaining the most critical bases was intended to avoid the formation of non-functional promoters [142], [160]. Indeed, in a parallel approach, which randomized all nucleotides of both boxes, a vast number of inactive promoters was generated as expected.

Active promoters of each library were identified as follows. The three amplified degenerated PCR products, each with its defined randomized regions, were assembled into an integration vector to drive the expression of *msfGFP* and transformed into *E. coli* PIR2. The recovery suspensions of each transformation were then screened for fluorescence of the expressed *msfGFP* by fluorescence-activated cell sorting (FACS) and single cells directly plated on solid growth media. The fluorescence phenotype of single colonies was confirmed in liquid microtiter plate assays. Constructs showing a fluorescent phenotype and a promoter sequence in consonance with the requirements described above were integrated into the *attTn7* locus of *E. coli* TOP10 and *P. taiwanensis* VLB120 (Figure 5).

Each promoter was characterized in both species by fluorescence equivalents per biomass and a specific GFP production rate expressed in molar fluorescence equivalents per biomass and time

unit (Figure 7). To derive the latter, we first translated the fluorescence output into μ molar fluorescent equivalents (MFE) by calibrating the fluorescence signal with fluorescein (see Material and Methods and Neves et al. [161]). The specific GFP activity, i.e., fluorescence equivalents per gram cell dry weight (CDW), was calculated by linear regression between the fluorescent equivalents and respective biomass concentration during exponential growth. This value was then multiplied by the specific growth rate to obtain a GFP production rate in MFE per gram CDW per hour. This promoter performance indicator describes the expression strength during exponential growth, compensating for potential differences arising due to discrepancies in growth rate. We chose this portrayal of promoter behavior as it resembles and anticipates the performance of the characterized promoters for metabolic engineering purposes, in which promoters are selected to adjust enzymatic activities expressed in equal units.

Fifty thousand cells were sorted for each library, and the fluorescence range was divided into quartiles (see Appendix Figure 21). From each fluorescence quartile of each library, 96 colonies were plated and pre-screened for fluorescence and growth. The number of strains that passed the pre-screen and sequencing quality control (QC) and the number of successfully integrated promoters in *E. coli* and *P. taiwanensis* is shown in Table 3.

Table 3. The number of clones at each step of the integration workflow for each library.

Library	N ⁰ passed pre-screen	N ⁰ passed for integration	QC	Integrated in Ec	Integrated in Pt	Integrated in both
SPL35	210	132		57	31	17
SPL42	220	83		37	30	21
SPA	330	160		81	71	55

3.1.3.2. Sequence diversity of generated promoter

The degenerate primers used in this study were designed to introduce up to seven and 17 nucleotide changes (compared to the template promoters) for the SPL and SPA libraries, respectively. To assess the randomization efficiency of the library generation, we inspected the sequences of the selected promoters.

Randomizing the spacer region led to the replacement of seven to 15 nucleotides and an average randomization efficiency of 76 % (12-13 nucleotide exchanges). In comparison, the randomization of the box regions was less efficient. Only one (promoter 42_104) of the 39 selected had all seven variable nucleotides exchanged, while, on average, only 3-4 nucleotide substitutions occurred. The randomization of the -10 and -35 boxes in the SPL42 library was relatively equal (55 % and 50 %, respectively). However, we observed a bias for the unmutated -35 box sequence in the SPL35 library, where nearly 40 % showed the consensus sequence of the template promoter.

The number of ambiguous nucleotide bases in the PCR template would allow the generation of 4^7 ($\sim 1.6 \cdot 10^4$) and 4^{17} ($\sim 1.7 \cdot 10^{10}$) possible promoter variants. This study's total of 95 promoters covers only a marginal fraction of this theoretical promoter space.

However, the calculation of the pairwise distance between all promoter sequences showed that the three-pronged approach of randomizing different promoter segments and template sequences resulted in a set of promoters with an overall good sequence diversity (Figure 6 A). This was further examined using the nucleotide sampling diversity at each position (Figure 6 B).

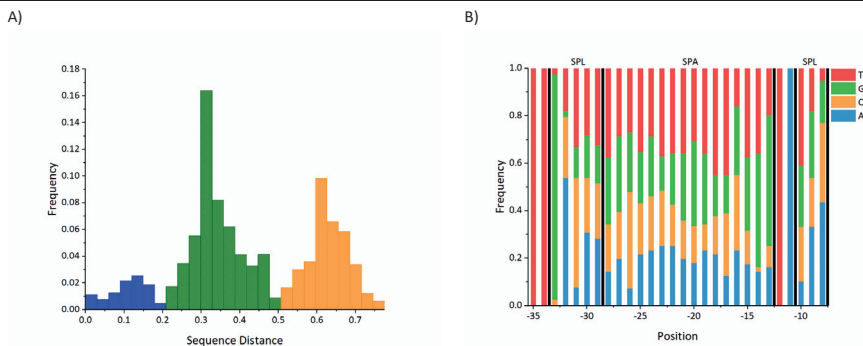


Figure 6. Statistical overview of the mutational landscape of the promoter libraries. A) Pairwise distance between all promoter sequences. The three regions represent the distance between promoter sequences of the SPL35 and the SPL42 library (blue), the distance of promoter sequences within the SPA library (green), and the distance between promoters of the SPL35 and SPA library (orange). B) Frequency of bases tested at each position. Positions -29 to -13 represent the sampling diversity of the SPA library only, -33 to -31 and -10 to -8 represent variations of the SPL libraries.

The stacked bar graph shows how often a nucleotide was tested on each randomized position, i.e., for the SPA library (positions -29 to -13) and the SPL library (-33 to -31 and -10 to -8). The spacer sequence was more uniformly sampled (if entirely random, the abundance of each nucleotide would be 25 %) than the boxes, for which there is a tendency to keep the consensus sequence (Appendix Table 8). The spacer sequence featured a slight dominance of guanine at positions -14 and -13 and thymine at -17 and -18. Discrimination against -33G promoters was likely introduced with the *E. coli*-based pre-screen, which selected promoters functional in this species. Although sampling was not uniform, the diversity of retrieved sequences from the three libraries was considerably broad, supporting the validity of the randomization approach.

3.1.3.3. Characterization of the synthetic promoter libraries in *E. coli* TOP10.

To assess the applicability of the synthetic promoters for microbial strain engineering, we first quantified the expression strength in *E. coli* and used the data as a benchmark for *P. taiwanensis*. The evaluation of the promoter libraries incorporated cellular fitness to determine a specific GFP production rate ($\text{MFE g}^{-1} \text{h}^{-1}$) as a novel measure for promoter strength. Since such a unit is not standard in promoter library characterizations, a comparison with the more commonly used biomass-specific fluorescence ($\text{MFE per gram cell dry weight, MFE g}^{-1}$) is included in Figure 7.

Interestingly, this comparison revealed a linear relationship between the rankings based on these performance indicators for weak promoters from the SPL35 and SPL42 libraries but a very dispersed distribution for stronger promoters from the SPA library (Figure 7). Therefore, we propose a specific GFP production rate as a more robust performance indicator for promoter libraries with large dynamic ranges, where strong expression can result in metabolic burden and interfere with cellular fitness and growth. This is especially important for metabolic engineering and growth-dependent production processes because of the implications on specific productivities.

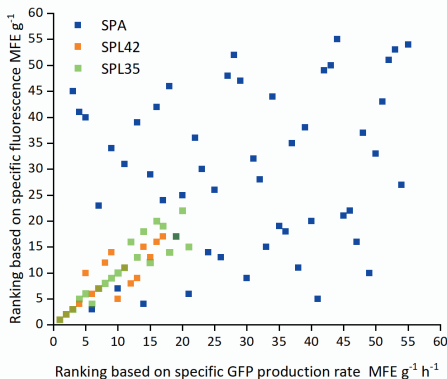
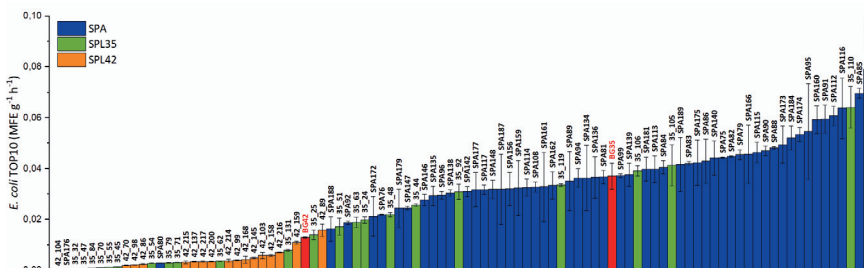


Figure 7. Comparison of promoter ranking based on the performance indicators. Comparison between the specific GFP production rate ($\text{MFE g}^{-1} \text{h}^{-1}$) and biomass-specific fluorescence (MFE g^{-1}) for the three libraries SPL35 (green), SPL42 (orange), and SPA (blue) in *E. coli*.

Considering the three genome-integrated libraries, a broad dynamic range of ca. 3,200-fold was achieved with a stepwise increase of promoter strength (Figure 8 A).

A)



B)

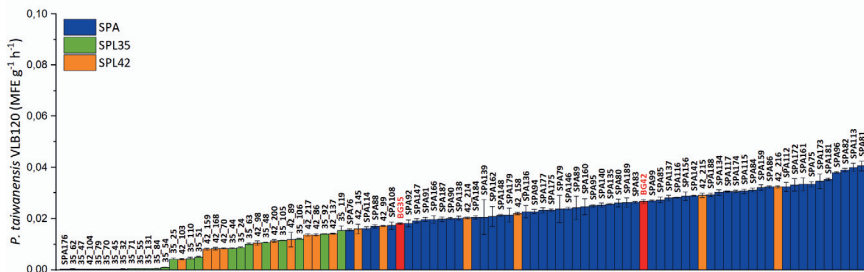


Figure 8. Overview of the expression strength of the three promoter libraries genomically integrated into A) *E. coli* TOP10 and B) *P. taiwanensis* VLB120. Error bars indicate the standard deviation of three biological replicates; the template promoters are highlighted in red. Promoter libraries SPL42 and SPA were derived from the template BG42. SPL35 was derived from BG35.

3.1.3.4. Characterization of the synthetic promoter libraries in *Pseudomonas taiwanensis* VLB120.

As an emerging cell factory, there is a lack of fundamental knowledge on *P. taiwanensis* VLB120 compared to, for example, *E. coli* or *P. putida* [162]. Therefore, oppositely to *E. coli*, a deeper analysis of the promoter sequence to performance relation was conducted.

The SP42 and SPL35 libraries with altered -35 and -10 boxes showed dynamic ranges of the specific GFP expression rate of 308- and 182-fold, respectively, whereas randomizing the spacer in the SPA library led to a 759-fold dynamic range, indicating a higher potential for modulating expression by changing the spacer sequence.

It is worth mentioning that the SPL42 library contains a more significant number of promoters with meaningful expression levels than the SPL35 library (Figure 8 B). Overall, the promoter libraries in *P. taiwanensis* VLB120 followed a continuous increase in strength, having only discontinuities in the lower expression range, which could facilitate expression fine-tuning.

All promoters within the SPL35 library had a weaker performance than the template promoter BG35 suggesting that in this weak promoter background, the consensus sequences are essential to retaining activity.

As with the SPL35 library, the SPL42 library was found to contain mainly promoters with weaker performance than the BG42 template promoter, with two exceptions (SPL42_216 and SPL42_215). In the strongest of these two, SPL42_216, the -35 box was modified to TTCGTT (GACA>CGTT) while the -10 box changed to TAGTTT (TA > GT), achieving a 1.2-fold stronger expression rate. In contrast, promoter SPL42_104 with the same -35 box showed a 124-fold lower performance than SPL42_216, indicating that the -10 box of SPL42_104 might be responsible for such a low expression rate. Unfortunately, an equivalent combination of the -35/-10 boxes was not found in the SPL35 library to further evaluate its impact on other promoter backgrounds.

Further comparison of the nucleotide abundances in SPL42 and SPL35 (Appendix Figure 22) revealed divergent nucleotide preferences at some positions. At position -30, the SPL35 promoters contained mostly adenine, whereas in the SPL42, most of the promoters contained either thymine or cytosine. For position -9, the nucleotide abundance was equally distributed over the four nucleotides in SPL35, while in SPL42, an enrichment in adenine and guanine was observed. At position -8, cytosine was preferred in SPL35, whereas in SPL42, over 60 % of the promoters contained adenine. The difference in position -30 is due to an enrichment of the native -35 box in SPL35, whereas the differences in positions -9 and -8 are caused by a preference for the -10 consensus sequence in SPL42.

One common feature between the two libraries is the occurrence of a guanine at position -33 in all promoters except for two SPL42 promoters. The two exceptions that did not contain guanine at position -33 showed the lowest and the strength of a medium expression promoter, underlining this nucleotide's relevance for promoter activity. Positions -30 and -9 showed more variability and could be possible targets for fine-tuning promoter strength. On the other hand, observing different preferences between these two libraries whose template promoters only differ in the spacer sequence shows that the different promoter segments do not contribute independently to promoter strength but influence each other. Such interdependency complicates the definition of guidelines for designing promoters and suggests the need for complex, nonlinear models or machine learning approaches.

The characterization of the two σ_{70} box libraries, SPL35 and SPL42, confirmed that the -35 and -10 consensus sequences are ideal for RNA polymerase binding in *P. taiwanensis* VLB120, and modulating their sequences to achieve higher gene expression is a limited approach as previously described [163], [164].

In contrast to the weakened activities found for SPL42 and SPL35, 43% of the spacer library SPA was composed of promoters stronger than the template BG42. The increase in expression strength correlated with a high GC content of the spacer sequence (Appendix Figure 23) with significant enrichment of guanine at positions -14 and -13, the two nucleotides upstream of the first nucleotide of the -10 box.

Since position-specific nucleotide enrichments are more perceptible when binning promoters according to their performance rates, the performance ranking was divided into three segments. Segment 1 includes the Q1 quartile promoters with 100-75% of the maximal specific GFP expression rate, whereas segment 2 contains promoters with performance rates between 50 % and 75 % of the maximal expression (Q2 quartile), and segment 3 holds all weaker promoters (Q3-Q4 quartiles, <50% of the maximal specific GFP expression rate). The deviation from the average frequency on a position among the segments is visualized via a Logo plot in Figure 9. In *E. coli* for the Q1 expression segment on position -16, the nucleotide 'C' was 18% less used compared to the mean of all quartiles, whereas the 'A' was 20% more frequent. High frequencies of $^{-29}\text{GGGG}^{-26}$ are enriched in Q3+4 in *E. coli*. *P. taiwanensis* Q1 sequences were enriched for $^{-17}\text{GGG}^{-15}$ while guanine was discriminated at these positions in Q3-4 (Figure 9) These observations could be used for future promoter designs in which the aim is to retrieve strong promoters in this *Pseudomonad*.

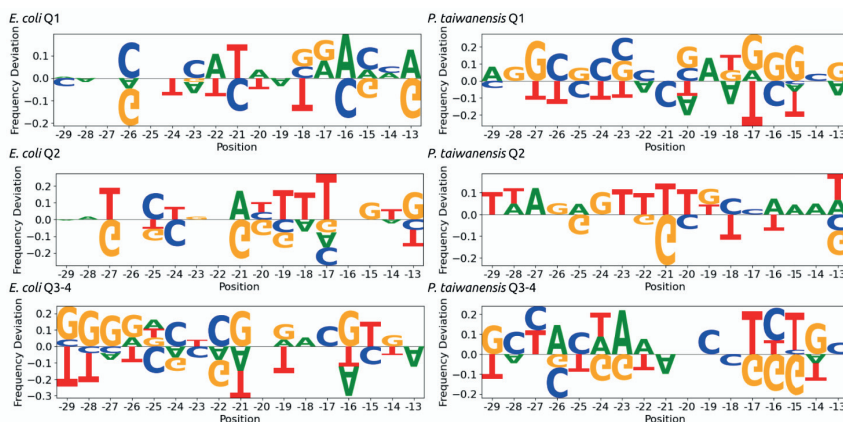


Figure 9. Representation of nucleotide frequency deviation of quartiles Q1, Q2, and Q3-4 from mean nucleotide frequencies for *E. coli* and *P. taiwanensis* VLB120. The expression was separated into quartiles and the average nucleotide frequency was calculated for all quartiles. The figure shows the nucleotide frequency differences greater than the standard deviation (Q1, 100-75%; Q2, 75-50%, and Q3-Q4, <50% of the maximal specific GFP expression rate).

Although the weakest promoter segment is characterized by its overall high AT content, guanine enrichment was observed at positions -14 and -13, a feature present throughout the SPA library. The conservation of guanine at position -13 was previously described for *E. coli* by

Djordjevic [165] in the context of the -15 element $^{-15}\text{TGNT}^{-12}$ [166]. The -15 element, $^{15}\text{TGNT}^{-12}$, supposed to be responsible for dsDNA- σ_{70} interactions [165], was only observed in the weakest segment, whereas in the strongest segment, the -15 element consisted of $^{-15}\text{GGGT}^{-12}$. Such -15 element comes closer to the λP_R promoter, $^{-15}\text{GGTG}^{-12}$ [167].

3.1.3.5. Common ground and disparities of σ_{70} -dependent promoters between *P. taiwanensis* VLB120 and *E. coli*.

As mentioned earlier, the homology between the RNA polymerase of *P. taiwanensis* VLB120 and *E. coli* might mislead to the assumption that a given promoter would function similarly in both organisms. This assumption was previously proven wrong and confirmed in this work since less than 10% of the characterized promoters had similar performance between the two strains (Figure 10) [153], [154].

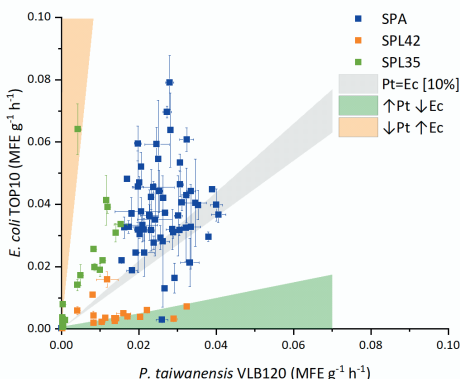


Figure 10. Performance comparison of the three promoter libraries SPA (blue), SPL42 (orange), and SPL35 (green) in *P. taiwanensis* VLB120 (Pt) and *E. coli* TOP10 (Ec). Highlighted areas contain promoters with relevant metabolic engineering applications, the grey area includes promoters with a 10% range of similar performance, whereas the green and orange area contains promoters with opposite outputs in the two strains. Error bars indicate the standard deviation of three biological replicas. The promoters enclosed within each set are listed in Appendix Table 9.

To further elucidate the low-performance similarity, we sought to identify nucleotide positions that drive divergent inter-species expression. We first scaled the measurements of the specific GFP production rate to zero mean and unit variance for each species to compare inter-species expression. The average expression for all nucleotides at each sequence position was then calculated and we tested significant differences in the expression variance at each position using Welch's t-test with a significance cut-off of $p < 0.05$ (Figure 11).

Overall, there are eight nucleotides on positions [-13, -15, -19, -27] for which the expression variance is different between *E. coli* and *P. taiwanensis* VLB120. For example, on position -13, the A and G show variance differences, and examining the normalized expression average on each position (Figure 12) confirms that the -13 G in *E. coli* was associated with an expression 8% below the *E. coli* average expression whereas in *P. taiwanensis* VLB120 the -13G was 10% above the average expression in *P. taiwanensis*.

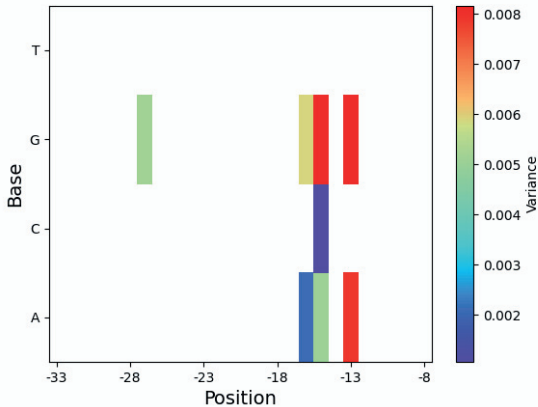


Figure 11. The variance of the mean for normalized expression for all nucleotide positions for the spacer region (-29 to -13) of the SPA library between *E. coli* and *P. taiwanensis* VLB120. Nucleotide positions with significantly different mean expression values (Welch's t-test with $p < 0.05$) were used to compute the variance. Red labels identify nucleotide positions associated with the most distinct mean expression for the respective nucleotide positions of the two strains; white patches represent nucleotide positions with insignificant differences in the mean; A, adenine; C, cytosine; G, guanine; T, thymine.

An elevated expression associated with G for *P. taiwanensis* VLB120 can be observed for multiple positions in Figure 12, although the significance is only valid for some positions (Figure 11).

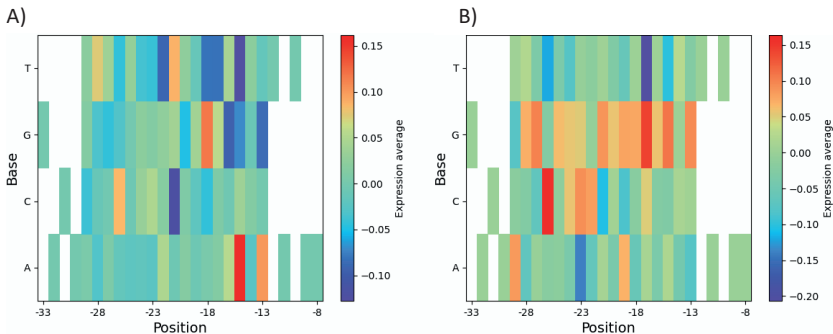


Figure 12. Normalized average expression for each nucleotide at each position for the SPA library in *E. coli* (A) and *P. taiwanensis* VLB120 (B). Red-labeled nucleotides at a given position indicate a correlation with strong expression levels, whereas blue-labeled nucleotides relate with weak expression. Including unchanged positions -33 to -30 and -12 to -8 serves the purpose of baseline references for mean expression.

The finding of a G-associated elevated expression for *P. taiwanensis* VLB120 is in line with the observation in this work that the strongest promoters in *P. taiwanensis* VLB120 had higher GC content, whereas in *E. coli*, the opposite was observed (Figure 9). A possible explanation for these tendencies is the evolution towards different genomic GC contents (*P. taiwanensis* VLB120 and *E. coli* TOP10 have a genomic GC content of 61.8% and 50.8%, respectively) as proposed by Johns et al [168].

Two of the three generated promoter libraries had an overall higher expression strength in *E. coli* than *P. taiwanensis* VLB120 (Figure 10). One plausible reason for this outcome could be the pre-screen of promoter libraries in *E. coli*, which may have favored the selection of active promoters in this organism. However, 5' regulatory sequences of *E. coli*, which includes promoters, were found to be very active in *P. aeruginosa* (which has a higher GC content than *P. taiwanensis* VLB120), suggesting that independently of a pre-screen bias towards active *E. coli* promoters these should be equally active in *Pseudomonas* [168]. Nevertheless, it has also been shown in the same work that 5' regulatory sequences of *P. aeruginosa* tend to be less active in *E. coli*, which could lead to a pre-screen bias toward weak promoters in *Pseudomonas*. The correlation between *P. aeruginosa* and *P. taiwanensis* VLB120 still needs to be confirmed to evaluate this bias further.

As mentioned previously, the characterization of the promoter libraries in the two strains was focused within the scope of metabolic engineering purposes. Promoters with a similar performance in *E. coli* and *P. taiwanensis* VLB120 (Figure 10) are especially desirable for cell factory development since they allow the proper comparison of these two strains as chassis. In the past years, the concept of 'adapt the strain to the product' has lost ground to 'find the strain for the product'. This shift is fuelled by the recent advancements in molecular biology tools which allow the manipulation of non-conventional organisms at rates usually confined to model organisms. This set of equally performing promoters in *E. coli* and *P. taiwanensis* VLB120 hopes to spark interest in creating common ground between different strains for proper strain benchmarking. The difficulty in selecting promoters with similar performance in *E. coli* and *P. taiwanensis* VLB120 raises the question if one should use orthologous or synthetic RNA polymerases, such as the T7 polymerase, in metabolic engineering applications to achieve species-independent expression levels. Besides the common strength promoters, promoters with opposite performances in the two strains have interesting applications. Promoters leading to weak expression in *P. taiwanensis* VLB120 and strong expression in *E. coli* could be advantageous for constructing weak expression cassettes in *P. taiwanensis* VLB120 that should have a strong selective phenotype in *E. coli* to facilitate assembly screening. However, the set of promoters that show strong expression in *P. taiwanensis* VLB120 and weak expression in *E. coli* is the one that gathers likely more interest. *Pseudomonads* are known to be able to produce products that are toxic to *E. coli*. Construction of constitutive expression systems for toxic compounds tends to be problematic in *E. coli* since the cells linger on toxicity effects during the construction of the genetic vectors. The knowledge of promoters that exhibit weak expression levels in *E. coli* and the opposite in the desired host would facilitate and fasten the construction of the desired expression strain.

3.1.4. Conclusion

This work contributed to the settlement that promoters behave differently in *E. coli* and *P. taiwanensis* VLB120 and that further studies are required to gain a mechanistic understanding of the distinct behavior, for example, by expressing one organism's RNA polymerase in the other. A more extensive study with hundreds of thousands of sequences is required to develop models for the quantitative prediction of sequence-function relationships. The presented data form a base for the informative design of promoter sequence libraries. These well-characterized libraries of σ_{70} dependent promoters for *E. coli* and *P. taiwanensis* VLB120 are valuable resources that can be used to select promoters for metabolic engineering purposes, especially when both species shall be tested as hosts and for cloning of genes challenging to express in *E. coli* due to toxicity issues. A predictive model of promoter strength in different species would allow the construction of expression systems with similar cross-species outputs, facilitating the search for the most favorable host.

Chapter 3.2

Pseudomonas mRNA 2.0: Boosting Gene Expression Through Enhanced mRNA Stability and Translational Efficiency

Partially published as

D. Neves, S. Vos, L. M. Blank, and B. E. Ebert, “*Pseudomonas* mRNA 2.0: Boosting Gene Expression Through Enhanced mRNA Stability and Translational Efficiency.” *Front. Bioeng. Biotechnol.*, 2020, doi: 10.3389/fbioe.2019.00458.

Contributions

Stefan Vos constructed the plasmid-based strains. Dário Neves constructed the genomically integrated strains and performed all the characterizations. Dário Neves prepared the figures and wrote the manuscript with the help of Birgitta Ebert and Lars M. Blank.

3.2. *Pseudomonas* mRNA 2.0: Boosting Gene Expression Through Enhanced mRNA Stability and Translational Efficiency

3.2.1. Abstract

High gene expression of enzymes partaking in recombinant production pathways is a desirable trait among cell factories belonging to all different kingdoms of life. High enzyme abundance is generally aimed for by utilizing strong promoters, which ramp up gene transcription and mRNA levels. Increased protein abundance can alternatively be achieved by optimizing the expression on the post-transcriptional level. Here, we evaluated protein synthesis with a previously proposed optimized gene expression architecture, in which mRNA stability and translation initiation are modulated by genetic parts such as self-cleaving ribozymes and a bicistronic design, which have initially been described to support the standardization of gene expression. The optimized gene expression architecture was tested in *Pseudomonas taiwanensis* VLB120, a promising, novel microbial cell factory. The expression cassette was employed on a plasmid basis and after single genomic integration. We used three constitutive and two inducible promoters to drive the expression of two fluorescent reporter proteins and a short acetoin biosynthesis pathway. The performance was confronted with that of a traditional expression cassette harboring the same promoter and gene of interest but lacking the genetic parts for increased expression efficiency. The optimized expression cassette granted higher protein abundance independently of the expression basis or promoter used proving its value for applications requiring high protein abundance. The highest increase in expression strength was observed when the optimized gene expression cassette was evaluated on a single genomic integration basis in which a 15 fold increase was observed.

3.2.2. Introduction

Cell factories have become an established role player in the sustainable production of chemicals and biological products proven with hundreds of billions of USD/year value on global markets [169]. A commonality in the development of such cell factories is the continuous pursuit of increased productivities through directed or selection-based genetic engineering methods. With both approaches, increasing activity of the partaking pathways commonly leads to the desired rise in productivity. High enzyme activity can be achieved by optimization of transcription, translation, post-translational modifications, and the process conditions [170]. A common strategy is to employ strong promoters to overexpress product biosynthesis genes. Highly active promoters achieve increased protein production rates by increasing the respective mRNA levels in the cell. However, previous studies have shown that high, recombinant gene expression leads to metabolic burden and consequently to growth impairment [171], [172]. Such hindrances are related to the drainage of biosynthetic precursors, such as nucleotides, or seizing of the cellular transcriptional machinery.

In recent years, Synthetic Biology parts emerged that support high enzyme activities without the need for strong gene expression, thereby contributing to diminishing competition and depletion of the cellular mRNA pool and lightening the metabolic burden. Two translation-focused approaches can be distinguished that target to optimize translation rather than transcription. To this end, the first approach attempts to stabilize mRNA, whereas the second

seeks to increase translational efficiency. Increasing mRNA stability is possible by placing stabilizing sequences in the 5' untranslated region (UTR) that avoid endoribonuclease attacks through their secondary structures as in *Escherichia coli* [173]. The implementation of ribozymes upstream of the ribosome binding site (RBS) allows the insulation of the desired expression cassette from the genetic context [174]. Besides the intrinsic cleaving activity, the ribozymes developed by Lou et al. contained a 23 nucleotide hairpin downstream of the catalytic core, which additionally adds an mRNA stabilizing trait to this genetic part [175].

One approach within the second category, which focuses on translational efficiency, allows increased expression levels by facilitating the access of the ribosome to the RBS. In the traditional operon architecture (Figure 13A), it is possible that gene of interest (GOI)-dependent secondary structures arise. This folding of the mRNA can block the access of ribosomes to the RBS thereby compromising the desired gene expression [176]. Mutalik et al. developed a 'bicistronic design' which takes advantage of the intrinsic helicase activity of ribosomes to unveil any RBS-GOI dependent secondary structure and consequently achieve GOI-independent expression [158]. In the bicistronic design, a short leading peptide cistron is allocated upstream of the GOI. The RBS of the GOI is enclosed within the coding sequence of the leading cistron, whereas the start codon of the GOI is fused to the stop codon of the leading cistron. The leading RBS-small peptide combination is known to not create any secondary structures, which assures the binding of a ribosome. Once the ribosome binds to the first RBS and starts to translate the leading peptide, any possible downstream RBS-GOI dependent secondary structures are unveiled by its intrinsic helicase activity exposing the RBS of the GOI. Otto et al. recently combined the bicistronic design with an upstream ribozyme to increase the translational efficiency of heterologous genes integrated in rRNA operons. Here the intention of the ribozyme integration was not to stabilize the mRNA but to increase translation efficiency by reducing a potential steric hindrance by the bulky 5' 16S mRNA flank and thereby facilitating ribosome docking. To this end, the ribozyme was placed upstream of the RBS, and this integration indeed resulted in a substantial increase in protein production [177].

Nielsen et al. proposed the compilation of these and further genetic parts into an overall standardized gene expression cassette for the assembly of genetic circuits (Figure 13B) [178].

Besides the incorporation of the gene expression parts described above, Nielsen et al. proposed the isolation of the expression cassette with bidirectional terminators on both ends and the integration of an RNase III site downstream of the GOI to further reduce context-specific effects.

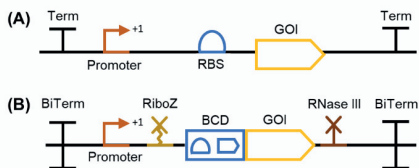


Figure 13. Gene expression cassette architectures represented with glyphs compliant with the Synthetic Biology Open Language Visual (SBOLv). (A) A traditional gene expression cassette comprising a promoter, an RBS, and a gene of interest (GOI) and a terminator (Term), (B) an optimized gene expression cassette as proposed in [178], framed between two bidirectional terminators (BiTerm.) and encompassing a promoter, a ribozyme (RiboZ), the bicistronic design (BCD) developed by Mutalik et al. [158], a GOI and an RNase III site.

The impact of an RNase III site downstream of the GOI was evaluated by Cambray et al. within the scope of reliable terminator characterization [179].

These promoter-independent gene expression tools have been individually characterized but, to our knowledge, a possible synergistic and expression enhancing effect of their combination is yet to be explored.

In this work we constructed optimized gene expression cassettes based on the architecture proposed by Nielsen et al. and evaluated the performance against traditional configurations using two fluorescence proteins (*msfGFP* and *mCherry*) and recombinant acetoin production as readout [180]. The constructed, optimized gene expression cassettes were evaluated on a plasmid basis and after single-copy genomic integration. Overall, the traditional and optimized gene expression cassette variants were characterized with three constitutive and two inducible promoters.

Reducing the overall size of the optimized gene expression cassette while maintaining its performance was also targeted in this work. Besides the characterization of several constructs, qPCR analysis was performed to elucidate the role of mRNA stability in altered protein expression.

We chose *Pseudomonas taiwanensis* VLB120 as expression host as this Gram-negative bacterium exhibits industrial relevant metabolic capabilities such as broad carbon source utilization, the ability to proliferate in the presence of organic solvents, and an almost byproduct free metabolism [108]. *P. taiwanensis* VLB120 has been proven a suitable biocatalyst to produce (S)-styrene oxide, phenol, isobutyric acid, and 4-hydroxybenzoic acid [131], [181], [182]. The novel expression device developed in this study contributes to more effective engineering of this emergent and promising biocatalysts and other prokaryotic cell factories.

3.2.3. Results and Discussion

3.2.3.1. Characterization of plasmid-based, constitutive fluorescent protein expression

The optimal gene expression profile depends on the specific application. Generally, the use of robust, constitutive promoters is prioritized over inducible promoters for large-scale production as they render the addition of inducers unnecessary and therefore contribute the cost efficiency of microbial fermentations.

To evaluate the impact and applicability of the consolidated, optimized expression architecture on this type of promoters, we selected two synthetic promoters, Syn42 and Syn35 (originally referred to as BG42 and BG35, respectively), created by Zobel et al. [128], whereas the third one, SPA75, was obtained from a synthetic promoter library created by Neves et al. (manuscript in preparation). The promoters Syn42 and SPA75 possess a similar high expression strength in *P. taiwanensis* VLB120, while the promoter Syn35 exhibits around 25 % of the expression strength of Syn42.

These promoters were encompassed within the optimized and traditional gene expression cassette in the pTN1 plasmid backbone, a vector used by the *Pseudomonas* scientific community (Figure 14) [183]–[185]. The optimized gene expression cassette was framed between two bidirectional terminators to uncouple transcription from its genetic context. For this purpose, two bidirectional terminators characterized by Chen et al., ECK120026481 and ECK120011170, were selected to insulate, respectively, the 5' and 3' end of the optimized gene expression

Results

cassette [186]. The ribozyme RiboJ, characterized by Lou et al., and the bicistronic design BCD2, developed by Mutalik et al., were placed downstream of the selected promoters [158], [174]. The last genetic part included was the RNase III site R1.1, characterized by Cambray et al., and placed downstream of the GOI [179]. The traditional versions of the gene expression cassettes were obtained by omitting the enhancing genetic parts and including the 2nd RBS of the BCD2 to maintain the ribosome affinity towards the mRNA between the two expression systems (Figure 14A). It has been demonstrated that certain combinations of RBS and gene of interest result in secondary structures, which inhibit translation [158]. The occurrence of such secondary structures in the tested traditional constructs cannot be excluded, and a contribution from the BCD to increased expression levels due to the abolishment of these structures should be considered.

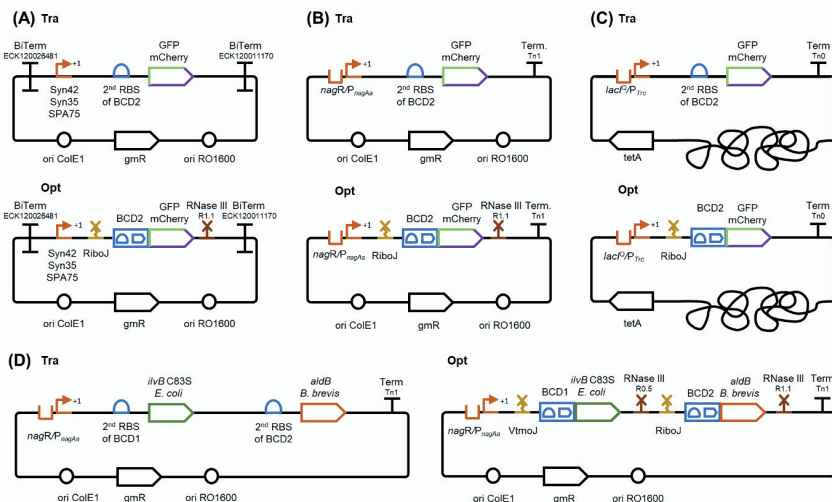


Figure 14. Gene expression constructs evaluated within this work. Traditional and optimized gene expression cassettes for (A) the plasmid-based expression of two fluorescent reporters (*msfGFP* and *mCherry*) under the control of three synthetic, constitutive promoters (*Syn42*, *Syn35*, and *SPA75*) and (B) the salicylate inducible *nagR/P_{nagAa}* promoter. The constructs for constitutive and inducible expression differ in the use of terminators. Bidirectional terminators were placed in front and at the end of the expression cassette in (A), while one unidirectional terminator was used in (B). (C) Traditional and optimized gene expression cassettes for single genomic integration into the *attTn7* site. The expression with these constructs was evaluated using the fluorescent reporter gene *msfGFP* under the control of the IPTG inducible *P_{trc}* promoter. The terminator *Tn0* was used here as in the original genome integration cassette [128]; (D) traditional and optimized gene expression cassettes for the plasmid-based evaluation of an acetoin pathway. The two-gene operon was expressed under the control of the salicylate inducible *P_{nagAa}* promoter; Tra, traditional gene expression cassette; Opt, optimized gene expression cassette; RBS, ribosomal binding site; Term / *BiTerm*, uni- / bidirectional terminator; BCD, bicistronic design; *VtmOJ*, *RiboJ*, synthetic ribozyme; *RNase III* R1.1 and R0.5, *RNase III* restriction sites; *gmR*, gentamycin resistance gene; *tetA*, tetracycline resistance gene; *ori ColE1* and *ori RO1600*, origins of replication.

We evaluated the twelve constructs in microtiter plate cultivations with online measurements of fluorescence and scattered light. The scattered light values were converted into cell dry weight units, whereas the arbitrary *msfGFP* fluorescence units were transformed into equivalents of fluorescein (MFE) to allow a direct comparison between experiments ran with different measurement settings. The *mCherry* fluorescence values were not converted since all

experiments were performed with the same settings. However, we propose the broad implementation of such standardized fluorescence units to facilitate results comparison within the scientific community. Gene expression with the different constructs was characterized by the slope of the linear regression between measured fluorescence and cell dry weight, which indicates a specific expression strength.

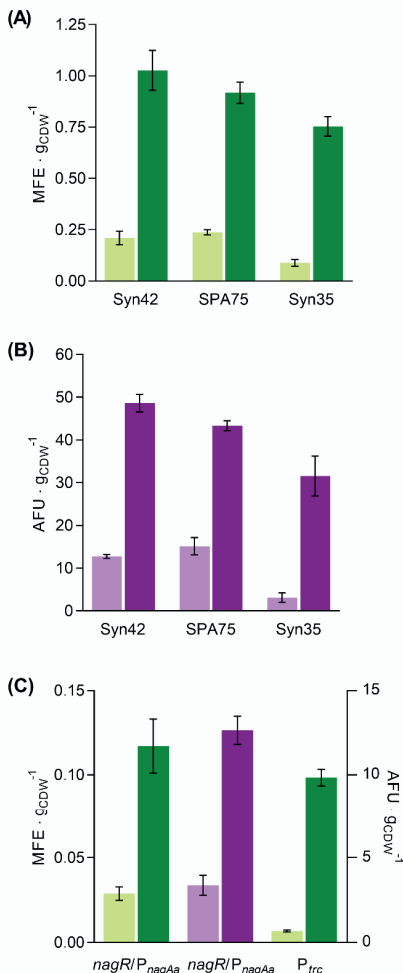


Figure 15. Evaluation of the developed gene expression constructs. Evaluation of plasmid-based expression of *msfGFP* (green) and *mCherry* (pink) with the traditional (light-colored) or optimized (dark-colored) expression cassette employing (A) constitutive and (B) the inducible *P_{nagAa}* promoter, (C) *msfGFP* expression under the control of the inducible *P_{Trc}* promoter from single copies of the traditional and optimized gene expression cassettes integrated into the *attTn7* site. Error bars indicate the standard deviation of three biological replicates except for the inducible *nagR/P_{nagAa}* construct expressing *mCherry* for which biological duplicates are represented. CDW, cell dry weight; MFE, μ moles of fluorescein equivalents; AFU, arbitrary fluorescence units.

All optimized gene expression constructs with the three tested constitutive promoters resulted in a substantial increase in fluorescence compared with their traditional counterparts (Figure 15A).

While the ranking of the promoter strength was maintained with the optimized gene expression cassettes, absolute differences in the level of expression were reduced as a much higher increase was observed for the weaker Syn35 promoter expressing *mCherry* (Table 4).

Table 4. Pairwise fold-changes of specific fluorescence (fluorescence per g cell dry weight) between the optimized and traditional gene expression cassettes. Calculated as described by Clifton et al. [175].

Expression system	pTN1 plasmid			-attTn7::	
Promoter	Syn35	Syn42	SPA75	<i>nagR</i> /P _{nagAa}	lacIq/P _{Trc}
<i>msfGFP</i>	8.7±1.6	5.0±0.9	3.9±0.3	4.1±0.7	14.7±1.6
<i>mCherry</i>	11.3±3.8	3.8±0.2	2.9±0.4	3.9±0.7	-

The lower fold increase in expression strength for the strong promoters suggests that the full potential of the optimized gene expression cassette in increasing protein expression is not reached here because of other cellular limitations, such as ribosome availability. This hypothesis is contrasted by a recent study, in which fluorescent protein expression in constructs harboring a RiboJ was evaluated using 24 different constitutive promoters covering a broad spectrum of expression strength.[175] From the presented single cell fluorescence values, a relatively stable fold change of the fluorescence output was observed for all tested constructs. Because of the distinct fluorescence measurements and standardization of the fluorescence values, the level of expression strength of the promoters used in the two studies cannot be compared. We can therefore not exclude that the SPA75 and Syn42 promoters used in our study are significantly stronger than the strongest promoters used by Clifton et al. and that an inverse correlation between fold change improvement and basic promoter strength is only observed for promoters exerting a very high expression strength.

3.2.3.2. Characterization of plasmid-based, inducible fluorescent protein expression

Controlled gene expression is required, for instance, in genetic circuits or when the synthesis of a target product harms cell fitness and needs to be decoupled from growth.[187]–[190] We, therefore, chose to further evaluate inducible gene expression by placing the two fluorescent reporter proteins under control of the *nagR*/P_{nagAa} promoter, inducible with low concentrations of the relatively cheap inducer salicylate.[191] In both, the traditional and optimized expression constructs, the bidirectional terminators were replaced with the unidirectional terminator Tn1 as the first attempt to reduce the overall size of the cassette. The removal of the bidirectional terminators should bear similar effects in both cassettes as they have the identical genetic context. Aside from the removal of the bidirectional terminators and the use of a different promoter, both expression cassettes contained the equal genetic parts used for the evaluation of the constitutive promoters (Figure 15B).

Under the control of the inducible *nagR*/P_{nagAa} promoter, the optimized gene expression cassette showed a similar behavior as with the strong constitutive promoters. The specific fluorescence was increased by 4-fold with the optimized gene expression cassette in comparison to their respective traditional counterparts (Figure 15C). A similar increase was observed for the

msfGFP signal under non-induced conditions whereas for the *mCherry* constructs only a 2-fold increase was observed (Appendix Figure 24).

The stable increase of the *msfGFP* signal under both induced and uninduced conditions supports the concept of a post-transcriptional gene expression enhancement. The lower fold ratio in the non-induced conditions observed with the *mCherry* constructs could be related to analytical inaccuracies of the weaker *mCherry* signal and longer maturation time of this fluorescent protein in comparison to *msfGFP*. Inducible promoters, such as the *nagR/P_{nagAa}* promoter system used in this work, tend to have a basal expression which could become problematic for the expression of toxic genes or their use in systems that need to be tightly regulated, *e. g.*, genetic circuits. Attempts to achieve non-leaky inducible expression systems have been made, but their number continues to be limited [192]. We propose the use of the optimized gene expression cassette in known non-leaky inducible promoter setups to increase the available expression range in such systems rather than aiming to engineer a novel non-leaky inducible variant. Since the additional parts of the optimized gene expression cassette tend to act on transcribed mRNA only, an optimized gene expression cassette harboring a tight, inducible promoter system could still exhibit the desired non-basal expression in the absence of the inducer and once induced, reach higher expression levels than the standard counterpart.

3.2.3.3. Characterization of inducible fluorescence expression of single, genome-integrated constructs

Genomic integration is generally preferred over plasmid-based expression when it comes to the stable construction of cell factories. Integrating the pathways into the genome grants higher genetic stability since it avoids common plasmid-based expression issues such as plasmid segregation and copy number variability, plasmid replication-related growth impairment, and antibiotic dependency [193]–[195]. However, genomic integration possesses specific disadvantages, like generally significantly lower expression levels and a limited number of characterized integration sites [196]. A common approach to overcome the low expression levels of single genomic integration is to directly or randomly integrate the desired expression cassette at multiple sites. However, the directed multiple integration procedure is laborious and limited by the number of characterized integration sites, whereas random integration requires high-throughput screening. As we had seen a significant increase in expression strength with the optimized cassettes located on a plasmid, we argued that this device might also be valuable to boost the output of genome-integrated constructs. To evaluate if the optimized gene expression cassette could relief the low expression limitation of genomic integrations, single genomic integration cassettes expressing *msfGFP* were constructed and integrated at the neutral *attTn7* site.

While Cambray et al. have shown a very beneficial effect on standardized gene expression in constructs with the T7 bacteriophage derived R1.1 RNase III cleavage site, a negative effect on absolute expression levels cannot be ruled out [179]. RNase III cleavage has been reported to have stabilizing as well as destabilizing effects depending on the mode of cleavage [197], [198]. While a single breakage, which leaves a folded structure at the 3' end, stabilizes the processed mRNA, a double breakage that removes the hairpin induces enhanced degradation. The mode of cleavage at the R1.1. RNase III site from the T7 bacteriophage used in this study is contradictorily

reported as harboring one or two cleavage sites and resulting in stabilized structures or mRNA molecules without 3' secondary structures [199]–[201]. We left out the RNase III cleavage site in the genome-integrated optimized construct to avoid a potentially adverse effect on mRNA stability and hence protein abundance. Further expansion of the promoter scope was sought by utilizing the standard LacI-repressed P_{Trc} promoter for driving the gene expression of genome integrated cassettes. As in the plasmid-based evaluations, the optimized gene expression cassette harbored the RiboJ and BCD2, whereas the traditional version contained the 2nd RBS of the BCD2 (Figure 14C).

Introducing this optimized gene expression cassette in the single genomic *attTn7* locus yielded a ca. 15-fold expression increase in comparison to the traditional analog, the highest fold increase observed in this work (Figure 15C). Even though RNase III is not the major endoribonuclease responsible for mRNA turnover in bacteria, the enzyme does contribute to mRNA degradation [202]. By removing the RNase III site from the optimized gene expression cassette, an mRNA degradation target was abolished, which might have resulted in an increased half-life of the transcripts and consequently higher expression levels.

The single, genome-integrated optimized expression cassette achieved expression levels of $0.098 \pm 0.005 \mu\text{mol fluorescein g}^{-1} \text{ cell dry weight (CDW)}$, an expression strength in the range of the plasmid-based optimized cassette under the control of the inducible promoter *nagR/P_{nagAa}* or the constitutive promoter Syn35 within the traditional cassette. Although the use of different promoters does not allow a fair comparison, it is still noteworthy to state that expression levels were achieved with the single genomic integration cassette, which are usually seen for episomally expressed genes.

3.2.3.4. Evaluation of a recombinant acetoin production pathway employing the optimized expression cassette

Finally, a heterologous acetoin pathway was cloned within the pTN1 plasmid backbone to further evaluate the optimized expression cassette in a production context. The acetoin pathway included a C83S mutant of the *E. coli* K-12 MG1655 acetolactate synthase (*ilvB*) and an acetolactate decarboxylase (*aldB*) from *Brevibacillus brevis* (Figure 4A). The *E. coli ilvB* C83S mutant was chosen due to its 4-fold lower K_m and 126% higher k_{cat}/K_m ratio compared with the wild type, making it one of the most efficient enzymes of this class so far characterized [203]. The *B. brevis aldB* was selected based on its low K_m value [204]. In the polycistronic design, expression of both genes was driven by the inducible *nagR/P_{nagAa}* promoter system while each gene was framed with a ribozyme, a bicistronic design version, and an RNase III site. The acetolactate synthase was framed with the VtmOJ ribozyme gene, the BCD1 bicistronic design, and the RNase III R0.5 site, whereas the acetolactate decarboxylase was surrounded with the RiboJ ribozyme gene, the BCD2 bicistronic design, and the RNase III R1.1 site (Figure 2D). The traditional expression cassette was obtained by removing the expression enhancing genetic parts while maintaining the 2nd RBS of BCD1 upstream of the *ilvB* and the 2nd RBS of BCD2 upstream of the *aldB* (Figure 14D).

Employing the optimized gene expression architecture to the acetoin pathway led to an acetoin accumulation of $5.5 \pm 0.76 \text{ mM}$, representing a 2.5-fold production increase when compared to the traditional counterpart (Figure 16B). The increase of acetoin production solely using the

optimized gene expression cassette shows that its use can be extended to production contexts. The optimized gene expression cassette could be advantageous for metabolic engineering approaches where high gene expression is required, such as redirecting native metabolites to the desired production pathway or for enzyme production for *in vitro* applications.

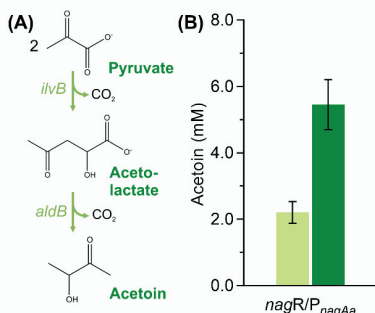


Figure 16. Acetoin production pathway comprising the C83S *ilvB* mutant from *E. coli* and *aldB* from *Brevibacillus brevis* (A). Acetoin titers achieved by the plasmid-based expression of the 2-gene operon under the control of the inducible P_{nagAa} promoter employing a traditional and an optimized expression cassette (B).

3.2.3.5. qPCR based elucidation of mRNA stability

The high fluorescence expression levels and increased acetoin production achieved by the optimized gene expression in this work arose from the combination of mRNA stabilizing and translation boosting genetic parts. Lou et al. integrated hairpins in both ribozymes used in this work, RiboJ and Vtmol, to expose the RBS and confirmed their catalytic functionality through rapid amplification of cDNA 5'-ends [174]. The presence of such hairpins in the 5'UTR region was reported to increase the respective mRNA half-life, which leads to higher protein production [205]. Further clarification of the stabilizing effect of the hairpin structure of RiboJ and its individual effect on protein expression has been published elsewhere [175]. To evaluate if such a phenomenon occurred in the optimized gene expression cassette and contributed to the lump sum of increased protein expression, qPCR assays were performed to compare the decay rates of the transcripts. For this purpose, cultivations of the strains expressing *msfGFP* under the control of the SPA75 promoter were treated with rifampicin and nalidixic acid in the early exponential growth phase, and mRNA samples were retrieved over time (Appendix Figure 25).

The addition of rifampicin inhibits bacterial RNA polymerase, whereas nalidixic acid inhibits a subunit of the DNA gyrase and topoisomerase. As the mRNA abundance data of the *msfGFP* were normalized with the data of the housekeeping gene *rpoB* to cancel out small differences in the template concentration, the determination of the absolute decay rate of the *msfGFP* transcript was not possible. Instead, we calculated the difference between the decay rates of the *rpoB* and the *msfGFP* mRNA (i.e., $k_{rpoB} - k_{msfGFP}$, with k being the decay rate). Given that the *rpoB* mRNA decay should be equal in both strains the delta can be used to reveal a possible difference in the *msfGFP* decay rates in the optimized and traditional expression architecture. As hypothesized, the data was significantly higher for the optimized construct (1.6-fold), which translates to a

Results

reduced decay rate of the *msfGFP* transcript (Figure 17). Hence, higher mRNA stability is indeed one factor contributing to the observed increase in fluorescence output and acetoin production.

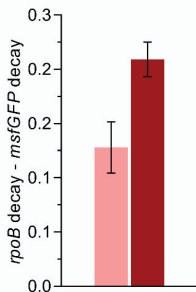


Figure 17. qPCR based elucidation of mRNA stability of *msfGFP* transcripts from the plasmid-based traditional (light-colored) and optimized (dark-colored) expression cassettes harboring the constitutive SPA75 promoter. Early exponential cultivations were treated with the antibiotics, nalidixic acid and rifampicin, to halt DNA replication and transcription, respectively. Samples were taken over time (time course data are shown in Error! Reference source not found.), and mRNA levels were assessed through qPCR. mRNA decay rates of transcripts from each expression cassette were retrieved through the difference between the decay rate of the housekeeping gene *rpoB* and the target *msfGFP*. Error bars indicate the standard deviation of two biological replicates.

3.2.4. Conclusion

In this study, the optimized gene expression cassette architecture proposed by Nielsen et al. was evaluated in *P. taiwanensis* VLB120 for the expression of fluorescent reporter genes and a 2-step acetoin biosynthesis operon [178]. The optimized gene expression cassette was characterized on a plasmid or single genomic integration basis with either constitutive or inducible promoters to cover all commonly used expression approaches in metabolic engineering. In all evaluations, the optimized gene expression cassette outperformed its traditional counterpart. The highest fold improvement was observed once the RNase III site was removed and evaluated on a single genomic integration basis under the control of the IPTG inducible P_{Ttc} promoter. Such a boost allowed a single genomic integration-based expression to achieve expression levels commonly reached with plasmids. Within the constitutive promoter paradigm, the optimized gene expression cassette increased expression levels of the strongest promoter of a promoter library, showing that this tool could be used to extend expression ranges further. The mRNA transcripts retrieved by the optimized gene expression cassette harnessed higher stability than the transcripts from the traditional counterpart, validating that mRNA stability contributed to the observed results. This work demonstrates the applicability of the optimized gene expression cassette as a tool to achieve high gene expression levels through transcription-independent approaches that rely on mRNA stability and translation efficiency.

Chapter 3.3

Expanding *Pseudomonas taiwanensis* VLB120's acyl-CoA portfolio: propionate production in mineral salt medium

Partially submitted as

D. Neves, D. Meinen, T. B. Alter, L. M. Blank and B. E. Ebert, "Expanding *Pseudomonas taiwanensis* VLB120's acyl-CoA portfolio: propionate production in mineral salt medium." *Microb. Biotechnol.*, 2023. doi: 10.1111/1751-7915.14309

Contributions

Dário Neves conceived the study and performed the experiments. Daniel Meinen constructed the propionyl-CoA chassis strain. Tobias Alter performed the flux balance analysis. Dário Neves prepared the figures and wrote the manuscript with the help of Birgitta Ebert and Lars M. Blank.

3.3. Expanding *Pseudomonas taiwanensis* VLB120's acyl-CoA portfolio: propionate production in mineral salt medium

3.3.1. Abstract

As one of the main precursors, acetyl-CoA leads to the predominant production of even-chain products. From an industrial biotechnology perspective, extending the acyl-CoA portfolio of a cell factory is vital to producing industrial relevant odd-chain alcohols, acids, ketones, and polyketides. The bioproduction of odd-chain molecules can be facilitated by incorporating propionyl-CoA into the metabolic network. The shortest pathway for propionyl-CoA production relies on succinyl-CoA catabolism, encoded by the sleeping beauty mutase operon. This work evaluated the use of the sleeping beauty mutase in *Pseudomonas taiwanensis* VLB120. A single genomic copy of the sleeping beauty mutase genes *scpA*, *argK*, and *scpB* combined with the deletion of the methylcitrate synthase PVLB_08385 was sufficient to observe propionyl-CoA accumulation in this *Pseudomonas*. The chassis' capability for odd-chain product synthesis was assessed by expressing an acyl-CoA hydrolase, which enabled propionate synthesis. Three fed-batch strategies during bioreactor fermentations were benchmarked for propionate production, in which a maximal propionate titer of 2.8 g L⁻¹ was achieved. Considering that the fermentations were carried out in mineral salt medium under aerobic conditions and that a single genome copy drove propionyl-CoA production, this result highlights the potential of *Pseudomonas* to produce propionyl-CoA derived, odd-chain products.

3.3.2. Introduction

Coenzyme A (CoA) activated carboxylic acids play a crucial role in microbial metabolism by acting as a carrier of reactive acyl groups and facilitating enzyme recognition [206]. The shortest acyl-CoA, acetyl-CoA, is a vital metabolite in the carbon metabolism of all living systems and essential for fuelling the TCA cycle and fatty acid biosynthesis [207]. All major workhorses in the metabolic engineering field are confined to dependency on acetyl-CoA, leading to the production of even-chain products. The production of odd-chain products requires the incorporation of propionyl-CoA into the metabolic network. Industrial-relevant products that rely on propionyl-CoA are odd-chain alcohols, acids, ketones, and polyketides such as 1-propanol [208], 1-pentanol [209], propionic acid [210], valeric acid [209], 2-butanone [211] or 6-deoxyerythronolide B [212]. Incorporating propionyl-CoA into a metabolism lacking this acyl-CoA, like *E. coli*'s metabolism, can be achieved, for instance, by feeding propionate or through fatty acid activation/degradation by adding odd-chain fatty acids [213]. Besides these feeding strategies, three *de novo* synthesis pathways of propionyl-CoA have been reported, a catabolic pathway of succinyl-CoA native to *E. coli* [214], [215], a heterologous catabolic pathway of 2-ketobutyrate [216], and the 3-hydroxypropionate cycle from thermoacidophilic crenarchae *Metallosphaera sedula* and *Sulfolobus tokodaii* [138] (

The three *de novo* synthesis pathways for propionyl-CoA production diverge from different points in the central carbon metabolism and differ in length. The catabolic succinyl-CoA pathway catalyzed by *E. coli*'s sleeping beauty mutase (*sbm*) requires only two reactions and is the shortest of the three alternatives.

Figure 18).

The three *de novo* synthesis pathways for propionyl-CoA production diverge from different points in the central carbon metabolism and differ in length. The catabolic succinyl-CoA pathway catalyzed by *E. coli*'s sleeping beauty mutase (*sbm*) requires only two reactions and is the shortest of the three alternatives.

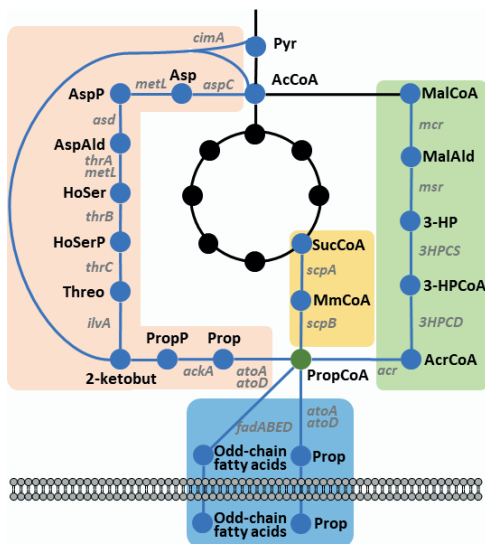


Figure 18. Strategies for propionyl-CoA production. Addition of odd-chain fatty acids and propionate to the cultivation medium (blue); catabolic pathway of 2-ketobutyrate (red); catabolic pathway of succinyl-CoA (yellow) employing the sleeping beauty mutase, and the 3-hydroxypropionate cycle from *Metallosphaera sedula* and *Sulfolobus tokodaii* (green). Asp, aspartate; AcCoA, acetyl-CoA; AspP, aspartyl-phosphate; AspAld, aspartate-semialdehyde; HoSer, homoserine; HoSerP, homoserine-phosphate; Threo, threonine; 2-ketobut, 2-ketobutyrate; PropP, propionyl-phosphate; Prop, propionate; PropCoA, propionyl-CoA; SucCoA, succinyl-CoA; MmCoA, methylmalonyl-CoA; MalCoA, malonyl-CoA; MalAld, malonic semialdehyde; 3-HP, 3-hydroxypropionate; 3-HPCoA, 3-hydroxypropionyl-CoA; AcrCoA, acryloyl-CoA; CimA, citramalate synthase; AspC, aspartate aminotransferase; MetL, aspartokinase/homoserine dehydrogenase 2; Asd, aspartate-semialdehyde dehydrogenase; ThrA, aspartokinase/homoserine dehydrogenase 1; ThrB, homoserine kinase; ThrC, threonine synthase; IlvA, threonine dehydratase; AckA, acetate kinase; AtoA, acetate CoA-transferase subunit B; AtoD, acetate CoA-transferase subunit A; FadA, 3-ketoacyl-CoA thiolase; FadB, fatty acid oxidation complex subunit alpha; FadE, acyl-CoA dehydrogenase; FadD, long chain fatty acid-CoA ligase; ScpA, methylmalonyl-CoA mutase; ScpB, methylmalonyl-CoA decarboxylase; Mcr, malonyl-CoA reductase; Msr, malonic semialdehyde reductase; 3HPCS, 3-hydroxypropionyl-CoA synthase; 3HPCD, 3-hydroxypropionyl-CoA dehydratase and Acr, acryloyl-CoA reductase.

The *sbm* operon has been successfully used for the production of several propionyl-CoA dependent products by either activation of the operon on the genome [210], [211], [217] or by plasmid-based overexpression [208], [218], [219]. The *sbm* operon of *E. coli* MG1655 comprises four genes encoding a methylmalonyl-CoA mutase (*scpA*), a membrane-bound ATP kinase (*argK*), a methylmalonyl-CoA decarboxylase (*scpB*), and a propionyl-CoA:succinate-CoA transferase (*scpC*). The function of the ATP kinase ArgK has not been fully elucidated but has been suggested

to interact with ScpA [214] and was described to contribute to enzyme activity [208]. Achievements in producing propionyl-CoA-derived products through metabolic engineering approaches have been comprehensively reviewed by Srirangan et al. [220].

Pseudomonas strains are generally discussed as promising hosts for industrial biotechnology because they harness distinctive features like broad carbon source utilization, the ability to proliferate in the presence of organic solvents, and non-fermentative growth [101], [108], [221]. This species has been successfully used to produce acetyl-CoA-derived products such as rhamnolipids [107], [222], methylketones [74], polyhydroxyalkanoates [223]–[225] and other natural products like terpenoids [226], polyketides [227], [228], and non-ribosomal peptides [229]. Contrarily, only a few examples of products synthesized from propionyl-CoA exist for this species and are mostly limited to the degradation of branched-chain amino acids and L-methionine [230], [231]. Propionyl-CoA has not been detected in *Pseudomonas* indicating low abundance or missing enzymatic capabilities to synthesize this acyl-CoA species. [232], [233]

However, we argue here that *Pseudomonas* could be turned into a superior host for propionyl-CoA biosynthesis from succinyl-CoA by harnessing its capability to supply this precursor at a high rate via its highly active TCA cycle flux reported for diverse strains of this species to reach values up to 4-times higher than in *E. coli* [112], [221], [234], [235]. Accordingly, this work aimed to couple this naturally high TCA cycle flux in *Pseudomonas* with heterologous expression of the sleeping beauty mutase from *E. coli* to derive a *P. taiwanensis* VLB120 [114] propionyl-CoA chassis and to showcase its potential for odd-chain length product synthesis on the example of the important building block propionate. This carboxylic acid has a broad application spectrum, including as an FDA-approved food preservative or herbicide [236] or additive in lacquer formulations and molding plastics [237], making it an interesting target for this study.

3.3.3. Results and Discussion

3.3.3.1. Extending the acyl-CoA portfolio of *P. taiwanensis* VLB120 by expressing the sleeping beauty mutase

The alternative propionyl-CoA synthesis pathways shown in Figure 18 were found to provide similar theoretical yields from glucose as carbon source (Table 5). We opted for the sleeping beauty mutase pathway due to the shorter length of the pathway when compared to alternative biosynthesis routes and the probability to achieve theoretical maximal yields as shown by an *in silico* flux balance analysis assuming TCA cycle fluxes previously observed for *P. putida* K2440 (Table 5) [112].

Table 5. Theoretical yields of propionate production from glucose for the three alternative propionyl-CoA pathways expressed in *P. taiwanensis* VLB120. Simulations are based on a genome-scale metabolic model of *P. taiwanensis* VLB120 constrained with physiological data taken from Ebert et al. [112].

Pathway	Theoretical [mol/mol]	yield
Succinyl-CoA catabolism	1.59	
2-ketobutyrate catabolism	1.59	
3-hydroxypropionate cycle	1.57	

Three out of the four *sbm* operon genes (*scpA*, *argK*, and *scpB*) were retrieved from the genome of *E. coli* MG1655 and assembled into a genomic integration construct, which placed this reduced

operon under the control of the salicylate inducible *nagR/P_{nagAa}* promoter system and incorporated it into the single, neutral *attTn7* site. The fourth gene, *scpC*, was omitted in the initial strain to avoid a possible loss of propionyl-CoA by transfer of the CoA group to succinate. Expressing this integration construct without further modification of *P. taiwanensis* VLB120 led to a marginal accumulation of propionyl-CoA (Table 6).

Propionyl-CoA is an intermediate of the β -oxidation of odd-chain fatty acids and amino acid degradation and is metabolized by the methylcitrate cycle, which it enters by condensation with oxaloacetate to 2-methylcitrate. Deletion of the gene PVLB_08385, which encodes the corresponding methylcitrate synthase, led to a 158-fold increase in propionyl-CoA accumulation, demonstrating the vital role of this knock-out for the successful construction of a *P. taiwanensis* VLB120 propionyl-CoA chassis strain (Table 6).

Table 6. Propionyl-CoA levels in constructed strains. Propionyl-CoA levels in the wild-type strain *P. taiwanensis* VLB120 (VLB120), the single genomic integrated strain at the *attTn7* site expressing the *sbm* operon (Tn7_*sbm*) and, the single genomic integrated construct in the PVLB_08385 knock out strain (Tn7_*sbm* Δ PVLB_08385). Errors indicate the standard deviation of biological duplicates.

Strain	Propionyl-CoA (nmol/g _{CDW})
VLB120	<0.01
Tn7_ <i>sbm</i>	0.02 \pm 0.01
Tn7_ <i>sbm</i> Δ PVLB_08385	3.56 \pm 1.03

Divergent statements regarding the auto sufficiency of the sleeping beauty mutase operon to convert succinyl-CoA to propionyl-CoA have risen in the past. Whereas Gonzalez-Garcia et al. [218] claimed the need for an epimerase to convert the stereoisomers of methylmalonyl-CoA, Haller et al. showed the conversion of succinyl-CoA into propionyl-CoA in *in vitro* enzymatic assays with methylmalonyl-CoA mutase (ScpA) and decarboxylase (ScpB) but lacking the epimerase [214]. Gonzalez-Garcia further alleged that without an epimerase, the production of propionate, and therefore also propionyl-CoA, is fueled by the degradation of amino acid provided by the yeast extract in the medium. In the present study, propionyl-CoA production was achieved in a mineral salt medium with no addition of yeast extract, giving evidence that ScpA and ScpB are sufficient to enable propionyl-CoA synthesis in *P. taiwanensis* VLB120, which to our knowledge, does not possess a methylmalonyl-CoA epimerase.

3.3.3.2. Propionate production in *P. taiwanensis* VLB120

Propionate was previously produced in reasonable amounts by knocking out the *ack* gene in the natural propionate producer *Propionibacterium acidipropionici* [238], activating the sleeping beauty mutase operon [210] or through L-threonine degradation in *E. coli* [216]. Further work with the sleeping beauty mutase for propionate production in *E. coli* was recently published by Miscovic et al., in which the role of each of the TCA metabolic routes was elucidated, and the deletions of Δ *sdhA* Δ *iclR* were shown to be vital to achieve a 30 g L⁻¹ propionate titer in M9 mineral salt medium supplemented with yeast extract [239]. Propionate was also produced in high amounts in *P. putida* KT2440 by the transformation of exogenous L-threonine to propionyl-CoA and further to propionate by action of a thioesterase [240]. However, the sleeping beauty mutase pathway has not been evaluated in this species yet.

We chose propionate synthesis as a case study to elucidate the potential of the *P. taiwanensis* VLB120 propionyl-CoA chassis because of the industrial relevance of this compound and its short

production pathway encompassing only one additional enzymatic step. The biocatalytic performance of two alternative enzymes with different catalytic mechanisms was evaluated. The acyl-CoA hydrolase YciA from *Haemophilus influenzae* (Uniprot P44886) was chosen because it does not require a CoA acceptor. The second enzyme, AarC, a CoA transferase from *Propionibacterium freudenreichii subsp. shermanii* (Uniprot A0A160VNBK6) is a monomer [241], an advantage from an expression burden point of view, and its overexpression in the native host was found to considerably improve propionate production [242]. The enzyme requires succinate as CoA acceptor, which allows CoA recycling into the TCA cycle, potentially leading to a less detrimental effect on the TCA cycle flux. The selection of *yciA* over the *scpC* from the sleeping beauty mutase operon of *E. coli* was based on superior kinetic enzymatic properties of *yciA*, namely, lower K_M and superior k_{cat} [214], [243]. Both enzymes were assembled into the pTN1_*nagR*_Tra and Opt plasmids [161] to evaluate two inducible expression cassettes with different expression levels and transformed into the propionyl-CoA chassis strain *P. taiwanensis* VLB120 ΔPVLB_08385 Tn7_sbm.

The pTN1_*nagR*_Tra plasmid expresses the genes from an operon consisting of the inducible promoter and an RBS. In contrast, the pTN1_*nagR*_Opt plasmid contains additionally a ribozyme, the bicistronic design developed by Mutalik et al. [158], and an RNase III restriction site which was shown to lead to higher expression levels [161]. Preliminary experiments showed that propionate production only started once the nitrogen source was depleted (data not shown). Therefore, the four constructed strains were evaluated under two growth conditions. One growth medium contained equimolar amounts of the carbon (glucose) and nitrogen (ammonium sulfate) source (C:N of 6:1), whereas the second contained only half of the nitrogen amount (C:N of 12:1) to assess if the excess carbon would be converted into propionate. Evaluation of the four strains under these two conditions showed that the strains expressing the *yciA* or the *aarC* gene in the traditional expression construct achieved the highest absolute propionate titer in the medium with equimolar amounts of carbon and nitrogen with the *yciA* slightly outperforming the *aarC* expressing strain. Surprisingly, propionate synthesis with presuming higher expression of both tested genes using the optimized expression constructs was outpaced by their traditional counterparts (Figure 19). This reduced performance cannot be attributed to a higher metabolic burden, or a metabolic imbalance caused by elevated pathway expression since the growth profiles of the strains harboring either the traditional or optimized constructs were similar (data not shown). This phenomenon is not novel since it was previously observed that higher gene expression does not necessarily translate into higher production rates [244].

Based on this initial screen, the strain with the genome-integrated sleeping beauty operon and void of the methylcitrate synthase expressing the pTN1_Tra_*yciA* plasmid was selected for evaluation in a bioreactor set-up.

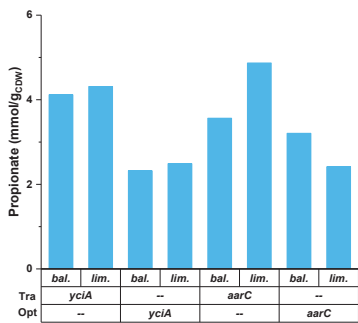


Figure 19. Specific propionate production by the propionyl-CoA chassis *P. taiwanensis* Tn7_sbm ΔPVLB_08385 expressing either the *yciA* or *aarC* in the pTn1 traditional (Tra) and optimized (Opt) variants using MSM₁₂ medium supplemented with 50 mM glucose with balanced amounts of nitrogen (bal.; C:N ratio of 6) or limited nitrogen content (lim.; C:N of 12). Data represents single biological experiments.

3.3.3.3. Benchmarking of fed-batch fermentation strategies for propionate production

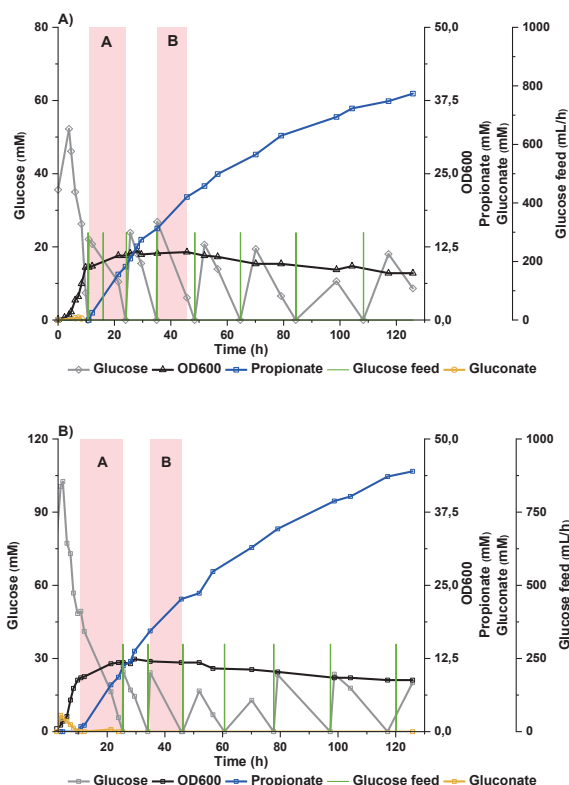
Bioreactor experiments were conducted with the *P. taiwanensis* VLB120 Tn7_sbm ΔPVLB_08385 expressing the pTn1_Tra_yciA plasmid to achieve increased propionate titers by performing the cultivations under controlled pH and prolonged nitrogen-limited conditions. Three fed-batch strategies were pursued to evaluate the influence of feeding regimes and feast-famine switches over the performance of the propionate-producing strain during bioreactor fermentations (Figure 20). Two of these strategies used a feeding script that added 25 mM glucose when the dissolved oxygen (DO) signal increased above 50 %. This procedure was repeated until the additional carbon did not lead to a decrease in the DO signal, indicating that the cells were no longer metabolically active. Two initial glucose concentrations of 50 mM and 100 mM were evaluated. The evaluation of different initial glucose amounts was motivated by the observation that production only started once the nitrogen source was depleted. The two different initial glucose concentrations aimed at achieving the first feast-famine switch, represented by the first glucose pulse, at two different fermentation stages: the late exponential stage at 50 mM and the late stationary stage at 100 mM initial glucose concentration, respectively. The feeding of the third strategy relied on an online feedback-loop unit, which monitored the glucose concentration inside the bioreactor through an enzymatic-amperometric module and continuously fed glucose to maintain a concentration of 25 mM throughout the fermentation. In the DO-controlled fed-batch strategy, the cells were submitted to stressful feast-famine switches, which were avoided in the feedback-loop controlled fed-batch fermentation with continuous glucose feed.

The *P. taiwanensis* VLB120 Tn7_sbm ΔPVLB_08385 pTn1_Tra_yciA exhibited similar growth rates and achieved similar propionate titers in all fed-batch regimes (Table 7). Product yields and productivities achieved with the three fed-batch fermentation strategies were calculated at the beginning of the stationary phase, at which product formation started, and at a later point to evaluate the robustness of the strain under the different fermentation conditions. In all three fermentations, the productivity declined over the course of the fermentation (Table 7). This decrease can be related to a higher metabolic fitness of the cells during the initial stationary

phase apparent from faster glucose consumption (Table 7). An opposite trend was observed for the product yields, which improved in all setups at the later fermentation stages. Although in both evaluated periods, the cells are in a stationary phase, the increased yield might be explained by the transient phase into the resting cell state at the early time point, where resources were still directed into growth as apparent from an increase in biomass.

In both the DO-controlled fed-batch starting with 50 mM glucose and the feedback-loop controlled fermentation, a maximal specific productivity of $11 \text{ mg h}^{-1} \text{ g}^{-1}$ was observed. The feedback-loop controlled fermentation achieved a product yield 13% higher than the DO-controlled 50 mM glucose fed-batch showing some benefits of the continuous glucose availability. However, despite the yield differences between the different fermentation strategies, there was no significant difference between the propionate titers.

The titers reached with this engineered *Pseudomonas* strain are far from the highest production levels published. However, in all reported studies, high amounts of yeast extract were added to the production media, contributing to propionate production through amino acid catabolism [210], [216], [238], [239]. For a fair benchmark with other cell factories, comparable conditions,



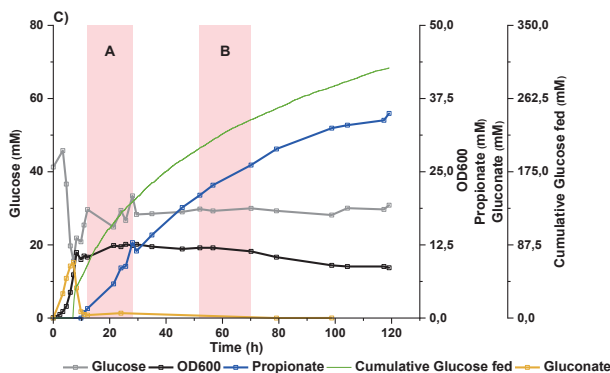


Figure 20. Representative fermentation profiles of the three evaluated fed-batch modes, DO triggered addition of 25 mM of glucose with a (A) 50 mM of initial glucose and (B) with 100 mM of initial glucose concentration and, (C) feedback-loop controlled fed-batch maintaining a constant glucose concentration of 25 mM. The time periods highlighted in red represent the initial, A, and later time periods, B, evaluated for productivities, titers and glucose uptake rates shown in Table 7.

namely, production in mineral salt medium without adding yeast extract and single-copy expression of the sleeping beauty mutase, need to be employed. Closest to this requirement is the work of Li et al. [219], who reported the production of 2.72 g L^{-1} propionate with *E. coli* expressing the sleeping beauty mutase from the medium-copy plasmid pET28a (~10-20 copies) under a strong constitutive promoter cultivated in mineral salt medium with glucose as sole carbon source. When a methylmalonyl-CoA mutase from *Methylobacterium extorquens* AM1 was co-expressed from the pACYC184 plasmid (~10 copies) under the control of the same strong promoter, the propionate titer increased to 4.95 g L^{-1} .

Although the titer achieved in the present work stayed below this benchmark, the following considerations underline the potential of *Pseudomonas*. Propionate production in *E. coli* was achieved under microaerobic conditions leading to fermentation and significant succinate secretion in the engineered strain void of lactate and formate production pathways. The strain was engineered to run the reverse TCA cycle and the significant succinate secretion reflects thermodynamic hindrances of its conversion to succinyl-CoA [219]. *Pseudomonas* fermentations are conducted under aerobic conditions in which the strain runs the oxidative TCA cycle, which might lead to lower yields due to carbon loss in form of CO_2 but is thermodynamically more favorable. Furthermore, the fact that no byproducts are produced might counterbalance the lower yield since according to Gonzalez-Garcia et al., one of the main reasons that makes biological propionate production not competitive is the complex downstream process required to remove the undesired fermentation byproducts [245].

Besides these metabolic advantages of *Pseudomonas*, it is important to reckon that minimal genetic engineering was employed to the production strain in this initial work, as in contrast to the previous *E. coli* work, which only lead to ca. 10% of the theoretical yield of propionate production in *P. taiwanensis* VLB120 with glucose as carbon source (Table 7). Anticipating that gene expression optimization has a similar impact on propionate production as in *E. coli*, there is

high potential to greatly improve propionate synthesis in *Pseudomonas* and propel it into competitive ranges.

Table 7. Comparison of yields, productivities, and glucose uptake rates of the *P. taiwanensis* VLB120 propionate production strain during the three evaluated fed-batch strategies. DO triggered with 50 mM (50 mM_i) and 100 mM (100 mM_i) of initial glucose and feedback-loop controlled fed-batch (TRACE) at two different fermentation stages (A and B). The errors in 50 mM_i and 100 mM_i represent biological replicates whereas the TRACE represents a single experiment.

Parameter	Period	Fermentation set-up		
		50 mM*	100 mM*	Trace
Max. specific growth rate (h ⁻¹)	-	0.19 ± 0.01	0.20 ± 0.01	0.22
Max. titer (mM)	-	36 ± 3	39 ± 6	35
Product yield (mg g _{CDW} ⁻¹)	A	83 ± 3	66 ± 19	95
	B	94 ± 11	100 ± 13	120
Productivity (mg L ⁻¹ h ⁻¹)	A	84 ± 3	67 ± 11	82
	B	62 ± 1	55 ± 2	44

*initial glucose concentration.

3.3.4. Conclusion

This study presents the engineering of the propionyl-CoA synthesis capabilities into *P. taiwanensis* VLB120 and demonstrated the capacity of this strain to produce products derived from propionyl-CoA from glucose as sole carbon source using propionate as a relevant example. A crucial step to produce this organic acid was the deletion of the methylcitrate synthase, encoded by PVLB_08385, which enabled propionyl-CoA accumulation in a strain expressing a single genomic integrated copy of the sleeping beauty mutase operon. The capability of this strain to produce propionate when co-expressing an acyl-CoA hydrolase was assessed in bioreactor fermentations and showed robust production performance under different fed-batch schemes. Besides robust behavior, the titers achieved are promising, considering that production was achieved with a minimal engineering approach, including a single-copy genome integration of the sleepy beauty mutase operon. Evaluating *P. taiwanensis* under stress conditions to increase TCA cycle activity as well as optimizing the expression of the sleepy beauty mutase and acyl-CoA hydrolase should be considered in future work. Nevertheless, this initial work showed the promising and expandable potential of *Pseudomonas* to produce propionyl-CoA derived products.

Chapter 4

General discussion

Contributions

This chapter was written by Dário Neves and reviewed by Lars M. Blank.

4. General Discussion

4.1. Development of cross-species genetic tools

Gene expression is the foundation on which cell factories rely to produce chemicals critical for human society. The main genetic part responsible for gene expression is promoters, which are the docking region for RNA polymerases. Several strategies to extend the affinity levels between promoters and RNA polymerase have been pursued, but are generally evaluated only in one specific organism and in most cases in model organisms like *E. coli* or *S. cerevisiae* [153], [246]. In the past, model organisms were commonly used as chassis to produce chemicals since these harnessed most of the information about metabolic networks, and the efficiencies of molecular biology tools in these always surpassed the ones in other microorganisms. This created a snowball effect that continuously increased the gap of characterized genetic parts between model and non-model organisms. In the past years, this gap has started to be narrowed down with the use of CRISPR-based technologies which allows engineering non-model organisms at rates usually confined to model organisms. This technological advance allied with the increasing pressure to obtain cell factories to replace petrochemical industries responsible for the growing global temperatures, started to melt the snowball which distanced model and non-model microorganisms for sustainable chemical production. The realization that model organisms have metabolic constraints and phenotypic shortcomings that compromise their industrialization boosted the focus on non-model organisms and the seek for the most suitable chassis for each product. Despite this, the knowledge gap regarding the performance of genetic parts in model and non-model organisms is still substantial and hinders the proper evaluation of which is the most suitable chassis for a specific product. The lack of genetic tools that guarantee similar gene expression of biosynthetic pathways in model and non-model organisms always raises the question if performance differences are related to divergent expression levels or intrinsic metabolic and phenotypic traits.

In this thesis, a contribution was made to close this gap between model and non-model organisms by characterizing three σ_{70} -dependent promoter libraries (SPL35, SPL42, and SPA) in *E. coli* and *P. taiwanensis* VLB120 and finding common ground between these two cell factories. These libraries were derived from two synthetic promoters, BG42 and BG35, which have distinct expression strengths and differ in the spacer sequence.[128] The SPLs were created by randomizing either the -35 and -10 consensus boxes of BG42 and BG35 whereas for the SPA the 17 nucleotide spacer was randomized of the BG42 sequence while maintaining the sequence length of the promoters and single segments. Some positions were kept constant in SPL42 and SPL35 to avoid the creation of non-functional promoters. Each promoter was characterized in both species by a specific GFP production rate expressed in molar fluorescence equivalents per biomass and time unit. This promoter performance indicator describes the expression strength during exponential growth, compensating for potential differences due to discrepancies in growth rate. It resembles and anticipates the performance of the characterized promoters for metabolic engineering purposes. The use of molar fluorescence equivalents should also permit inter-laboratory and interexperiment comparison of gene expression and allow the compilation of standardized experimental data for machine learning purposes.

The synthetic promoters were first characterized in *E. coli*, and the data served as a benchmark for comparison with *P. taiwanensis* VLB120. The promoters were characterized using this novel GFP production rate metric and comparison with the more commonly used biomass-specific fluorescence unit showed a linear relationship for weak promoters but a dispersed distribution for stronger promoters. This suggests that the specific GFP production rate could be a more robust indicator for promoter libraries with large dynamic ranges, particularly for metabolic engineering and growth-dependent production processes.

The promoter libraries were also characterized in *P. taiwanensis* VLB120, and the results showed, just like in *E. coli*, a higher potential for modulating expression by changing the spacer sequence rather than the consensus boxes. It was also observed that the different promoter segments influence each other, rather than contributing independently to promoter strength, which complicates the definition of guidelines for designing promoters and suggests the need for complex, nonlinear models, or machine-learning approaches. Finding common ground between *E. coli* and *P. taiwanensis* VLB120 seemed to be rather a difficult road since less than 10% of the promoters had similar performance in both strains, confirming that the assumption that a given promoter works similarly in both organisms is inappropriate.[153], [154] Also, it was found that the strongest promoters in *P. taiwanensis* VLB120 had higher GC content, while in *E. coli* the opposite was true. This may be due to the evolution towards different genomic GC contents in the two species.[168] Three sets of inter-species performing promoters were identified: those with similar behaviour in both strains, those with stronger performance in *E. coli*, and those with stronger performance in *P. taiwanensis* VLB120. Promoters with similar performance in both strains would be particularly useful for cell factory development as they allow for proper comparison of the two strains. Promoters with stronger performance in *P. taiwanensis* VLB120 could be beneficial to facilitate the construction of expression constructs that tend to be toxic in *E. coli* since the lower gene expression in this organism would avoid interferences during the gene assembly workflow.

In addition to the work described in this thesis, there are several potential avenues for future research. One possibility is to expand the promoter libraries to increase the coverage of the promoter combination space. This could potentially identify additional promoters with similar expression in both *E. coli* and *P. taiwanensis* VLB120, which could be useful for cell factory development. Another important area for future work is to test the promoters with similar expression in both organisms in pathway assemblies and compare the outcomes. This would provide further insight into the utility of these promoters for metabolic engineering purposes. It would also be interesting to test the promoter characterization workflow described in this text with other organisms. This could provide a more comprehensive understanding of the applicability of this approach to different species and could help identify any generalizable patterns that might be useful for promoter design. Testing other reporter genes besides *msfGFP* could help to determine whether the outcomes of this work are reporter gene independent. This could be useful for understanding the robustness of the findings and for identifying promoters that might be useful for a wide range of applications. Finally, it might be interesting to explore other promoter classes, such as T7 or Sp6-dependent promoters, to gain a more complete understanding of the diversity of promoters available for use in metabolic engineering and possibly identify promoter classes that are more suitable for cross-species studies.

4.2. Development of enhanced gene expression architectures

Cell factories, which are used to produce chemicals and biological products, often seek to increase productivity through genetic engineering methods. One strategy for increasing enzyme activity is the use of strong promoters to overexpress product biosynthesis genes. However, this approach can have drawbacks, as the use of strong promoters can lead to metabolic burden and growth impairment by high jacking the transcriptional machinery of the cell. In recent years, synthetic biology parts have been developed that support high gene expression without relying on strong promoters. These parts target translation rather than transcription and can be divided into two categories: those that stabilize mRNA and those that increase translational efficiency.

In this thesis, both approaches have been combined into an optimized gene expression cassette to achieve high gene expression. The genetic elements incorporated to stabilize mRNA consisted of ribozymes and RNase III sites whereas the bicistronic design was responsible to increase the translational efficiency.[158], [174], [199]–[201] The optimized gene expression cassette was tested using different promoters and vectors to express reporter genes and an acetoin production pathway. In all the tested combinations the optimized gene expression cassettes outperformed their traditional counterparts, which were assembled by omitting the translation-enhancing genetic elements while maintaining the ribosome affinity towards the mRNA. The role of mRNA stability in the observed increase of gene expression by the optimized gene expression cassette was elucidated through qPCR-based decay rates comparisons. The increase in expression levels between the optimized and traditional cassette was not proportional between the different tested promoters, having the highest fold increase been observed in the weakest of these promoters. This suggests that the other promoters could be too strong and that an expression plateau was reached when combined with the optimized gene expression architecture. It would be interesting to increase the number of promoters tested and rather focus on weaker promoters to properly evaluate the potential of this tool. In the future, further investigation could focus on the application of this tool in pathway assembly for cell factories, particularly on bottleneck steps where gene expression is a limiting factor. Additionally, the application of this tool for protein production could be of particular interest, as high expression levels can be achieved with a single genomic integration, potentially avoiding the use of plasmids and antibiotics in these processes.

4.3. Extending the acyl-CoA portfolio of *Pseudomonas taiwanensis*

P. taiwanensis VLB120 is generally considered a promising host for industrial biotechnology due to its distinctive features such as the ability to utilize a broad range of carbon sources, the ability to grow in the presence of organic solvents, and the non-fermentative growth.[101], [108], [221] While this species has been successfully used to produce a variety of products derived from acetyl-CoA, examples of products synthesized from propionyl-CoA are rather scarce. Propionyl-CoA, a vital intermediate for the synthesis of odd-chain products has not been detected in Pseudomonads, suggesting a limited capacity to produce these types of products. To expand the metabolic capabilities of *Pseudomonas* and enable the production of propionyl-CoA-dependent products, it is necessary to incorporate this acyl-CoA into the metabolic network of the organism. In this work, the implementation of the sleepy beauty mutase operon from *E. coli* was proven to extend the acyl-CoA portfolio of *P. taiwanensis* VLB120 and was showcased with the production

of propionate. However, the sole implementation of the sleepy beauty mutase was not enough to observe propionyl-CoA accumulation and required the deletion of the methylcitrate synthase, encoded by PVLB_08385. The potential of *P. taiwanensis* VLB120 to produce propionyl-CoA-dependent products in this work was barely explored since the propionyl-CoA synthesis was reliant on a single genomic copy of the sleepy beauty mutase and the capability of this strain to provide higher TCA cycle fluxes than *E. coli*, and therefore a higher pool of the precursor succinyl-CoA, was untouched. Despite this, *P. taiwanensis* VLB120 was able to reach similar propionate titers to previous studies performed in comparable conditions with minimal genetic manipulations. The engineered *P. taiwanensis* VLB120 for propionate production was further evaluated in bioreactor fermentations to assess how this strain would perform when subjected to different fed-batch strategies. The different fed-batch strategies targeted how the strain would respond to different feeding regimes and feast-famine switches to understand, which fermentation strategy could manipulate the overall metabolism to increase the fluxes through the TCA cycle to enhance the accumulation of succinyl-CoA. Such strategies focused on starting the fermentations with different C:N ratios to reach the stationary phase with either a depletion or a surplus of carbon source. Besides this, the effect of feast-famine switches was also evaluated by either adding carbon source once it was depleted or by continuously feeding glucose to maintain a certain concentration within the bioreactor. Notably, the propionate titers reached in the tested conditions were rather similar observing mainly differences in product yield and productivities. This demonstrates that *P. taiwanensis* VLB120 has a relatively robust performance for propionate production, which could be rather interesting for industrial purposes since it could handle heterogeneity within the bioreactor.

With this, the potential of Pseudomonads to produce odd-chain products was revealed and opened several avenues for future research. In this thesis, minimal genetic engineering was employed to reach propionate production, which could be further optimized by attempting to increase the copy number of the sleepy beauty mutase operon in the genome. This could be achieved through multiple genomic integrations using systems like the Tn5 transposon which deploys randomly the integration cassette in the genome. Such an approach would however require screening since the random integration could hit important genes for proper metabolic function or regulatory factors. Besides improving the accumulation of propionyl-CoA per se, evaluating this propionyl-CoA chassis to produce other odd-chain products could be pursued. One of these products is 2-butanone, a ketone that recently was shown to have similar combustion properties to gasoline while at the same having lower soot, hydrocarbon, and nitric oxide emissions [248]. One of the pathways for 2-butanone relies on the condensation of propionyl-CoA and acetyl-CoA which could be of particular interest to evaluate in the propionyl-CoA *P. taiwanensis* VLB120 chassis in conditions where higher TCA cycle fluxes are reached [211].

4.4. Conclusion

This thesis targeted three venues of synthetic biology of *Pseudomonas taiwanensis* VLB120, the characterization of synthetic promoters to control gene expression and their performance comparison in the model organism *E. coli*, the development of a high gene expression cassette architecture in which one of the synthetic promoters was incorporated, and the application of these tools to create a chassis strain to widen the product portfolio of this important cell factory.

The development of synthetic promoters in *P. taiwanensis* VLB120 and their comparison in *E. coli* showed that the performance transposability between these two organisms is rather limited and that there is an urgent need to characterize genetic parts in *P. taiwanensis* and to extend its genetic toolbox for advanced strain engineering. Within the development of synthetic promoters, a standard for fluorescent-based synthetic biology tools characterization was proposed and its advantages should facilitate inter-laboratory comparisons and contribute to the standardization of developed tools. The assembly of an optimized gene expression cassette and its achievement of high gene expression relying on translation efficiency rather than transcription exploration showed that there are alternatives for gene expression manipulation in *P. taiwanensis* VLB120. It would be of interest to characterize the optimized gene expression cassette using the proposed performance unit used in the development of synthetic promoters and assess the applicability of this standard for benchmarking synthetic biology tools aiming at the same goal through alternative paths.

Expanding the product portfolio of *P. taiwanensis* VLB120 was achieved by incorporating an odd-chain intermediate in the metabolism. The applicability of work described in *E. coli* in this *Pseudomonas* fast-tracks the development of *P. taiwanensis* VLB120 since previously described metabolic pathway exploration can be applied in this organism. Theoretically, it also indicates that the product portfolio of *E. coli* can be extended to *Pseudomonas*. It is therefore vital to identify products whose pitfalls in *E. coli* can be overcome by the superior intrinsic metabolic traits of *P. taiwanensis* VLB120 and extend the list of relevant products for human society produced not by exploiting fossil resources but as a component of a sustainable circular bioeconomy.

Appendix

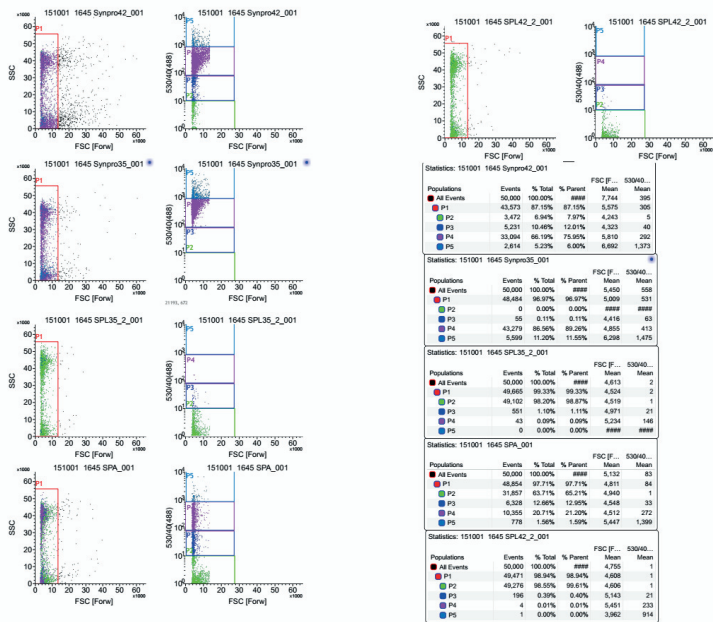


Figure 21. FACS distribution of the promoter libraries templates BG42 (SynPro 42) and BG35 (SynPro 35) and the three generated promoter libraries SPL35, SPL42 and SPA expressed in the pTn7 plasmid in *E. coli* PIR2.

Appendix

Table 8. Sequence and characterization of each promoter in *E. coli* TOP10 and *P. taiwanensis* VLB120.

Promoter	Sequence	<i>E. coli</i> TOP10		<i>P. taiwanensis</i> VLB120	
		MFE g ⁻¹ h ⁻¹	Std. Dev.	MFE g ⁻¹ h ⁻¹	Std. Dev.
SynPro35	TTTATTGACATGCGTGATGTTTAGAATTATAATTGGGG	3.70E-02	5.12E-03	1.81E-02	2.38E-04
SynPro42	GCCATTGACAAGGCTCTCGCGCCAGGTATAATTGCACG	1.30E-02	2.51E-04	2.67E-02	7.42E-04
SPA75	GCCATTGACAACACTATTTTTGATACTATAATTGCACG	4.43E-02	1.89E-04	3.35E-02	1.06E-03
SPA76	GCCATTGACACGTGTACTGTGACGGTTATAATTGCACG	2.19E-02	2.17E-04	1.56E-02	4.40E-04
SPA79	GCCATTGACATGGTAATGAAGCCGGTGTAATTGCACG	4.55E-02	1.95E-03	2.38E-02	5.32E-03
SPA80	GCCATTGACAAGGAGTTGCGGAGGTGTATAATTGCACG	2.89E-03	8.99E-05	2.60E-02	1.51E-03
SPA81	GCCATTGACAACGCGTCCACGTGGGGGTATAATTGCACG	3.67E-02	2.55E-03	4.06E-02	1.88E-03
SPA82	GCCATTGACATTGCGGTCTGTGGGTGTATAATTGCACG	4.48E-02	2.00E-04	3.89E-02	7.02E-04
SPA83	GCCATTGACATTGCGGTATTGCTAGTTTATAATTGCACG	4.21E-02	7.58E-04	2.64E-02	4.52E-04
SPA84	GCCATTGACATAGCTACGGTTGTTTATATAATTGCACG	4.06E-02	2.55E-03	3.12E-02	6.87E-04
SPA85	GCCATTGACATATCTTCATTGGTGCTATAATTGCACG	6.97E-02	1.92E-03	2.73E-02	1.10E-03
SPA86	GCCATTGACAAGGACGTTCTGCGAGGTATAATTGCACG	4.29E-02	8.73E-03	3.23E-02	4.43E-04
SPA88	GCCATTGACACCCCTCTTGACTTATTATAATTGCACG	4.82E-02	4.85E-04	1.70E-02	6.30E-04
SPA89	GCCATTGACATTACTACGCTCACTCGGTATAATTGCACG	3.51E-02	1.16E-02	2.42E-02	4.51E-03
SPA90	GCCATTGACATTGCCACATTGACCTGGTATAATTGCACG	4.70E-02	1.81E-03	2.01E-02	4.28E-04
SPA91	GCCATTGACAATTAGTATGGGGCAAGGTATAATTGCACG	5.95E-02	5.57E-03	1.97E-02	8.29E-04
SPA92	GCCATTGACAGCCAATACGGTTTCTGCTATAATTGCACG	1.88E-02	6.27E-04	1.82E-02	1.37E-03
SPA94	GCCATTGACAACGTGTTGTTTATATAATTGCACG	3.63E-02	3.62E-03	2.28E-02	7.26E-04
SPA95	GCCATTGACACTTTCAAAGTACCAGTTATAATTGCACG	5.46E-02	1.89E-02	2.50E-02	4.24E-04
SPA96	GCCATTGACAAGTACCCCTGGATCCGTGTAATTGCACG	2.96E-02	1.50E-03	3.80E-02	2.55E-04
SPA99	GCCATTGACATTGCAGTTTGCTCATGTATAATTGCACG	3.72E-02	7.36E-04	2.68E-02	3.76E-04
SPA108	GCCATTGACACTCACCAGCCTACTCGGTATAATTGCACG	3.27E-02	2.03E-03	1.73E-02	1.42E-03
SPA112	GCCATTGACACTGTACTGAGACATTGCTATAATTGCACG	6.08E-02	3.82E-03	3.24E-02	1.80E-03
SPA113	GCCATTGACAATCCACAAGGACATCTGTATAATTGCACG	3.98E-02	5.18E-03	4.00E-02	1.56E-03
SPA114	GCCATTGACAACATTGTGACAATTTGGTATAATTGCACG	3.25E-02	3.39E-03	1.62E-02	5.93E-04
SPA115	GCCATTGACACTACGCGCTGGCAAGATATAATTGCACG	4.64E-02	4.01E-03	3.07E-02	8.25E-04
SPA116	GCCATTGACAAGATGGTTTGCCAAAGTATAATTGCACG	6.38E-02	1.20E-02	2.82E-02	2.73E-04
SPA117	GCCATTGACATTGGTGAGACATTGGGGTATAATTGCACG	3.18E-02	1.82E-03	3.05E-02	2.86E-04
SPA134	GCCATTGACACTACAGTGTGGGCTGGTATAATTGCACG	3.63E-02	1.29E-02	3.02E-02	1.07E-03
SPA135	GCCATTGACACGCGCAATTTTTCGGGTATAATTGCACG	2.93E-02	3.83E-03	2.56E-02	2.57E-04
SPA136	GCCATTGACATAGAAATATTACTGTATAATTGCACG	3.65E-02	8.20E-03	2.27E-02	2.36E-03
SPA137	GCCATTGACAGTAGGCGGGAAGTAGATATAATTGCACG	7.91E-02	8.72E-03	2.80E-02	1.08E-03
SPA138	GCCATTGACATCTCGATGCAATTCCTGTATAATTGCACG	3.04E-02	1.25E-03	2.02E-02	7.30E-04
SPA139	GCCATTGACAACTTTTATCTTTCGGGTATAATTGCACG	3.77E-02	4.54E-03	2.06E-02	6.80E-03
SPA140	GCCATTGACAACCTCTATCCGAAGCGATATAATTGCACG	4.42E-02	6.74E-03	2.52E-02	8.31E-04
SPA142	GCCATTGACAACATCTACAATGTGTAGTATAATTGCACG	3.10E-02	1.93E-03	2.89E-02	1.34E-04
SPA146	GCCATTGACATTTCTGACGTTATTGGTATAATTGCACG	2.76E-02	2.21E-03	2.39E-02	5.37E-04
SPA147	GCCATTGACAAGTCTCAAGGTTTGTGTATAATTGCACG	2.45E-02	7.06E-04	1.92E-02	7.88E-04
SPA148	GCCATTGACAGGCGCGCTGTTTAGTTTATAATTGCACG	3.18E-02	3.62E-03	2.14E-02	3.01E-04
SPA156	GCCATTGACATATGCACTCGCATCGGTATAATTGCACG	3.20E-02	6.50E-03	2.87E-02	1.65E-03
SPA159	GCCATTGACACGTTGATTTGTTCCGGGTATAATTGCACG	3.24E-02	1.08E-02	3.22E-02	1.12E-03
SPA160	GCCATTGACATCCCGGGTGAAGAAATTTATAATTGCACG	5.93E-02	5.47E-03	2.46E-02	3.16E-03
SPA161	GCCATTGACATGTCTGGGAGGTGGATGTATAATTGCACG	3.28E-02	1.36E-02	3.34E-02	2.45E-03
SPA162	GCCATTGACATATTTTAAATTCGCGATATAATTGCACG	3.34E-02	5.39E-03	2.09E-02	3.86E-03
SPA166	GCCATTGACAGGCTCATCTACTCTGCTATAATTGCACG	4.57E-02	1.15E-02	1.97E-02	1.52E-03
SPA172	GCCATTGACAGGGGGCGGGAATTCGGTGTATAATTGCACG	2.13E-02	7.76E-03	3.32E-02	2.36E-03
SPA173	GCCATTGACACGCTTCAGGTGGCGTGATAATTGCACG	4.05E-02	1.40E-02	3.46E-02	2.77E-03
SPA174	GCCATTGACAATGGCGCGTATGTGCTTATAATTGCACG	5.34E-02	2.67E-03	3.06E-02	4.23E-04
SPA175	GCCATTGACAGGATACAATAATGACTATATAATTGCACG	4.23E-02	8.92E-03	2.32E-02	4.29E-04
SPA176	GCCATTGACAGAGTGTAAAGCCTGTAGTATAATTGCACG	2.44E-04	2.16E-05	1.10E-04	2.75E-05
SPA177	GCCATTGACATTTGTTGAAACTATATTATAATTGCACG	3.17E-02	6.74E-03	2.32E-02	9.72E-04
SPA179	GCCATTGACACGCGACGCCTATTAGGGTATAATTGCACG	2.44E-02	7.46E-03	2.14E-02	2.63E-03
SPA181	GCCATTGACAGAGCTTCAGCGGCATAGTATAATTGCACG	3.98E-02	4.68E-03	3.53E-02	4.72E-04

Table 8. (Continued)

Promoter	Sequence	<i>E. coli</i> TOP10		<i>P. taiwanensis</i> VLB120	
		MFE g ⁻¹ h ⁻¹	Std. Dev.	Promoter	Sequence
SPA184	GCCCAATTGACACTGTTTATTCTTTTGATATAATTGCACG	5.21E-02	4.65E-03	2.05E-02	6.73E-04
SPA187	GCCCAATTGACAGTTGATAATTTGTATATATAATTGCACG	3.19E-02	1.38E-02	1.98E-02	9.44E-04
SPA188	GCCCAATTGACACTACTCTTTTAACTGTTGATAATTGCACG	1.63E-02	4.83E-03	2.93E-02	6.23E-04
SPA189	GCCCAATTGACAATCTGTGTTTTCGCTCTATAATTGCACG	2.81E-02	2.10E-02	2.62E-02	1.83E-03
42_70	GCCCAATTGCTTAGGCTCTCGCGGCCAGGTAGTATTGCACG	1.93E-03	7.42E-05	8.35E-03	2.71E-04
42_86	GCCCAATTGCTTAGGCTCTCGCGGCCAGGTAGATAATTGCACG	2.48E-03	2.19E-04	1.38E-02	3.85E-04
42_89	GCCCAATTGCTTAGGCTCTCGCGGCCAGGTATGATTGCACG	1.58E-02	2.48E-03	1.18E-02	2.83E-03
42_98	GCCCAATTACTAGGCTCTCGCGGCCAGGTATGATTGCACG	2.17E-03	7.62E-05	1.04E-02	8.45E-04
42_99	GCCCAATTGACCAAGGCTCTCGCGGCCAGGTACGCTTGCACG	3.91E-03	1.88E-04	1.71E-02	1.91E-04
42_103	GCCCAATTGATCAGGCTCTCGCGGCCAGGTATTATTGCACG	5.89E-03	1.27E-03	4.14E-03	2.49E-04
42_104	GCCCAATTCGTTAGGCTCTCGCGGCCAGGTAGGCTTGCACG	1.60E-04	5.62E-05	2.60E-04	1.58E-05
42_137	GCCCAATTGATAAGGCTCTCGCGGCCAGGTATCATTGCACG	3.41E-03	1.89E-04	1.41E-02	1.81E-04
42_145	GCCCAATTGCTTAGGCTCTCGCGGCCAGGTACAATTGCACG	4.98E-03	3.25E-04	1.61E-02	1.85E-03
42_158	GCCCAATTGACCAAGGCTCTCGCGGCCAGGTACAGTTGCACG	5.95E-03	3.17E-04	2.21E-02	5.52E-04
42_159	GCCCAATTGACCAAGGCTCTCGCGGCCAGGTACGATTGCACG	1.09E-02	5.74E-04	8.06E-03	3.87E-04
42_168	GCCCAATTGTAGGCTCTCGCGGCCAGGTACTACTGCACG	4.23E-03	1.44E-03	8.30E-03	4.50E-04
42_200	GCCCAATTGATCAGGCTCTCGCGGCCAGGTATGATTGCACG	3.49E-03	1.04E-04	1.13E-02	4.42E-04
42_214	GCCCAATTGACCAAGGCTCTCGCGGCCAGGTAAGTTGCACG	3.80E-03	6.12E-04	2.04E-02	3.02E-04
42_215	GCCCAATTGCAAAAGGCTCTCGCGGCCAGGTATGCTTGCACG	3.16E-03	5.09E-04	2.91E-02	8.90E-04
42_216	GCCCAATTGACAAGGCTCTCGCGGCCAGGTAGTTTGCACG	7.16E-03	1.78E-04	3.24E-02	3.77E-04
42_217	GCCCAATTGCGGAGGCTCTCGCGGCCAGGTAGATAATTGCACG	3.43E-03	2.40E-04	1.36E-02	5.56E-04
35_24	TTTATTTGACATGCGTGATGTTTAGAATTAACTTTGGGG	1.99E-02	1.24E-03	8.59E-03	4.04E-04
35_25	TTTATTTGACCTGCGTGATGTTTAGAATTATAATTTGGGG	1.41E-02	1.85E-03	4.13E-03	4.97E-04
35_32	TTTATTTGTGTGCGTGATGTTTAGAATTAGCATTGGGG	5.57E-04	9.86E-05	3.18E-04	3.78E-05
35_44	TTTATTTGACATGCGTGATGTTTAGAATTACCTTTGGGG	2.57E-02	5.09E-04	8.36E-03	1.98E-04
35_45	TTTATTTGTTGTGCGTGATGTTTAGAATTATCTTTGGGG	1.34E-03	5.15E-05	2.84E-04	3.72E-05
35_47	TTTATTTGTTTGTGCGTGATGTTTAGAATTATCGTTTGGGG	5.90E-04	7.13E-05	2.42E-04	8.64E-06
35_48	TTTATTTGACATGCGTGATGTTTAGAATTACACTTTGGGG	2.20E-02	8.28E-04	1.07E-02	1.21E-04
35_51	TTTATTTGACGTGCGTGATGTTTAGAATTAATTTGGGG	1.72E-02	3.40E-03	4.96E-03	2.51E-04
35_54	TTTATTTGTAATGCGTGATGTTTAGAATTAGACTTTGGGG	2.80E-03	1.20E-04	9.76E-04	9.54E-05
35_55	TTTATTTGCATTGCGTGATGTTTAGAATTACGGTTTGGGG	1.21E-03	4.13E-05	3.52E-04	1.82E-05
35_62	TTTATTTGTGCTGCGTGATGTTTAGAATTATCTTTGGGG	3.67E-03	1.12E-04	2.39E-04	1.18E-04
35_63	TTTATTTGACATGCGTGATGTTTAGAATTATCCTTTGGGG	1.89E-02	2.08E-03	9.98E-03	5.24E-04
35_70	TTTATTTGATGTGCGTGATGTTTAGAATTACATTTGGGG	1.02E-03	1.71E-05	2.83E-04	1.13E-05
35_71	TTTATTTGCTCTGCGTGATGTTTAGAATTATTGTTTGGGG	3.13E-03	6.73E-05	3.31E-04	1.40E-04
35_79	TTTATTTGCTGTGCGTGATGTTTAGAATTAGGGTTTGGGG	2.94E-03	1.20E-04	2.65E-04	2.23E-06
35_84	TTTATTTGCGTTGCGTGATGTTTAGAATTAGGGTTTGGGG	8.02E-04	3.75E-05	4.81E-04	3.22E-05
35_92	TTTATTTGACATGCGTGATGTTTAGAATTATCATTGGGG	3.09E-02	2.98E-03	1.40E-02	1.75E-04
35_105	TTTATTTGACATGCGTGATGTTTAGAATTACCATTTGGGG	4.13E-02	8.02E-03	1.16E-02	1.03E-04
35_106	TTTATTTGACATGCGTGATGTTTAGAATTATGCTTTGGGG	3.92E-02	1.98E-03	1.20E-02	3.10E-04
35_110	TTTATTTGACGTGCGTGATGTTTAGAATTAACCTTTGGGG	6.41E-02	8.18E-03	4.22E-03	7.99E-04
35_131	TTTATTTGTTTGTGCGTGATGTTTAGAATTAGTATTGGGG	7.91E-03	3.06E-04	4.18E-04	2.31E-05

Appendix

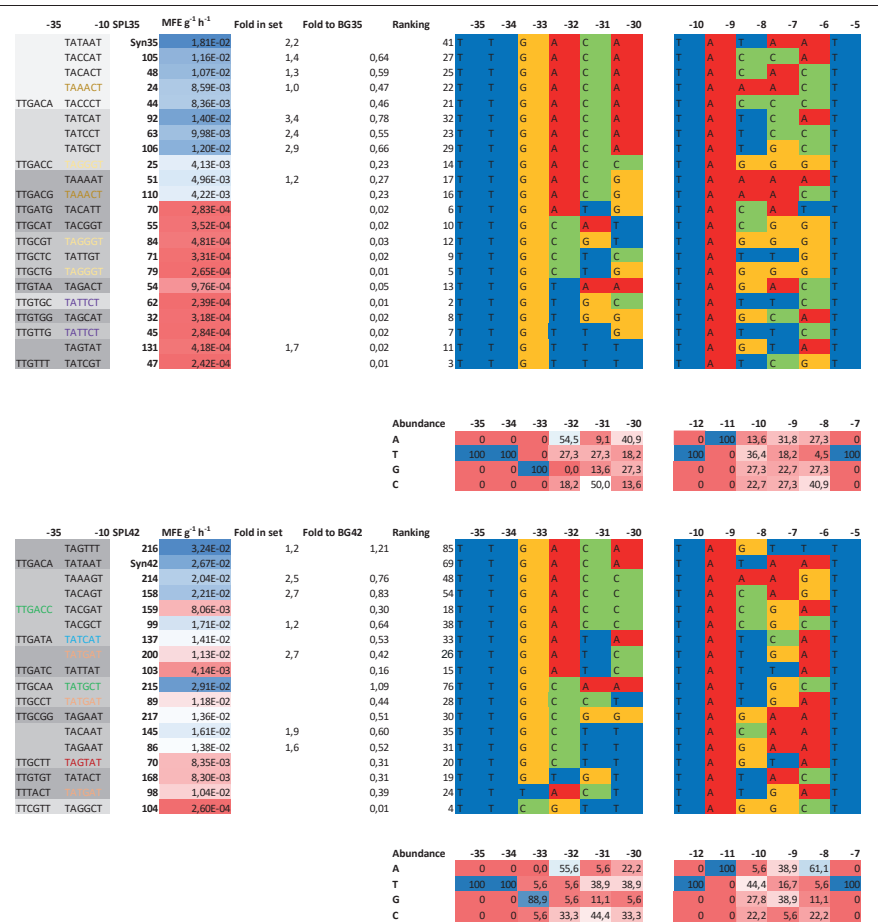


Figure 22. Nucleotide abundances in the promoter libraries SPL35 and SPL42 in *P. taiwanensis* VLB120. A=adenine, T= thymine, G=guanine and C=cytosine.

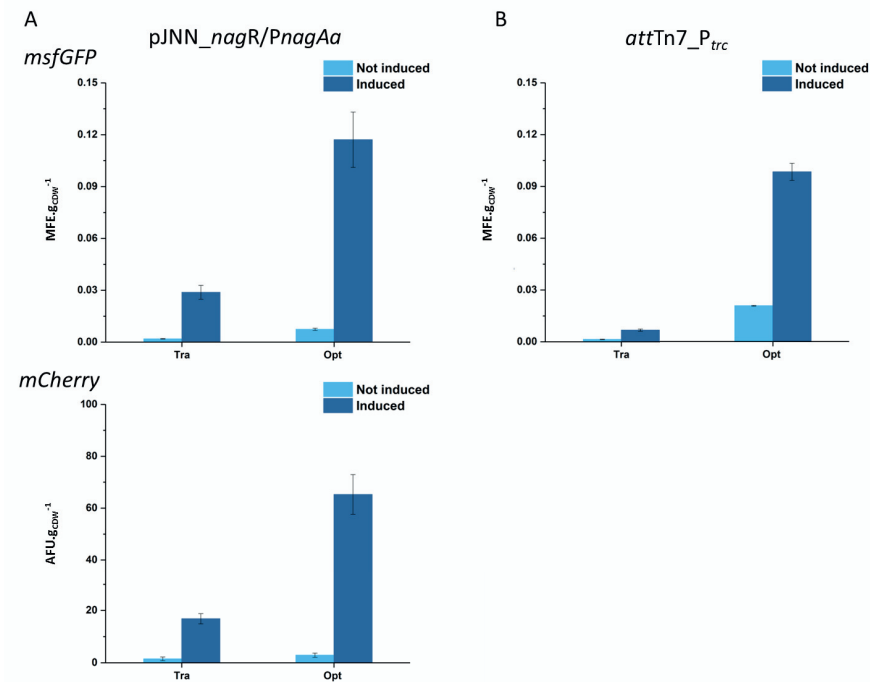


Figure 24. Evaluation of the developed inducible gene expression constructs under induced (dark blue) and non-induced (light blue) conditions. (A) plasmid-based expression of *msfGFP* and *mCherry* under the control of the *nagR/PnagAa* promoter, (B) genomic integrated expression of *msfGFP* at the *attTn7* site under the control of the *P_{trc}* promoter.

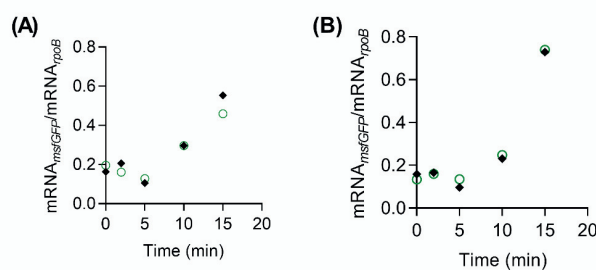


Figure 25. Time course of mRNA abundance of the *msfGFP* gene normalized with the transcript level of the housekeeping gene *rpoB* for the traditional (A) and the optimized expression cassette (B).

References

- [1] R. K. P. and L. A. M. (eds. . Core Writing Team, "IPCC, 2014: Climate change 2014: synthesis report. contribution of working groups i, ii and iii to the fifth assessment report of the intergovernmental panel on climate change," Geneva, Switzerland, 2014.
- [2] G. Yvon-Durocher *et al.*, "Methane fluxes show consistent temperature dependence across microbial to ecosystem scales," *Nature*, vol. 507, no. 7493, pp. 488–491, 2014.
- [3] P. Morrison, "The discovery of global warming," *Phys. Today*, vol. 57, no. 6, pp. 60–61, Jun. 2004.
- [4] NASA Global Climate Change, "NASA Vital signs-global temperature." [Online]. Available: <https://climate.nasa.gov/vital-signs/global-temperature/%0A>. [Accessed: 29-Dec-2020].
- [5] CO2-Earth, "Historical CO2 datasets." [Online]. Available: <https://www.co2.earth/historical-co2-datasets%0A>. [Accessed: 29-Dec-2020].
- [6] R. S. Nerem, B. D. Beckley, J. T. Fasullo, B. D. Hamlington, D. Masters, and G. T. Mitchum, "Climate-change-driven accelerated sea-level rise detected in the altimeter era," *Proc. Natl. Acad. Sci.*, vol. 115, no. 9, pp. 2022–2025, Feb. 2018.
- [7] M. Hulme, "Attributing weather extremes to 'climate change': A review," *Prog. Phys. Geogr.*, vol. 38, no. 4, pp. 499–511, 2014.
- [8] P. Stott, "How climate change affects extreme weather events," *Science (80-.)*, vol. 352, no. 6293, pp. 1517–1518, 2016.
- [9] National Climate Assessment and NASA's Goddard Space Flight Center Scientific Visualization Studio, "National climate assessment: 21st century temperature scenarios." [Online]. Available: <https://svs.gsfc.nasa.gov/4029>. [Accessed: 04-Jan-2020].
- [10] National Climate Assessment and NASA's Goddard Space Flight Center Scientific Visualization Studio, "Megadroughts in U.S. west projected to be worst of the millennium." [Online]. Available: <https://svs.gsfc.nasa.gov/4270>. [Accessed: 05-Jan-2021].
- [11] K. E. Taylor, R. J. Stouffer, and G. A. Meehl, "An overview of CMIP5 and the experiment design," *Bull. Am. Meteorol. Soc.*, vol. 93, no. 4, pp. 485–498, 2012.
- [12] G. A. Meehl *et al.*, "Decadal prediction," *Bull. Am. Meteorol. Soc.*, vol. 90, no. 10, pp. 1467–1486, Oct. 2009.
- [13] J. R. Fleming, "Joseph Fourier, the 'greenhouse effect', and the quest for a universal theory of terrestrial temperatures," *Endeavour*, vol. 23, no. 2, pp. 72–75, 1999.
- [14] R. J. Charlson and H. Rodhe, *The legacy of Svante Arrhenius: understanding the greenhouse effect*. Stockholm : Royal Swedish Academy of Sciences, 1998.
- [15] R. J. Russell, "Climate and man: 1941 yearbook of agriculture," *JAMA J. Am. Med. Assoc.*, vol. 118, no. 9, p. 765, Feb. 1942.
- [16] S. R. Weart, "The discovery of the risk of global warming," *Phys. Today*, vol. 50, no. 1, pp. 34–40, 1997.
- [17] G. C. Simpson, "Past Climates," *Nature*, vol. 124, no. 3139, pp. 988–991, Dec. 1929.
- [18] K. Angstrom, "Knut Angstrom on atmospheric absorption.," *Mon. Wea. Rev.*, vol. 29, no. 6, p. 268, 1901.
- [19] G. S. Callendar, "The artificial production of carbon dioxide and its influence on temperature," *Q. J. R. Meteorol. Soc.*, vol. 64, no. 275, pp. 223–240, 1938.
- [20] G. S. Callendar, "Variations of the amount of carbon dioxide in different air currents," *Q. J. R. Meteorol. Soc.*, vol. 66, no. 287, pp. 395–400, Sep. 1940.
- [21] G. S. Callendar, "Can carbon dioxide influence climate?," *Weather*, vol. 4, no. 10, pp. 310–314, Oct. 1949.
- [22] H. E. Suess, "Radiocarbon concentration in modern wood," *Science (80-.)*, vol. 122, no. 3166, pp. 415–417, Sep. 1955.
- [23] J. S. Sawyer, "Man-made carbon dioxide and the 'greenhouse' effect," *Nature*, vol. 239, no. 5366, pp. 23–26, Sep. 1972.

-
- [24] N. Nicholls, "Climate: Sawyer predicted rate of warming in 1972," *Nature*, vol. 448, no. 7157, pp. 992–992, Aug. 2007.
- [25] "About the IPCC." [Online]. Available: <https://www.ipcc.ch/about/>. [Accessed: 09-Jan-2021].
- [26] J. Hansen *et al.*, "Efficacy of climate forcings," *J. Geophys. Res. D Atmos.*, vol. 110, no. 18, pp. 1–45, 2005.
- [27] T. P. Barnett, J. C. Adam, and D. P. Lettenmaier, "Potential impacts of a warming climate on water availability in snow-dominated regions," *Nature*, vol. 438, no. 7066, pp. 303–309, 2005.
- [28] The Royal Society of London, "A guide to facts and fiction about climate change," *R. Soc.*, no. March, p. 19, 2005.
- [29] UN Treaty Database, "Kyoto Protocol." 1997.
- [30] United Nations Treaty Collection, "Paris Agreement." 2016.
- [31] "About the UNFCCC." [Online]. Available: <https://unfccc.int/about-us/about-the-secretariat>. [Accessed: 10-Jan-2021].
- [32] M. I. Kabir, M. B. Rahman, W. Smith, M. A. F. Lusha, S. Azim, and A. H. Milton, "Knowledge and perception about climate change and human health: Findings from a baseline survey among vulnerable communities in Bangladesh," *BMC Public Health*, vol. 16, no. 1, pp. 1–10, 2016.
- [33] A. L. Taylor, S. Dessai, and W. Bruine de Bruin, "Public perception of climate risk and adaptation in the UK: A review of the literature," *Clim. Risk Manag.*, vol. 4, pp. 1–16, 2014.
- [34] A. Sullivan and D. D. White, "An assessment of public perceptions of climate change risk in three western U.S. Cities," *Weather. Clim. Soc.*, vol. 11, no. 2, pp. 449–463, 2019.
- [35] J. C. Semenza, D. E. Hall, D. J. Wilson, B. D. Bontempo, D. J. Sailor, and L. A. George, "Public perception of climate change," *Am. J. Prev. Med.*, vol. 35, no. 5, pp. 479–487, Nov. 2008.
- [36] NASA Global Climate Change, "Responding to climate change." [Online]. Available: <https://climate.nasa.gov/solutions/adaptation-mitigation/>. [Accessed: 10-Jan-2021].
- [37] H. Ritchie and M. Roser, "CO₂ and greenhouse gas emissions," *Our World Data*, 2017.
- [38] United Nations Department of economic and social affairs population division, "Probabilistic population projections based on the world population prospects 2019," 2019.
- [39] Ellen MacArthur Foundation, "Towards the circular economy-economic and business rationale for an accelerated transition," 2013. [Online]. Available: <https://www.ellenmacarthurfoundation.org/assets/downloads/publications/Ellen-MacArthur-Foundation-Towards-the-Circular-Economy-vol.1.pdf>. [Accessed: 31-Jan-2021].
- [40] M. Carus and L. Dammer, "The Circular Bioeconomy—concepts, opportunities, and limitations," *Ind. Biotechnol.*, vol. 14, no. 2, pp. 83–91, 2018.
- [41] M. Kardung *et al.*, "Development of the Circular Bioeconomy: drivers and indicators," *Sustainability*, vol. 13, no. 1, p. 413, 2021.
- [42] European Commission, "Communication from the Commission to the European Parliament, the European Council, the Council, the European economic and social Committee and the Committee of the regions, The European Green Deal, COM/2019/640 final," 2019. [Online]. Available: <https://eur-lex.europa.eu/legal-content/EN/TXT/?uri=CELEX%3A52019DC0640>. [Accessed: 31-Jan-2021].
- [43] J. Wesseler and J. Von Braun, "Measuring the bioeconomy: economics and policies," *Annu. Rev. Resour. Econ.*, vol. 9, no. June, pp. 275–298, 2017.
- [44] The White House, "National bioeconomy blueprint," *Ind. Biotechnol.*, vol. 8, no. 3, pp. 97–102, Jun. 2012.
-

-
- [45] I. Virgin and E. J. Morris, *Creating sustainable bioeconomies*. Routledge, 2016.
- [46] M. Hanewinkel, B. Muys, and M. Ollikainen, *Leading the way to a european circular bioeconomy strategy*, no. October. 2017.
- [47] “EFIB2020 goes digital – EuropaBio hosts 13th annual european industrial biotechnology and bioeconomy conference.” [Online]. Available: <https://efibforum.com/topics/green-circular-sustainable/>. [Accessed: 20-Feb-2021].
- [48] Confederation of European Paper Industries, “Bioeconomy and the Green Deal: matching Europe’s climate neutrality and competitiveness goals?,” 2021. [Online]. Available: <https://www.cepi.org/bioeconomy-and-the-green-deal-matching-europes-climate-neutrality-and-competitiveness-goals/>. [Accessed: 20-Feb-2021].
- [49] K. P. Purnhagen and J. H. H. Wessler, “Maximum vs minimum harmonization: what to expect from the institutional and legal battles in the EU on gene editing technologies,” *Pest Manag. Sci.*, vol. 75, no. 9, pp. 2310–2315, 2019.
- [50] D. Eriksson *et al.*, “A comparison of the EU regulatory approach to directed mutagenesis with that of other jurisdictions, consequences for international trade and potential steps forward,” *New Phytol.*, vol. 222, no. 4, pp. 1673–1684, 2019.
- [51] K. Purnhagen and J. Wessler, “EU regulation of new plant breeding technologies and their possible economic implications for the EU and beyond,” *Appl. Econ. Perspect. Policy*, vol. 00, no. 00, pp. 1–17, 2020.
- [52] Y. Jin, D. Drabik, N. Heerink, and J. Wessler, “Getting an imported GM crop approved in China,” *Trends Biotechnol.*, vol. 37, no. 6, pp. 566–569, 2019.
- [53] R. Carlson, “Estimating the biotech sector’s contribution to the US economy,” *Nat. Biotechnol.*, vol. 34, no. 3, pp. 247–255, 2016.
- [54] L. Clarke and R. Kitney, “Developing synthetic biology for industrial biotechnology applications,” *Biochem. Soc. Trans.*, vol. 48, no. 1, pp. 113–122, 2020.
- [55] J. D. Keasling, “Manufacturing molecules through metabolic engineering,” *Science (80-.)*, vol. 330, no. 6009, pp. 1355–1358, 2010.
- [56] C. E. Nakamura and G. M. Whited, “Metabolic engineering for the microbial production of 1,3-propanediol,” *Curr. Opin. Biotechnol.*, vol. 14, no. 5, pp. 454–459, 2003.
- [57] Y. S. Ko *et al.*, “Tools and strategies of systems metabolic engineering for the development of microbial cell factories for chemical production,” *Chem. Soc. Rev.*, vol. 49, no. 14, pp. 4615–4636, 2020.
- [58] J. W. Xu, Y. N. Xu, and J. J. Zhong, “Enhancement of ganoderic acid accumulation by overexpression of an n-terminally truncated 3-hydroxy-3-methylglutaryl coenzyme a reductase gene in the basidiomycete *Ganoderma lucidum*,” *Appl. Environ. Microbiol.*, vol. 78, no. 22, pp. 7968–7976, 2012.
- [59] M. J. Dunlop *et al.*, “Engineering microbial biofuel tolerance and export using efflux pumps,” *Mol. Syst. Biol.*, vol. 7, no. 487, p. 487, 2011.
- [60] J. H. Park, J. E. Oh, K. H. Lee, J. Y. Kim, and S. Y. Lee, “Rational design of *Escherichia coli* for l-isoleucine production,” *ACS Synth. Biol.*, vol. 1, no. 11, pp. 532–540, Nov. 2012.
- [61] K. H. Lee, J. H. Park, T. Y. Kim, H. U. Kim, and S. Y. Lee, “Systems metabolic engineering of *Escherichia coli* for L-threonine production,” *Mol. Syst. Biol.*, vol. 3, no. 149, 2007.
- [62] B. F. Pflieger, M. Gossing, and J. Nielsen, “Metabolic engineering strategies for microbial synthesis of oleochemicals,” *Metab. Eng.*, vol. 29, pp. 1–11, 2015.
- [63] H. M. van Rossum, B. U. Kozak, J. T. Pronk, and A. J. A. van Maris, “Engineering cytosolic acetyl-coenzyme A supply in *Saccharomyces cerevisiae*: Pathway stoichiometry, free-energy conservation and redox-cofactor balancing,” *Metab. Eng.*, vol. 36, pp. 99–115, 2016.
- [64] M. A. Asadollahi, J. Maury, K. R. Patil, M. Schalk, A. Clark, and J. Nielsen, “Enhancing
-

- sesquiterpene production in *Saccharomyces cerevisiae* through in silico driven metabolic engineering," *Metab. Eng.*, vol. 11, no. 6, pp. 328–334, Nov. 2009.
- [65] Y. Y. Cui, C. Ling, Y. Y. Zhang, J. Huang, and J. Z. Liu, "Production of shikimic acid from *Escherichia coli* through chemically inducible chromosomal evolution and cofactor metabolic engineering," *Microb. Cell Fact.*, vol. 13, no. 1, pp. 1–11, 2014.
- [66] S. Y. Lee and H. U. Kim, "Systems strategies for developing industrial microbial strains," *Nat. Biotechnol.*, vol. 33, no. 10, pp. 1061–1072, 2015.
- [67] J.-H. Lee, D.-E. Lee, B. Lee, and H. Kim, "Global analyses of transcriptomes and proteomes of a parent strain and an l-threonine-overproducing mutant strain," *J. Bacteriol.*, vol. 185, no. 18, pp. 5442–5451, Sep. 2003.
- [68] A. L. Rodrigues *et al.*, "Systems metabolic engineering of *Escherichia coli* for production of the antitumor drugs violacein and deoxyviolacein," *Metab. Eng.*, vol. 20, pp. 29–41, 2013.
- [69] K. Qi, J.-J. Zhong, and X.-X. Xia, "Triggering respirofermentative metabolism in the Crabtree-negative yeast *Pichia guilliermondii* by disrupting the CAT8 gene," *Appl. Environ. Microbiol.*, vol. 80, no. 13, pp. 3879–3887, Jul. 2014.
- [70] C. Kiel, E. Yus, and L. Serrano, "Engineering signal transduction pathways," *Cell*, vol. 140, no. 1, pp. 33–47, 2010.
- [71] S. Y. Park, R. M. Binkley, W. J. Kim, M. H. Lee, and S. Y. Lee, "Metabolic engineering of *Escherichia coli* for high-level astaxanthin production with high productivity," *Metab. Eng.*, vol. 49, no. July, pp. 105–115, Sep. 2018.
- [72] H. Yim *et al.*, "Metabolic engineering of *Escherichia coli* for direct production of 1,4-butanediol," *Nat. Chem. Biol.*, vol. 7, no. 7, pp. 445–452, 2011.
- [73] M. A. Islam, N. Hadadi, M. Ataman, V. Hatzimanikatis, and G. Stephanopoulos, "Exploring biochemical pathways for mono-ethylene glycol (MEG) synthesis from synthesis gas," *Metab. Eng.*, vol. 41, pp. 173–181, 2017.
- [74] S. C. Nies *et al.*, "High titer methyl ketone production with tailored *Pseudomonas taiwanensis* VLB120," *Metab. Eng.*, vol. 62, no. July, pp. 84–94, 2020.
- [75] M. C. Bassalo, R. Liu, and R. T. Gill, "Directed evolution and synthetic biology applications to microbial systems," *Curr. Opin. Biotechnol.*, vol. 39, pp. 126–133, 2016.
- [76] S. H. Park, H. U. Kim, T. Y. Kim, J. S. Park, S. S. Kim, and S. Y. Lee, "Metabolic engineering of *Corynebacterium glutamicum* for L-arginine production," *Nat. Commun.*, vol. 5, 2014.
- [77] S. B. Jennifer Kan, X. Huang, Y. Gumulya, K. Chen, and F. H. Arnold, "Genetically programmed chiral organoborane synthesis," *Nature*, vol. 552, no. 7683, pp. 132–136, 2017.
- [78] C. D. Herring *et al.*, "Comparative genome sequencing of *Escherichia coli* allows observation of bacterial evolution on a laboratory timescale," *Nat. Genet.*, vol. 38, no. 12, pp. 1406–1412, 2006.
- [79] R. A. LaCroix *et al.*, "Use of adaptive laboratory evolution to discover key mutations enabling rapid growth of *Escherichia coli* K-12 MG1655 on glucose minimal medium," *Appl. Environ. Microbiol.*, vol. 81, no. 1, pp. 17–30, 2015.
- [80] Z. D. Blount, J. E. Barrick, C. J. Davidson, and R. E. Lenski, "Genomic analysis of a key innovation in an experimental *Escherichia coli* population," *Nature*, vol. 489, no. 7417, pp. 513–518, 2012.
- [81] T. Tiso *et al.*, "Towards bio-upcycling of polyethylene terephthalate," *Metab. Eng.*, vol. 66, no. March, pp. 167–178, 2021.
- [82] H. Goodarzi *et al.*, "Regulatory and metabolic rewiring during laboratory evolution of ethanol tolerance in *E. coli*," *Mol. Syst. Biol.*, vol. 6, no. 378, pp. 1–12, 2010.
- [83] M. Dragosits and D. Mattanovich, "Adaptive laboratory evolution - principles and applications for biotechnology," *Microb. Cell Fact.*, vol. 12, no. 1, pp. 1–17, 2013.

- [84] E. T. Mohamed *et al.*, “Generation of a platform strain for ionic liquid tolerance using adaptive laboratory evolution,” *Microb. Cell Fact.*, vol. 16, no. 1, pp. 1–15, 2017.
- [85] “SynbiCITE start-up survey,” 2017. [Online]. Available: <http://www.synbicite.com/news-events/materials/uk-Synthetic-biology-start-up-survey-2017/>. [Accessed: 25-Jul-2021].
- [86] “Synthetic biology UK – a decade of rapid progress 2009–2019,” 2019. [Online]. Available: <https://ktn-uk.org/wp-content/uploads/2020/08/SBLC-combined-final.pdf>. [Accessed: 25-Jul-2021].
- [87] R. A. Le Feuvre and N. S. Scrutton, “A living foundry for synthetic biological materials: a synthetic biology roadmap to new advanced materials,” *Synth. Syst. Biotechnol.*, vol. 3, no. 2, pp. 105–112, 2018.
- [88] A. P. Jacobus, J. Gross, J. H. Evans, S. R. Ceccato-Antonini, and A. K. Gombert, “*Saccharomyces cerevisiae* strains used industrially for bioethanol production,” *Essays Biochem.*, vol. 65, no. 2, pp. 147–161, Jul. 2021.
- [89] C. Patermann and A. Aguilar, “The origins of the bioeconomy in the European Union,” *N. Biotechnol.*, vol. 40, pp. 20–24, 2018.
- [90] R. H. Davis, “The age of model organisms,” *Nat. Rev. Genet.*, vol. 5, no. 1, pp. 69–76, 2004.
- [91] E. Freed *et al.*, “Building a genome engineering toolbox in nonmodel prokaryotic microbes,” *Biotechnol. Bioeng.*, vol. 115, no. 9, pp. 2120–2138, 2018.
- [92] H. Raschmanová, A. Weninger, A. Glieder, K. Kovar, and T. Vogl, “Implementing CRISPR-Cas technologies in conventional and non-conventional yeasts: Current state and future prospects,” *Biotechnol. Adv.*, vol. 36, no. 3, pp. 641–665, 2018.
- [93] E. Palazzotto, Y. Tong, S. Y. Lee, and T. Weber, “Synthetic biology and metabolic engineering of actinomycetes for natural product discovery,” *Biotechnol. Adv.*, vol. 37, no. 6, 2019.
- [94] Q. Wang and J. J. Coleman, “Progress and challenges: development and implementation of CRISPR/Cas9 technology in filamentous fungi,” *Comput. Struct. Biotechnol. J.*, vol. 17, pp. 761–769, 2019.
- [95] I. S. Ng, B. B. Keskin, and S. I. Tan, *A critical review of genome editing and synthetic biology applications in metabolic engineering of microalgae and cyanobacteria*, vol. 15, no. 8. 2020.
- [96] S. Santala and V. Santala, “*Acinetobacter baylyi* ADP1—naturally competent for synthetic biology,” *Essays Biochem.*, vol. 65, no. 2, pp. 309–318, Jul. 2021.
- [97] N. L. Bitzenhofer *et al.*, “Towards robust *Pseudomonas* cell factories to harbour novel biosynthetic pathways,” *Essays Biochem.*, vol. 65, no. 2, pp. 319–336, 2021.
- [98] S. Ikeda *et al.*, “*Shewanella oneidensis* MR-1 as a bacterial platform for electro-biotechnology,” *Essays Biochem.*, vol. 65, no. 2, p. 355, 2021.
- [99] F. Thoma and B. Blombach, “Metabolic engineering of *Vibrio natriegens*,” *Essays Biochem.*, vol. 65, no. 2, pp. 381–392, 2021.
- [100] J. W. Ye and G. Q. Chen, “*Halomonas* as a chassis,” *Essays Biochem.*, vol. 65, no. 2, pp. 393–403, 2021.
- [101] I. Poblete-Castro, J. Becker, K. Dohnt, V. M. Dos Santos, and C. Wittmann, “Industrial biotechnology of *Pseudomonas putida* and related species,” *Appl. Microbiol. Biotechnol.*, vol. 93, no. 6, pp. 2279–2290, 2012.
- [102] J. I. Jiménez, B. Miñambres, J. L. García, and E. Díaz, “Genomic analysis of the aromatic catabolic pathways from *Pseudomonas putida* KT2440,” *Environ. Microbiol.*, vol. 4, no. 12, pp. 824–841, 2002.
- [103] B. Cao, K. Nagarajan, and K. C. Loh, “Biodegradation of aromatic compounds: current status and opportunities for biomolecular approaches,” *Appl. Microbiol. Biotechnol.*, vol. 85, no. 2, pp. 207–228, 2009.

-
- [104] R. Gross, K. Buehler, and A. Schmid, "Engineered catalytic biofilms for continuous large scale production of n-octanol and (S)-styrene oxide," *Biotechnol. Bioeng.*, vol. 110, no. 2, pp. 424–436, Feb. 2013.
- [105] A. S. Klein *et al.*, "New prodigiosin derivatives obtained by mutasynthesis in *Pseudomonas putida*," *ACS Synth. Biol.*, vol. 6, no. 9, pp. 1757–1765, 2017.
- [106] J. M. Borrero-de Acuña *et al.*, "Production of medium chain length polyhydroxyalkanoate in metabolic flux optimized *Pseudomonas putida*," *Microb. Cell Fact.*, vol. 13, no. 1, pp. 1–15, 2014.
- [107] T. Tiso *et al.*, "Designer rhamnolipids by reduction of congener diversity: Production and characterization," *Microb. Cell Fact.*, vol. 16, no. 1, pp. 1–14, 2017.
- [108] K. A. K. Köhler *et al.*, "Complete genome sequence of *Pseudomonas* sp. strain VLB120 a solvent tolerant, styrene degrading bacterium, isolated from forest soil," *J. Biotechnol.*, vol. 168, no. 4, pp. 729–730, 2013.
- [109] K. A. K. Köhler, L. M. Blank, O. Frick, and A. Schmid, "D-Xylose assimilation via the Weimberg pathway by solvent-tolerant *Pseudomonas taiwanensis* VLB120," *Environ. Microbiol.*, vol. 17, no. 1, pp. 156–170, 2015.
- [110] G. G. Wordofa and M. Kristensen, "Tolerance and metabolic response of *Pseudomonas taiwanensis* VLB120 towards biomass hydrolysate-derived inhibitors," *Biotechnol. Biofuels*, vol. 11, no. 1, pp. 1–11, 2018.
- [111] M. Chavarria, P. I. Nikel, D. Pérez-Pantoja, and V. De Lorenzo, "The Entner-Doudoroff pathway empowers *Pseudomonas putida* KT2440 with a high tolerance to oxidative stress," *Environ. Microbiol.*, vol. 15, no. 6, pp. 1772–1785, 2013.
- [112] B. E. Ebert, F. Kurth, M. Grund, L. M. Blank, and A. Schmid, "Response of *Pseudomonas putida* KT2440 to increased NADH and ATP demand," *Appl. Environ. Microbiol.*, vol. 77, no. 18, pp. 6597–6605, 2011.
- [113] P. I. Nikel, M. Chavarria, T. Fuhrer, U. Sauer, and V. de Lorenzo, "*Pseudomonas putida* KT2440 strain metabolizes glucose through a cycle formed by enzymes of the Entner-Doudoroff, Embden-Meyerhof-Parnas, and pentose phosphate pathways," *J. Biol. Chem.*, vol. 290, no. 43, pp. 25920–25932, 2015.
- [114] S. Panke, B. Witholt, A. Schmid, and M. G. Wubbolts, "Towards a biocatalyst for (S)-styrene oxide production: characterization of the styrene degradation pathway of *Pseudomonas* sp. strain VLB120," *Appl. Environ. Microbiol.*, vol. 64, no. 6, pp. 2032–2043, 1998.
- [115] C. E. French, B. Boonstra, K. A. J. Bufton, and N. C. Bruce, "Cloning, sequence, and properties of the soluble pyridine nucleotide transhydrogenase of *Pseudomonas fluorescens*," *J. Bacteriol.*, vol. 179, no. 8, pp. 2761–2765, 1997.
- [116] H. J. Heipieper, F. J. Weber, J. Sikkema, H. Keweloh, and J. A. M. de Bont, "Mechanisms of resistance of whole cells to toxic organic solvents," *Trends Biotechnol.*, vol. 12, no. 10, pp. 409–415, Oct. 1994.
- [117] H. J. Heipieper, G. Neumann, S. Cornelissen, and F. Meinhardt, "Solvent-tolerant bacteria for biotransformations in two-phase fermentation systems," *Appl. Microbiol. Biotechnol.*, vol. 74, no. 5, pp. 961–973, Mar. 2007.
- [118] F. J. Weber, L. P. Ooijkaas, R. M. Schemen, S. Hartmans, and J. A. de Bont, "Adaptation of *Pseudomonas putida* S12 to high concentrations of styrene and other organic solvents," *Appl. Environ. Microbiol.*, vol. 59, no. 10, pp. 3502–3504, 1993.
- [119] J. A. m. De Bont, "Solvent-tolerant bacteria in biocatalysis," *Trends Biotechnol.*, vol. 16, no. 12, pp. 493–499, 1998.
- [120] Y. N. Sardessai and S. Bhosle, "Industrial potential of organic solvent tolerant bacteria," *Biotechnol. Prog.*, vol. 20, no. 3, pp. 655–660, 2004.
- [121] J. L. Ramos *et al.*, "Mechanisms of solvent tolerance in gram-negative bacteria," *Annu.*
-

-
- Rev. Microbiol.*, vol. 56, pp. 743–768, 2002.
- [122] C. Eberlein, T. Baumgarten, S. Starke, and H. J. Heipieper, “Immediate response mechanisms of Gram-negative solvent-tolerant bacteria to cope with environmental stress: cis-trans isomerization of unsaturated fatty acids and outer membrane vesicle secretion,” *Appl. Microbiol. Biotechnol.*, vol. 102, no. 6, pp. 2583–2593, Mar. 2018.
 - [123] H. J. Heipieper, F. Meinhardt, and A. Segura, “The cis-trans isomerase of unsaturated fatty acids in *Pseudomonas* and *Vibrio*: biochemistry, molecular biology and physiological function of a unique stress adaptive mechanism,” *FEMS Microbiol. Lett.*, vol. 229, no. 1, pp. 1–7, Dec. 2003.
 - [124] H. Kusumawardhani, R. Hosseini, and J. H. de Winde, “Solvent tolerance in bacteria: fulfilling the promise of the biotech era?,” *Trends Biotechnol.*, vol. 36, no. 10, pp. 1025–1039, 2018.
 - [125] S. Hartmans, J. P. Smits, M. J. Van der Werf, F. Volkering, and J. A. M. de Bont, “Metabolism of styrene oxide and 2-phenylethanol,” *Appl. Environ. Microbiol.*, vol. 55, no. 11, pp. 2850–2855, 1989.
 - [126] D. G. Gibson, L. Young, R. Y. Chuang, J. C. Venter, C. A. Hutchison, and H. O. Smith, “Enzymatic assembly of DNA molecules up to several hundred kilobases,” *Nat. Methods*, vol. 6, no. 5, pp. 343–345, 2009.
 - [127] P. Puigbo, E. Guzman, A. Romeu, and S. Garcia-Vallve, “OPTIMIZER: a web server for optimizing the codon usage of DNA sequences,” *Nucleic Acids Res.*, vol. 35, no. Web Server, pp. W126–W131, 2007.
 - [128] S. Zobel, I. Benedetti, L. Eisenbach, V. de Lorenzo, N. Wierckx, and L. M. Blank, “Tn7-based device for calibrated heterologous gene expression in *Pseudomonas putida*,” *ACS Synth. Biol.*, vol. 4, no. 12, pp. 1341–1351, Dec. 2015.
 - [129] P. Chomczynski and M. Rymaszewski, “Alkaline polyethylene glycol-based method for direct PCR from bacteria, eukaryotic tissue samples, and whole blood,” *Biotechniques*, vol. 40, no. 4, pp. 454–458, 2006.
 - [130] E. Martínez-García and V. de Lorenzo, “Engineering multiple genomic deletions in gram-negative bacteria: analysis of the multi-resistant antibiotic profile of *Pseudomonas putida* KT2440,” *Environ. Microbiol.*, vol. 13, no. 10, pp. 2702–2716, 2011.
 - [131] B. Wynands, C. Lenzen, M. Otto, F. Koch, L. M. Blank, and N. Wierckx, “Metabolic engineering of *Pseudomonas taiwanensis* VLB120 with minimal genomic modifications for high-yield phenol production,” *Metab. Eng.*, vol. 47, no. December 2017, pp. 121–133, 2018.
 - [132] D. Hanahan, “Techniques for transformation of *E. coli*,” *DNA cloning a Pract. approach*, vol. 1, pp. 109–135, 1985.
 - [133] “E. coli PIR2 ThermoFisher Scientific.” [Online]. Available: <https://www.thermofisher.com/order/catalog/product/C111110>. [Accessed: 20-Dec-2021].
 - [134] G. Ditta, S. Stanfield, D. Corbin, and D. R. Helinski, “Broad host range DNA cloning system for gram-negative bacteria: construction of a gene bank of *Rhizobium meliloti*,” *Proc. Natl. Acad. Sci.*, vol. 77, no. 12, pp. 7347–7351, 1980.
 - [135] “E. coli TOP10 Invitrogen.” [Online]. Available: <https://www.thermofisher.com/order/catalog/product/C404010>. [Accessed: 17-Dec-2021].
 - [136] J. Hemmerich, W. Wiechert, and M. Oldiges, “Automated growth rate determination in high-throughput microbioreactor systems,” *BMC Res. Notes*, vol. 10, no. 1, pp. 1–7, 2017.
 - [137] J. Beal *et al.*, “Quantification of bacterial fluorescence using independent calibrants,” *PLoS One*, vol. 13, no. 6, pp. 1–15, 2018.
-

- [138] S. Yuzawa, N. Chiba, L. Katz, and J. D. Keasling, "Construction of a part of a 3-hydroxypropionate cycle for heterologous polyketide biosynthesis in *Escherichia coli*," *Biochemistry*, vol. 51, no. 49, pp. 9779–9781, Dec. 2012.
- [139] R. Balakrishnan *et al.*, "Principles of gene regulation quantitatively connect DNA to RNA and proteins in bacteria," *Science (80-.)*, vol. 378, Dec. 2022.
- [140] A. H. Yona, E. J. Alm, and J. Gore, "Random sequences rapidly evolve into de novo promoters," *Nat. Commun.*, vol. 9, no. 1, pp. 1–10, 2018.
- [141] R. P. Patwardhan *et al.*, "Massively parallel functional dissection of mammalian enhancers *in vivo*," *Nat. Biotechnol.*, vol. 30, no. 3, pp. 265–270, 2012.
- [142] H. Alper, C. Fischer, E. Nevoigt, and G. Stephanopoulos, "Tuning genetic control through promoter engineering," *Proc. Natl. Acad. Sci. U. S. A.*, vol. 102, no. 36, pp. 12678–12683, 2005.
- [143] A. Hossain *et al.*, "Automated design of thousands of nonrepetitive parts for engineering stable genetic systems," *Nat. Biotechnol.*, vol. 38, no. 12, pp. 1466–1475, 2020.
- [144] U. W. Liebal, S. Köbbing, L. Netze, A. M. Schweidtmann, A. Mitsos, and L. M. Blank, "Insight to gene expression from promoter libraries with the machine learning workflow Exp2lpynb," *Front. Bioinforma.*, vol. 1, no. October, pp. 1–9, 2021.
- [145] M. Zhao, Z. Yuan, L. Wu, S. Zhou, and Y. Deng, "Precise prediction of promoter strength based on a de novo synthetic promoter library coupled with machine learning," *ACS Synth. Biol.*, vol. 11, no. 1, pp. 92–102, 2022.
- [146] S. Ohuchi, T. Mascher, and B. Suess, "Promoter RNA sequencing (PRSeq) for the massive and quantitative promoter analysis *in vitro*," *Sci. Rep.*, vol. 9, no. 1, pp. 1–7, 2019.
- [147] D. Del Vecchio, "Modularity, context-dependence, and insulation in engineered biological circuits," *Trends Biotechnol.*, vol. 33, no. 2, pp. 111–119, 2015.
- [148] S. Klumpp, Z. Zhang, and T. Hwa, "Growth rate-dependent global effects on gene expression in bacteria," *Cell*, vol. 139, no. 7, pp. 1366–1375, 2009.
- [149] L. Jin, S. Nawab, M. Xia, X. Ma, and Y. X. Huo, "Context-dependency of synthetic minimal promoters in driving gene expression: a case study," *Microb. Biotechnol.*, vol. 12, no. 6, pp. 1476–1486, 2019.
- [150] A. Weimer, M. Kohlstedt, D. C. Volke, P. I. Nikel, and C. Wittmann, "Industrial biotechnology of *Pseudomonas putida*: advances and prospects," *Appl. Microbiol. Biotechnol.*, vol. 104, no. 18, pp. 7745–7766, 2020.
- [151] M. Lonetto, M. Gribskov, and C. A. Gross, "The $\sigma 70$ family: sequence conservation and evolutionary relationships," *J. Bacteriol.*, vol. 174, no. 12, pp. 3843–3849, 1992.
- [152] S. Borukhov and E. Nudler, "RNA polymerase holoenzyme: structure, function and biological implications," *Curr. Opin. Microbiol.*, vol. 6, no. 2, pp. 93–100, 2003.
- [153] J. Park and H. H. Wang, "Systematic dissection of $\sigma 70$ sequence diversity and function in bacteria," *Cell Rep.*, vol. 36, no. 8, p. 109590, 2021.
- [154] T. Gardella, H. Moyle, and M. M. Susskind, "A mutant *Escherichia coli* $\sigma 70$ subunit of RNA polymerase with altered promoter specificity," *J. Mol. Biol.*, vol. 206, no. 4, pp. 579–590, 1989.
- [155] D. A. Siegele, J. C. Hu, W. A. Walter, and C. A. Gross, "Altered promoter recognition by mutant forms of the $\sigma 70$ subunit of *Escherichia coli* RNA polymerase," *J. Mol. Biol.*, vol. 206, no. 4, pp. 591–603, 1989.
- [156] C. Waldburger, T. Gardella, R. Wong, and M. M. Susskind, "Changes in conserved region 2 of *Escherichia coli* $\sigma 70$ affecting promoter recognition," *J. Mol. Biol.*, vol. 215, no. 2, pp. 267–276, 1990.
- [157] S. P. Haugen, W. Ross, and R. L. Gourse, "Advances in bacterial promoter recognition and its control by factors that do not bind DNA," *Nat. Rev. Microbiol.*, vol. 6, no. 7, pp. 507–

-
- 519, 2008.
- [158] V. K. Mutalik *et al.*, "Precise and reliable gene expression via standard transcription and translation initiation elements.," *Nat. Methods*, vol. 10, no. 4, pp. 354–60, 2013.
 - [159] C. Solem and P. R. Jensen, "Modulation of gene expression made easy," *Appl. Environ. Microbiol.*, vol. 68, no. 5, pp. 2397–2403, 2002.
 - [160] R. M. Saecker, M. T. Record, and P. L. Dehaseth, "Mechanism of bacterial transcription initiation: RNA polymerase - promoter binding, isomerization to initiation-competent open complexes, and initiation of RNA synthesis," *J. Mol. Biol.*, vol. 412, no. 5, pp. 754–771, 2011.
 - [161] D. Neves, S. Vos, L. M. Blank, and B. E. Ebert, "Pseudomonas mRNA 2.0: boosting gene expression through enhanced mRNA stability and translational efficiency," *Front. Bioeng. Biotechnol.*, vol. 7, no. January, pp. 1–11, 2020.
 - [162] J. R. Elmore, A. Furches, G. N. Wolff, K. Gorday, and A. M. Guss, "Development of a high efficiency integration system and promoter library for rapid modification of *Pseudomonas putida* KT2440," *Metab. Eng. Commun.*, vol. 5, pp. 1–8, Dec. 2017.
 - [163] P. R. Jensen and K. Hammer, "The sequence of spacers between the consensus sequences modulates the strength of prokaryotic promoters.," *Appl. Environ. Microbiol.*, vol. 64, no. 1, pp. 82–7, Jan. 1998.
 - [164] A. Kanhere, "Structural properties of promoters: similarities and differences between prokaryotes and eukaryotes," *Nucleic Acids Res.*, vol. 33, no. 10, pp. 3165–3175, Jun. 2005.
 - [165] M. Djordjevic, "Redefining *Escherichia coli* σ 70 promoter elements: -15 motif as a complement of the -10 motif," *J. Bacteriol.*, vol. 193, no. 22, pp. 6305–6314, 2011.
 - [166] S. Keilty and M. Rosenberg, "Constitutive function of a positively regulated promoter reveals new sequences essential for activity.," *J. Biol. Chem.*, vol. 262, no. 13, pp. 6389–6395, 1987.
 - [167] E. F. Ruff, M. Thomas Record, and I. Artsimovitch, "Initial events in bacterial transcription initiation," *Biomolecules*, vol. 5, no. 2, pp. 1035–1062, 2015.
 - [168] N. I. Johns *et al.*, "Metagenomic mining of regulatory elements enables programmable species-selective gene expression," *Nat. Methods*, vol. 15, no. 5, pp. 323–329, 2018.
 - [169] A. M. Davy, H. F. Kildegaard, and M. R. Andersen, "Cell factory engineering," *Cell Syst.*, vol. 4, no. 3, pp. 262–275, Mar. 2017.
 - [170] L. Liu *et al.*, "How to achieve high-level expression of microbial enzymes," *Bioengineered*, vol. 4, no. 4, pp. 212–223, Jul. 2013.
 - [171] S. Carneiro, E. C. Ferreira, and I. Rocha, "Metabolic responses to recombinant bioprocesses in *Escherichia coli*," *J. Biotechnol.*, vol. 164, no. 3, pp. 396–408, Apr. 2013.
 - [172] O. Borkowski, F. Ceroni, G. B. Stan, and T. Ellis, "Overloaded and stressed: whole-cell considerations for bacterial synthetic biology," *Curr. Opin. Microbiol.*, vol. 33, pp. 123–130, 2016.
 - [173] T. A. Carrier and J. D. Keasling, "Engineering mRNA stability in *E. coli* by the addition of synthetic hairpins using a 5' cassette system," *Biotechnol. Bioeng.*, vol. 55, no. 3, pp. 577–580, Aug. 1997.
 - [174] C. Lou, B. Stanton, Y.-J. Chen, B. Munsy, and C. A. Voigt, "Ribozyme-based insulator parts buffer synthetic circuits from genetic context.," *Nat. Biotechnol.*, vol. 30, no. 11, pp. 1137–42, 2012.
 - [175] K. P. Clifton *et al.*, "The genetic insulator RiboJ increases expression of insulated genes," *J. Biol. Eng.*, vol. 12, no. 1, p. 23, Dec. 2018.
 - [176] H. M. Salis, E. A. Mirsky, and C. A. Voigt, "Automated design of synthetic ribosome binding sites to control protein expression," *Nat. Biotechnol.*, vol. 27, no. 10, pp. 946–950, 2009.
 - [177] M. Otto *et al.*, "Targeting 16S ribosomal DNA for stable recombinant gene expression in
-

- Pseudomonas*," *ACS Synth. Biol.*, p. acssynbio.9b00195, 2019.
- [178] A. a. K. Nielsen, T. H. Segall-Shapiro, and C. a. Voigt, "Advances in genetic circuit design: novel biochemistries, deep part mining, and precision gene expression," *Curr. Opin. Chem. Biol.*, vol. 17, no. 6, pp. 878–892, 2013.
- [179] G. Cambray *et al.*, "Measurement and modeling of intrinsic transcription terminators," *Nucleic Acids Res.*, vol. 41, no. 9, pp. 5139–5148, 2013.
- [180] D. Landgraf, "Quantifying localizations and dynamics in single bacterial cells," Doctoral dissertation, Harvard University, 2012.
- [181] K. Lang, J. Zierow, K. Buehler, and A. Schmid, "Metabolic engineering of *Pseudomonas* sp. strain VLB120 as platform biocatalyst for the production of isobutyric acid and other secondary metabolites," *Microb. Cell Fact.*, vol. 13, no. 1, p. 2, 2014.
- [182] C. Lenzen *et al.*, "High-yield production of 4-hydroxybenzoate from glucose or glycerol by an engineered *Pseudomonas taiwanensis* VLB120," *Front. Bioeng. Biotechnol.*, vol. 7, no. June, pp. 1–17, Jun. 2019.
- [183] N. J. P. Wierckx, H. Ballerstedt, J. A. M. de Bont, and J. Wery, "Engineering of solvent-tolerant *Pseudomonas putida* S12 for bioproduction of phenol from glucose," *Appl. Environ. Microbiol.*, vol. 71, no. 12, pp. 8221–8227, Dec. 2005.
- [184] S. Verhoef, N. Wierckx, R. G. M. Westerhof, J. H. De Winde, and H. J. Ruijsseenaars, "Bioproduction of p-hydroxystyrene from glucose by the solvent-tolerant bacterium *Pseudomonas putida* S12 in a two-phase water-decanol fermentation," *Appl. Environ. Microbiol.*, vol. 75, no. 4, pp. 931–936, 2009.
- [185] S. Schmitz, S. Nies, N. Wierckx, L. M. Blank, and M. A. Rosenbaum, "Engineering mediator-based electroactivity in the obligate aerobic bacterium *Pseudomonas putida* KT2440," *Front. Microbiol.*, vol. 6, no. APR, pp. 1–13, 2015.
- [186] Y.-J. Chen *et al.*, "Characterization of 582 natural and synthetic terminators and quantification of their design constraints," *Nat. Methods*, vol. 10, no. 7, pp. 659–664, 2013.
- [187] K. Terpe, "Overview of bacterial expression systems for heterologous protein production: From molecular and biochemical fundamentals to commercial systems," *Appl. Microbiol. Biotechnol.*, vol. 72, no. 2, pp. 211–222, 2006.
- [188] C. A. Voigt, "Genetic parts to program bacteria," *Curr. Opin. Biotechnol.*, vol. 17, no. 5, pp. 548–557, 2006.
- [189] R. Chen, "Bacterial expression systems for recombinant protein production: *E. coli* and beyond," *Biotechnol. Adv.*, vol. 30, no. 5, pp. 1102–1107, 2012.
- [190] B. Jusiak, S. Cleto, P. Perez-Piñera, and T. K. Lu, "Engineering synthetic gene circuits in living cells with CRISPR technology," *Trends Biotechnol.*, vol. 34, no. 7, pp. 535–547, 2016.
- [191] L. E. Hüskén, R. Beeftink, J. A. M. De Bont, and J. Wery, "High-rate 3-methylcatechol production in *Pseudomonas putida* strains by means of a novel expression system," *Appl. Microbiol. Biotechnol.*, vol. 55, no. 5, pp. 571–577, 2001.
- [192] L. Horbal and A. Luzhetskyy, "Dual control system - a novel scaffolding architecture of an inducible regulatory device for the precise regulation of gene expression," *Metab. Eng.*, vol. 37, pp. 11–23, 2016.
- [193] M. Jahn *et al.*, "Accurate determination of plasmid copy number of flow-sorted cells using droplet digital PCR," *Anal. Chem.*, vol. 86, no. 12, pp. 5969–5976, 2014.
- [194] M. Lindmeyer, M. Jahn, C. Vorpahl, S. Müller, A. Schmid, and B. Bühler, "Variability in subpopulation formation propagates into biocatalytic variability of engineered *Pseudomonas putida* strains," *Front. Microbiol.*, vol. 6, no. OCT, pp. 1–15, 2015.
- [195] J. Mi *et al.*, "Investigation of plasmid-induced growth defect in *Pseudomonas putida*," *J. Biotechnol.*, vol. 231, pp. 167–173, 2016.
- [196] M. Otto *et al.*, "Targeting 16S ribosomal DNA for stable recombinant gene expression in

-
- Pseudomonas*," *ACS Synth. Biol.*, p. acssynbio.9b00195, Jul. 2019.
- [197] D. Court, "RNA processing and degradation by RNase III," in *Control of Messenger RNA Stability*, Belasco JG and Brawerman G, Eds. New York: Academic, 1993, pp. 71–116.
- [198] S. Laalami, L. Zig, and H. Putzer, "Initiation of mRNA decay in bacteria," *Cell. Mol. Life Sci.*, vol. 71, no. 10, pp. 1799–1828, 2014.
- [199] N. Panayotatos and K. Truong, "Cleavage within an RNase III site can control mRNA stability and protein synthesis in vivo," *Nucleic Acids Res.*, vol. 13, no. 7, pp. 2227–2240, 1985.
- [200] I. Calin-Jageman and A. W. Nicholson, "Mutational analysis of an RNA internal loop as a reactivity epitope for *Escherichia coli* ribonuclease III substrates," *Biochemistry*, vol. 42, no. 17, pp. 5025–34, 2003.
- [201] J. Xiao, C. E. Feehery, G. Tzertzinis, and C. V. Maina, "*E. coli* RNase III(E38A) generates discrete-sized products from long dsRNA," *Rna*, vol. 15, no. 5, pp. 984–991, 2009.
- [202] M. P. Deutscher, "Degradation of RNA in bacteria: comparison of mRNA and stable RNA," *Nucleic Acids Res.*, vol. 34, no. 2, pp. 659–666, 2006.
- [203] I. Belenky, A. Steinmetz, M. Vyazmensky, Z. Barak, K. Tittmann, and D. M. Chipman, "Many of the functional differences between acetohydroxyacid synthase (AHAS) isozyme I and other AHASs are a result of the rapid formation and breakdown of the covalent acetolactate-thiamin diphosphate adduct in AHAS I," *FEBS J.*, vol. 279, no. 11, pp. 1967–1979, Jun. 2012.
- [204] J. B. Rostgaard, I. Svendsen, and M. Oitese, "Isolation and characterization of an alpha-acetolactate decarboxylase useful for accelerated beer maturation," in *Journal of the Institute of Brewing*, 1987, vol. 93, no. 3, p. 160.
- [205] S. C. Viegas, P. Apura, E. Martínez-García, V. De Lorenzo, and C. M. Arraiano, "Modulating heterologous gene expression with portable mRNA-stabilizing 5'-UTR sequences," *ACS Synth. Biol.*, vol. 7, no. 9, pp. 2177–2188, 2018.
- [206] E. P. Brass, "Overview of coenzyme A metabolism and its role in cellular toxicity," *Chem. Biol. Interact.*, vol. 90, no. 3, pp. 203–214, 1994.
- [207] A. Krivoruchko, Y. Zhang, V. Siewers, Y. Chen, and J. Nielsen, "Microbial acetyl-CoA metabolism and metabolic engineering," *Metab. Eng.*, vol. 28, pp. 28–42, 2015.
- [208] K. Srirangan *et al.*, "Manipulating the sleeping beauty mutase operon for the production of 1-propanol in engineered *Escherichia coli*," *Biotechnol. Biofuels*, vol. 6, no. 1, pp. 1–14, 2013.
- [209] H. C. Tseng and K. L. J. Prather, "Controlled biosynthesis of odd-chain fuels and chemicals via engineered modular metabolic pathways," *Proc. Natl. Acad. Sci. U. S. A.*, vol. 109, no. 44, pp. 17925–17930, 2012.
- [210] L. Akawi, K. Srirangan, X. Liu, M. Moo-Young, and C. Perry Chou, "Engineering *Escherichia coli* for high-level production of propionate," *J. Ind. Microbiol. Biotechnol.*, vol. 42, no. 7, pp. 1057–1072, 2015.
- [211] K. Srirangan, X. Liu, L. Akawi, M. Bruder, M. Moo-Young, and C. P. Chou, "Engineering *Escherichia coli* for microbial production of butanone," *Appl. Environ. Microbiol.*, vol. 82, no. 9, pp. 2574–2584, May 2016.
- [212] B. A. Pfeifer, S. J. Admiraal, H. Gramajo, D. E. Cane, and C. Khosla, "Biosynthesis of complex polyketides in a metabolically engineered strain of *E. coli*," *Science (80-)*, vol. 291, no. 5509, pp. 1790–1792, 2001.
- [213] C. Dellomonaco, C. Rivera, P. Campbell, and R. Gonzalez, "Engineered respiro-fermentative metabolism for the production of biofuels and biochemicals from fatty acid-rich feedstocks," *Appl. Environ. Microbiol.*, vol. 76, no. 15, pp. 5067–5078, 2010.
- [214] T. Haller, T. Buckel, J. Rétey, and J. A. Gerlt, "Discovering new enzymes and metabolic pathways: conversion of succinate to propionate by *Escherichia coli*," *Biochemistry*, vol.
-

- 39, no. 16, pp. 4622–4629, Apr. 2000.
- [215] R. A. Gonzalez-Garcia, T. McCubbin, M. S. Turner, L. K. Nielsen, and E. Marcellin, “Engineering *Escherichia coli* for propionic acid production through the Wood–Werkman cycle,” *Biotechnol. Bioeng.*, vol. 117, no. 1, pp. 167–183, Jan. 2020.
- [216] Y. Jun Choi, J. Hwan Park, T. Yong Kim, and S. Yup Lee, “Metabolic engineering of *Escherichia coli* for the production of 1-propanol,” *Metab. Eng.*, vol. 14, no. 5, pp. 477–486, 2012.
- [217] K. Srirangan *et al.*, “Biochemical, genetic, and metabolic engineering strategies to enhance coproduction of 1-propanol and ethanol in engineered *Escherichia coli*,” *Appl. Microbiol. Biotechnol.*, vol. 98, no. 22, pp. 9499–9515, 2014.
- [218] R. A. Gonzalez-Garcia, T. McCubbin, A. Wille, M. Plan, L. K. Nielsen, and E. Marcellin, “Awakening sleeping beauty: production of propionic acid in *Escherichia coli* through the *sbm* operon requires the activity of a methylmalonyl-CoA epimerase,” *Microb. Cell Fact.*, vol. 16, no. 1, pp. 1–14, 2017.
- [219] J. Li, X. Zhu, J. Chen, D. Zhao, X. Zhang, and C. Bi, “Construction of a novel anaerobic pathway in *Escherichia coli* for propionate production,” *BMC Biotechnol.*, vol. 17, no. 1, pp. 1–9, 2017.
- [220] K. Srirangan *et al.*, “Recent advances in engineering propionyl-CoA metabolism for microbial production of value-added chemicals and biofuels,” *Crit. Rev. Biotechnol.*, vol. 37, no. 6, pp. 701–722, 2017.
- [221] J. Rühl, A. Schmid, and L. M. Blank, “Selected *Pseudomonas putida* strains able to grow in the presence of high butanol concentrations,” *Appl. Environ. Microbiol.*, vol. 75, no. 13, pp. 4653–4656, 2009.
- [222] M. M. Müller, B. Hörmann, C. Syltatk, and R. Hausmann, “*Pseudomonas aeruginosa* PAO1 as a model for rhamnolipid production in bioreactor systems,” *Appl. Microbiol. Biotechnol.*, vol. 87, no. 1, pp. 167–174, 2010.
- [223] I. Poblete-Castro, A. L. Rodriguez, C. M. Chi Lam, and W. Kessler, “Improved production of medium-chain-length polyhydroxyalkanoates in glucose-based fed-batch cultivations of metabolically engineered *Pseudomonas putida* strains,” *J. Microbiol. Biotechnol.*, vol. 24, no. 1, pp. 59–69, 2014.
- [224] D. Cha, H. Seok Ha, and S. Kuk Lee, “Metabolic engineering of *Pseudomonas putida* for the production of various types of short-chain-length polyhydroxyalkanoates from levulinic acid,” *Bioresour. Technol.*, p. 123332, Apr. 2020.
- [225] J. Mozejko-Ciesielska, K. Szacherska, and P. Marciniak, “*Pseudomonas* species as producers of eco-friendly polyhydroxyalkanoates,” *J. Polym. Environ.*, vol. 27, no. 6, pp. 1151–1166, 2019.
- [226] J. Mi *et al.*, “De novo production of the monoterpene geranic acid by metabolically engineered *Pseudomonas putida*,” *Microb. Cell Fact.*, vol. 13, no. 1, pp. 1–11, 2014.
- [227] A. Martinez *et al.*, “Genetically modified bacterial strains and novel bacterial artificial chromosome shuttle vectors for constructing environmental libraries and detecting heterologous natural products in multiple expression hosts,” *Appl. Environ. Microbiol.*, vol. 70, no. 4, pp. 2452–2463, 2004.
- [228] F. Gross *et al.*, “Bacterial type III polyketide synthases: phylogenetic analysis and potential for the production of novel secondary metabolites by heterologous expression in pseudomonads,” *Arch. Microbiol.*, vol. 185, no. 1, pp. 28–38, 2006.
- [229] A. Loeschcke and S. Thies, “*Pseudomonas putida*—a versatile host for the production of natural products,” *Appl. Microbiol. Biotechnol.*, pp. 6197–6214, 2015.
- [230] V. dePaul Marshall and J. R. Sokatch, “Regulation of valine catabolism in *Pseudomonas putida*,” *J. Bacteriol.*, vol. 110, no. 3, pp. 1073–1081, Jun. 1972.

-
- [231] B. P. Mooney, J. A. Miernyk, and D. D. Randall, "The complex fate of α -ketoacids," *Annu. Rev. Plant Biol.*, vol. 53, pp. 357–375, 2002.
- [232] F. Gross *et al.*, "Metabolic engineering of *Pseudomonas putida* for methylmalonyl-CoA biosynthesis to enable complex heterologous secondary metabolite formation," *Chem. Biol.*, vol. 13, no. 12, pp. 1253–1264, 2006.
- [233] D. Bannerjee, L. E. Sanders, and J. R. Sokatch, "Properties of purified methylmalonate semialdehyde dehydrogenase of *Pseudomonas aeruginosa*," *J. Biol. Chem.*, vol. 245, no. 7, pp. 1828–1835, Apr. 1970.
- [234] C. P. Long, J. E. Gonzalez, A. M. Feist, B. O. Palsson, and M. R. Antoniewicz, "Fast growth phenotype of *E. coli* K-12 from adaptive laboratory evolution does not require intracellular flux rewiring," *Metab. Eng.*, vol. 44, pp. 100–107, Nov. 2017.
- [235] L. M. Blank, G. Ionidis, B. E. Ebert, B. Bühler, and A. Schmid, "Metabolic response of *Pseudomonas putida* during redox biocatalysis in the presence of a second octanol phase," *FEBS J.*, vol. 275, no. 20, pp. 5173–5190, 2008.
- [236] M. J. Zidwick, J.-S. Chen, and P. Rogers*, "Organic acid and solvent production: propionic and butyric acids and ethanol," in *The Prokaryotes*, vol. 9783642313, E. Rosenberg, E. F. DeLong, S. Lory, E. Stackebrandt, and F. Thompson, Eds. Berlin, Heidelberg: Springer Berlin Heidelberg, 2013, pp. 135–167.
- [237] C. R. Álvarez-Chávez, S. Edwards, R. Moure-Eraso, and K. Geiser, "Sustainability of bio-based plastics: general comparative analysis and recommendations for improvement," *J. Clean. Prod.*, vol. 23, no. 1, pp. 47–56, 2012.
- [238] S. Suwannakham, Y. Huang, and S.-T. Yang, "Construction and characterization of ack knock-out mutants of *Propionibacterium acidipropionici* for enhanced propionic acid fermentation," *Biotechnol. Bioeng.*, vol. 94, no. 2, pp. 383–395, Jun. 2006.
- [239] D. Miscevic, J. Mao, M. Moo-Young, and C. P. Chou, "High-level heterologous production of propionate in engineered *Escherichia coli*," *Biotechnol. Bioeng.*, vol. 117, no. 5, pp. 1304–1315, May 2020.
- [240] C. Ma *et al.*, "Bio-production of high-purity propionate by engineering l-threonine degradation pathway in *Pseudomonas putida*," *Appl. Microbiol. Biotechnol.*, Apr. 2020.
- [241] Z. Wang, "Process development and metabolic engineering for enhanced propionic acid production by *Propionibacterium freudenreichii* subsp. *shermanii*," The Ohio State University, 2013.
- [242] Z. Wang, E. M. Ammar, A. Zhang, L. Wang, M. Lin, and S.-T. Yang, "Engineering *Propionibacterium freudenreichii* subsp. *shermanii* for enhanced propionic acid fermentation: effects of overexpressing propionyl-CoA: Succinate CoA transferase," *Metab. Eng.*, vol. 27, pp. 46–56, 2015.
- [243] Z. Zhuang *et al.*, "Divergence of function in the hot dog fold enzyme superfamily: the bacterial thioesterase YciA," *Biochemistry*, vol. 47, no. 9, pp. 2789–2796, 2008.
- [244] T. E. Saleski, M. T. Chung, D. N. Carruthers, A. Khasbaatar, K. Kurabayashi, and X. N. Lin, "Optimized gene expression from bacterial chromosome by high-throughput integration and screening," *Sci. Adv.*, vol. 7, no. 7, p. eabe1767, 2021.
- [245] R. Gonzalez-Garcia, T. McCubbin, L. Navone, C. Stowers, L. Nielsen, and E. Marcellin, "Microbial propionic acid production," *Fermentation*, vol. 3, no. 2, p. 21, 2017.
- [246] S. Köbbing, L. M. Blank, and N. Wierckx, "Characterization of context-dependent effects on synthetic promoters," *Front. Bioeng. Biotechnol.*, vol. 8, no. June, pp. 1–13, 2020.
- [247] T. La Fleur, A. Hossain, and H. M. Salis, "Automated model-predictive design of synthetic promoters to control transcriptional profiles in bacteria," *bioRxiv*, p. 2021.09.01.458561, 2021.
- [248] F. Hoppe, U. Burke, M. Thewes, A. Heufer, F. Kremer, and S. Pischinger, "Tailor-made fuels
-

References

from biomass: potentials of 2-butanone and 2-methylfuran in direct injection spark ignition engines," *Fuel*, vol. 167, pp. 106–117, 2016.

Curriculum vitae

Personal data

Name: Dário Jorge Silva Neves
Born: March 20, 1990 in Angra do Heroísmo, Portugal
Nationality: Portuguese

Education

02/2015-08/2019 **PhD student**
Institute of Applied Microbiology, RWTH Aachen, Germany
2013-2015 **Research Scholarship**
ITQB, Portugal
2011-2013 **Master of Science program: Molecular Biotechnology**
University of Aveiro, Aveiro, Portugal
University of Lund, Lund, Sweden
2008-2011 **Bachelor of Science program: Biotechnology**
University of Aveiro, Aveiro, Portugal
2001-2008 **High School**
Instituto D. João V, Louriçal, Portugal

Awards and grants

2018 Junior Research Grant for Metabolic Engineering 12 Conference

Extracurricular activities

2021- Mentor at IMFAHE
2015-2019 Coach/Captain of the Alemannia Aachen Futsal Team

Publications

D. Neves, S. Vos, L. M. Blank, and B. E. Ebert, "Pseudomonas mRNA 2.0: boosting gene expression through enhanced mRNA stability and translational efficiency," *Front. Bioeng. Biotechnol.*, vol. 7, no. January, pp. 1–11, 2020

G. Sandström, H. Almqvist, D. Portugal-Nunes, **D. Neves**, G. Lidén, and M. F. Gorwa-Grauslund, "Saccharomyces cerevisiae: a potential host for carboxylic acid production from lignocellulosic feedstock?," *Appl. Microbiol. Biotechnol.*, vol. 98, no. 17, pp. 7299–7318, Sep. 2014.

M. Tokic, N. Hadadi, M. Ataman, **D. Neves**, B. E. Ebert, L. M. Blank, L. Miskovic, V. Hatzimanikatis, "Discovery and evaluation of biosynthetic pathways for the production of five methyl ethyl ketone precursors," *ACS Synth. Biol.*, vol. 7, no. 8, pp. 1858–1873, Aug. 2018.

J. Deischter, K. Schute, **D. S. Neves**, B. E. Ebert, L. M. Blank, and R. Palkovits, "Aromatisation of bio-derivable isobutyraldehyde over HZSM-5 zeolite catalysts," *Green Chem.*, vol. 21, no. 7, pp. 1710–1717, 2019.

D. Neves, U. Liebal, S. C. Nies, T. B. Alter, C. Pitzler, L. M. Blank and B. E. Ebert, "Cross-species synthetic promoter library: finding common ground between *Pseudomonas taiwanensis* VLB120 and *Escherichia coli*." *ACS Syn. Bio.*, 2023.

D. Neves, D. Meinen, T. B. Alter, L. M. Blank and B. E. Ebert, "Expanding *Pseudomonas taiwanensis* VLB120's acyl-CoA portfolio: propionate production in mineral salt medium." *Micro. Biotechnol.*, 2023.

Poster presentations

D. Neves, S. Nies, B. E. Ebert L. M. Blank, (February 23, 2016) Comprehensive analysis and cross-species comparison of synthetic promoters. 3rd Meeting on Applied Synthetic Biology in Europe, Lisbon, Portugal

D. Neves, B. E. Ebert L. M. Blank, (June 24-28, 2018) A guide for novel synthetic pathways: principles and tools. Metabolic engineering 12: systems metabolic engineering for superior bio-production, Munique, Germany

D. Neves, B. E. Ebert L. M. Blank, M. Mann, G. Wandrey, N. Ilhing, J. Buechs (June 24-28, 2018) Conversion of methane to value added products. Metabolic engineering 12: systems metabolic engineering for superior bio-production, Munique, Germany

D. Neves, B. E. Ebert L. M. Blank, (March 21-24, 2018) A guide for novel synthetic pathways: principles and tools. Mosbacher Kolloquium "Synthetic Biology-from understanding to application", Mosbach, Germany